A Method Of Measuring Degree Of Dispersion In Dried Ink Films.

INFORMATION TO USERS

This was produced from a copy of a document sent to us for microfilming. While the most advanced technological means to photograph and reproduce this document have been used, the quality is heavily dependent upon the quality of the material submitted.

The following explanation of techniques is provided to help you understand markings or notations which may appear on this reproduction.

1. The sign or "target" for pages apparently lacking from the document photographed is "Missing Page(s)". If it was possible to obtain the missing page(s) or section, they are spliced into the film along with adjacent pages. This may have necessitated cutting through an image and duplicating adjacent pages to assure you of complete continuity.

2. When an image on the film is obliterated with a round black mark it is an indication that the film inspector noticed either blurred copy because of movement during exposure, or duplicate copy. Unless we meant to delete copyrighted materials that should not have been filmed, you will find a good image of the page in the adjacent frame.

3. When a map, drawing or chart, etc., is part of the material being photographed the photographer has followed a definite method in "sectioning" the material. It is customary to begin filming at the upper left hand corner of a large sheet and to continue from left to right in equal sections with small overlaps. If necessary, sectioning is continued again—beginning below the first row and continuing on until complete.

4. For any illustrations that cannot be reproduced satisfactorily by xerography, photographic prints can be purchased at additional cost and tipped into your xerographic copy. Requests can be made to our Dissertations Customer Services Department.

5. Some pages in any document may have indistinct print. In all cases we have filmed the best available copy.

University Microfilms International

300 N. ZEEB ROAD, ANN ARBOR, MI 48106
18 BEDFORD ROW, LONDON WC1R 4EJ, ENGLAND

NIPPERT, CHARLES R., JR.
A METHOD OF MEASURING DEGREE OF DISPERSION IN DRIED INK FILMS.

LEHIGH UNIVERSITY, PH.D., 1979

PLEASE NOTE:

In all cases this material has been filmed in the best possible way from the available copy. Problems encountered with this document have been identified here with a check mark ✓.

1. Glossy photographs _____
2. Colored illustrations _____
3. Photographs with dark background _____
4. Illustrations are poor copy _____
5. Print shows through as there is text on both sides of page _____
6. Indistinct, broken or small print on several pages _____ throughout _____
7. Tightly bound copy with print lost in spine _____
8. Computer printout pages with indistinct print ✓
9. Page(s) _____ lacking when material received, and not available from school or author _____
10. Page(s) _____ seem to be missing in numbering only as text follows _____
11. Poor carbon copy _____
12. Not original copy, several pages with blurred type _____
13. Appendix pages are poor copy _____
14. Original copy with light type _____
15. Curling and wrinkled pages _____
16. Other _____

University Microfilms International

300 N. ZEEB RD., ANN ARBOR, MI 48106 (313) 761-4700

A METHOD OF MEASURING DEGREE OF DISPERSION IN DRIED INK FILMS

By

Charles R. Nippert, Jr.

A Dissertation

Presented to the Graduate Committee

of Lehigh University

in Candidacy for the Degree of

Doctor of Philosophy

Lehigh University

1978

Approved and recommended for acceptance as a dissertation in partial fulfillment of the requirements for the degree of Doctor of Philosophy.

_____
(date)

J. W. Vandeventer
Professor in Charge

Accepted _____
(date)

Special committee directing the doctoral work of Charles R. Nippert

J. W. Vandeventer
Chairman

Gary Poehlein

Eugene M. Allen

M. R. Dassey

D. J. Mueller

ACKOWLEDGEMENTS

The author wishes to acknowledge the gracious contributions of the following people and groups.

Prof. J. W. Vanderhoff for his patience and advice during the research and in reviewing the manuscripts.

Profs. M. S. El-Aasser, E. M. Allen, F. J. Micale and G. W. Poehlein, whose assistance throughout this work was deeply appreciated.

The National Printing Ink Research Institute which funded the project.

Ms. J. M. Fetsko, and Ms. J. Lavelle for their willingness to share the knowledge of their extensive background in ink research.

In addition, the author would like to acknowledge the following companies for providing material during the work:

E. I. DuPont de Nemours & Co.

American Cyanamid

Ciba-Geigy

Capitol Printing Ink

TABLE OF CONTENTS

List of Tables

List of Figures

List of Appendices

ABSTRACT

The quality of a pigmented dispersion is an important consideration in ink manufacture, both in quality control and in basic research. A study has been made of various aspects of dispersion measurement. The purposes of this work were: 1) to investigate qualitatively the relationship between the color strength of ink prints and various industrial measurements of degree of dispersion, 2) to consider potential new methods of measurment, and 3) to develop a better theory of the process of pigment dispersion. To achieve these goals, a series of copper phthalocyanine blue dispersions were made using commercially available pigments and a standard alkyd resin. This experimental work confirmed the inadequacy of existing bleach test methods and demonstrated the advantages of determining color strength directly from prints. This new

method was compared with more sophisticated colorimetric models based upon Kubelka-Munk theory and was found to have potential for industrial use.

While preparing the dispersions used in the previously mentioned colorimetric measurements, experimental data were obtained relating the change of various quality control measurements (i.e., wet gloss, grindometer scratch count, tinting strength and transfer properties) to milling time. A theoretical model of the dispersion of pigments in process equipment which explained these data was derived. This model was based on: 1) the assumption that shear-induced collisions between particles cause dispersion (the mathematics for describing such collisions was developed by Smoluchowski) and 2) a theoretical model of grinding developed by Austin. The final model correctly

describes the change in the aggregate size distribution as a function of milling time and correctly predicts the qualitatively observed relationship between degree of dispersion, pigment loading and dispersion time.

INTRODUCTION

The improvement of ink properties with increasing dispersion times is of basic importance to the ink industry. Inks are commonly manufactured in two ways: 1) they can be manufactured from "dry color", that is, from pigment in the form of a dry, finely ground powder that must be wet with the ink vehicle and dispersed; or 2) they can be manufactured from "flushed color" which is a dispersion of pigment in oil. In general, longer milling times produce better inks. This relationship for dry color pigments provides an easily controllable process parameter, especially when ink is produced in sand or ball mills.

"Dry color" is produced by drying the filtered products of the pigment synthesis. "Flushed color" is produced by displacing the water in the filter cake with oil or varnish. The "press cake", containing 30 to 80% water,

is mixed with oil or varnish. As the pigment is wet by the oil (for which it has greater affinity), the water is flushed out of the press cake. The last traces of water are then removed by heat or vacuum (1). With the use of either system, both the ink maker and the pigment supplier are intimately concerned about dispersion quality and measurement. The degree of dispersion can be controlled and must be measured during flushing and during the final manufacture of ink.

Poor dispersions have, in general, lower color strengths. In extreme cases, they may also contain large pigment particles which interfere with the printing process and may damage the printing plate. Furthermore, ink properties are determined by the size of pigment aggregates rather than by the size of primary particles. Nonetheless, the particle size distribution (which, in other dispersed systems is synonymous

with the term "degree of dispersion") is not measurable for most lithographic inks because they are too viscous and their pigment loadings are too high for convention particle size analysis.

Adjusting the properties of an ink to allow for such measurement could change the size of the aggregates to be measured. For instance, diluting the ink to a pigment loading at which aggregates would be visible using an electron microscope or diluting to a viscosity at which centrifugation tests could be performed would require both adding mechanical energy to the system and changing the chemical composition of the vehicle. Either method may change the aggregate size distribution. Therefore, the size distribution of pigment aggregates in inks is not generally measured directly.

An exception is the measurement of the

largest aggregates (normally 1 μ m or more in diameter). These can be detected routinely by a grindometer (2, 3). Nonetheless, the degree of dispersion of a colored ink is most often measured by its "color strength" and the two terms are frequently interchangeable in the ink industry. This ambiguity of terms occurs because the color strength (or tinting strength) generally increases as the dispersion time (and hence degree of dispersion) increases. It should be noted that this principle is a general rule, not an absolute "law", and that exceptions have been reported (4) and can be expected from the predictions of Mie theory (5). Nonetheless, the general principle cited above does hold in the great majority of cases (6, 7) and the concept of measuring degree of dispersion by measuring color strength is well established.

Color strength can be defined broadly as

the ability of a colored material, such as an ink, to impart its color to a particular white medium. Increasing the color strength of an ink while holding its other properties constant is desirable because the printer can then achieve either: 1) a darker color with the same thickness of ink; or 2) the same color with less ink. It should be noted that reducing the ink film thickness is desirable because that not only reduces the consumption of ink but also reduces wear on the lithographic plate and permits more efficient press operation (8, 9).

The standard method of measuring the color strength of an ink relative to another ink is the "tinting strength test". In this test (such as NPIRI TM-E2) a sample ink is mixed with a white paste. The resulting bleach is compared visually with a similar bleach made from the same white paste and a reference ink. This comparison is made from

side-by-side drawdowns of the two bleaches. Successive bleaches are made by varying the ratio of test ink to paste until a match is achieved. The result is normally expressed as 100 times the ratio of the concentration of reference ink to the concentration of test ink.

Bleach tests have several inherent problems associated with them. First, the procedure for preparing bleaches is time-consuming and the results are operator-dependent. Second, the test leaves no permanent record other than the operator's written comments because the bleach drawdowns age quickly. Third, it is a "wet test", that is, it is based upon the color of wet ink rather than dried ink films. Therefore, bleach tests themselves are significantly different from the end use of the ink (i.e., printed on a substrate) and do not accurately represent the ink's color or degree of dispersion in

piece of printed matter. A new test that can quickly and easily measure color strength from printed materials is desirable. Further, because ink makers normally make sample prints ("proof prints") from batches of colored inks, the development of such "printing strength test" using proof prints would be easily incorporated into their laboratory procedure.

Yet another consideration in ink manufacture is the absence of a mathematically rigorous theory based on principles of surface chemistry, which can account, at least qualitatively, for the relationship between pigment loading and degree of dispersion observed in ink manufacture. A mathematical treatment has been developed to describe the changes in particle size distributions during grinding. In Part I, this treatment will be applied to develop a model of the dispersion of pigment during milling.

PART I

ABSTRACT

A kinetic model of the process of dispersing a pigment in a binder is developed assuming that 1) shear-induced collisions of aggregates cause dispersion and that 2) some aggregates may not break up in the shear field encountered in a particular piece of dispersion equipment. A system of differential equations is proposed which describes the rate of change of the aggregate size distribution. The change in grindometer scratch count as a function of milling conditions is predicted from this model and is compared qualitatively to experimental measurements.

Additional measurements were performed that establish that gloss readings made on grindometer drawdowns could be used as a measure of the degree of dispersion.

CHAPTER I

Dispersion of Inks as a Rate-Controlled Process

Introduction

The preparation of dispersions is the basic operation in the manufacture of inks, paints and many coatings and can be divided into two processes: 1) the wetting of a solid (usually a pigment or a filler) by the binder or vehicle; and 2) the breaking up of aggregates to the desired size (which is normally determined by such factors as color, viscosity, flocculation rate, size of the primary particles and the end use of the finished material). In the manufacture of printing inks from dry color, these two processes can be roughly equated to two separate operations; premixing and milling. The pigment is wetted with binder, typically in a stirred tank, and the dispersion of the resulting "premix" is carried out in a mill.

Little research has been done in the development of a theoretical model that can be used to relate the kinetics of milling (that is, the process of converting premixes to inks) to pigment surface properties and aggregate size distribution. Specifically, there have been few attempts to explain some of the differences between dispersions produced from the same ingredients in various pieces of equipment or the relationship between milling time and dispersion "quality" (an imprecise term because the aggregate size distribution cannot be measured easily). Dispersion research has lagged far behind the field of grinding in attempting to develop kinetic models, even though the importance of dispersion rates to the manufacturer has long been recognized and has been discussed by Vanderhoff (9).

A mathematical treatment has been

developed to describe grinding (10), a process defined as the brittle fracture of large particles to form smaller ones. The model is based upon the assumption that the rate of destruction of large particles (and the rate of formation of smaller particles) is proportional to the number of large particles present. Austin (10) traces the development of grinding theories and describes how to predict changes in particle size distribution. However, a model of ink milling must include the fact that not all the aggregates of a particular size may be dispersed under a given set of conditions. Therefore, different pieces of equipment dispersing the same premix for very long times may produce dispersions of different quality.

It should be noted that, although the phrase "grinding pigment" is sometimes used, the process of pigment dispersion is

fundamentally different than conventional grinding, such as the grinding of stones. "Grinding" can be defined as fracturing individual particles, often individual crystals or crystallites, usually by brittle failure resulting from impact. "Dispersion of pigments", on the other hand, involves the tearing apart of aggregates of particles held together by surface forces.

That the processes are different was demonstrated by Taylor (11) in 1959. Using a roll mill with a fixed gap setting, Taylor first crushed glass beads (a grinding operation), then milled a white ink (a dispersion operation). The largest glass particles were about the same size as the clearance between the rolls (typically 20-70 microns); on the other hand, the largest particle size in the inks was 2 microns.

Nonetheless, there are obvious

similarities between dispersion and grinding. First, the same equipment (ball mills and sand mills, for instance) can be used for both processes. Second, both processes involve the reduction of the average size of a collection of "units" (either primary particles or aggregates) by forming smaller units from larger ones. These similarities allow for the use of Austin's mathematical formulism in the treatment of the dispersion process.

Grinding Theory

The development of the mathematical treatment of grinding as a rate process has been detailed by Austin (10). An outline based on that work will be presented as background material.

Uniform particle sizes rarely occur in grinding operations, but rather, a broad range of sizes is found. The range of particle sizes, from the smallest to the largest, is frequently presented in a cumulative distribution curve

similar to that shown in Fugure 1. For this development, the particle size distribution may be divided into a series of small size intervals similar to the size intervals resulting from a sieve analysis. It is assumed that the rate of breakage of particles in a particular size interval is proportional to the number of particles present. Sedlatschek and Bass (12) demonstrated that this assumption can be derived from probability theory by assuming that breakage results from a fraction of the collisions in a grinding operation. This assumption predicts that the rate of breakage can be represented by a first-order differential equation analogous to those frequently found in chemical engineering reaction kinetics:

rate of loss from the i-th interval =

$$S_i w_i(t) \qquad (1)$$

where S_i = the specific rate of breakage (a function of the equipment and the material being ground).

Figure 1 - Cumulative Particle Size Distribution
(according to Austin (10))

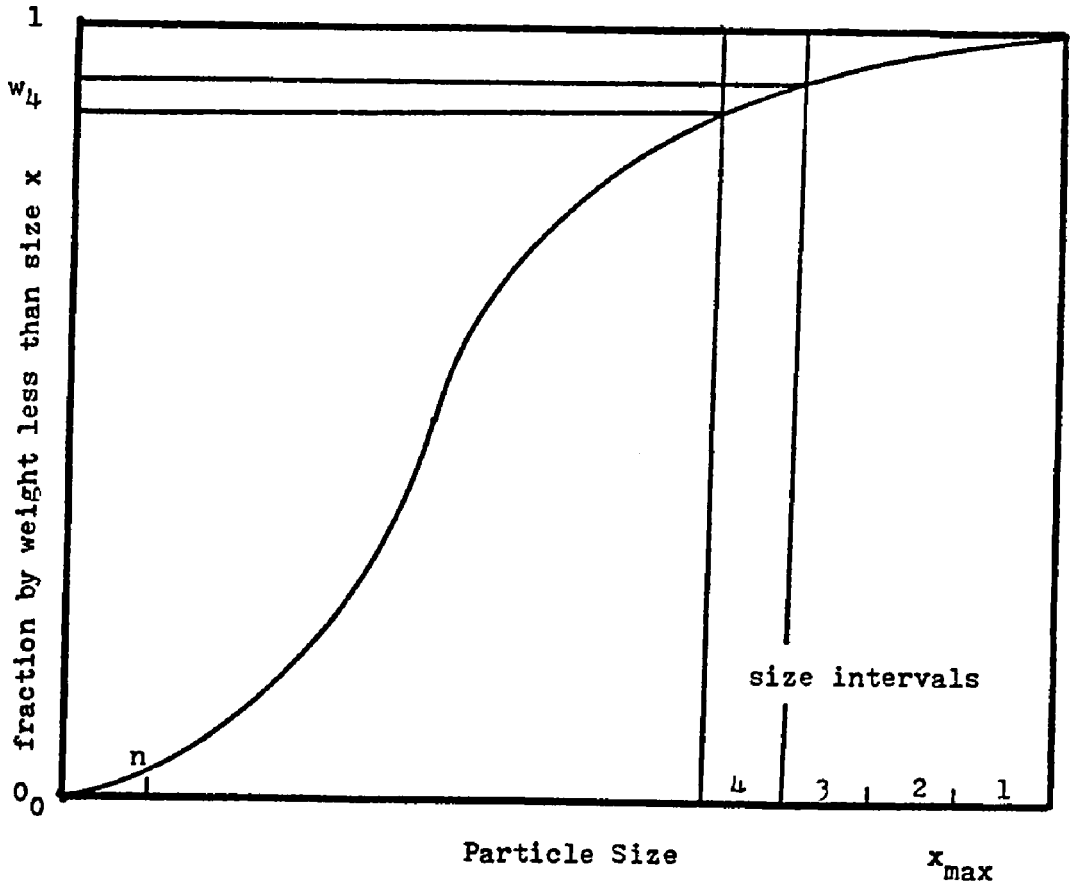

Nomenclature of size-weight distributions

$w_i(t)$ = the amount of material of the i-th size interval present at time t.

It should be noted that Austin's nomenclature and definitions (10) are preserved in this chapter.

The rate of change of the number of particles in the i-th size interval will be the sum of: 1) the rate of loss of particles resulting from grinding particles in that interval, and 2) the rate of gain resulting from grinding larger particles to form particles in the i-th size interval. When considering the rate of <u>formation</u> of i-th sized particles, it is important to note that a particle will, in general, form several smaller particles as a result of fracture. These products of fracture will have a size distribution ranging from the smallest size interval to a size just below that of the original particle. The rate of change of i-th sized particles, therefore, is the sum of the rate of which i-th sized

material is destroyed plus a function of the destruction rates of larger particles. These effects are described by a differential equation for the rate of change in the amount of material in any size interval. This equation is shown in equation 2.

$$dw_i(t)/dt = \sum_{j=1}^{i-1} S_j b_{i,j} w_j(t) \quad -S_i w_i(t) \qquad (2)$$

i 1

where j = $1,2,\ldots,n$

n = the number of intervals

$b_{i,j}$ = the fraction of material in size interval j that forms i-sized particles after breaking.

It is important to note that for the largest particle size the summation vanishes. The resulting differential equation can be solved for these largest particles to obtain an exponential decay shown in equation 3.

$$w_i(t) = w_i(0)e^{-s_i t} \qquad (3)$$

Derivation of a Model os Dispersion for Inks

In ink research, first order-rates of loss of large aggregates have been postulated by Schmitz, Kroker and Pluhar (13), who determined relative tinting strength as a function of dispersion time for several inks, and Zroll (14), who attempted to include the effects of reagglomeration of smaller particles into an empirical model. These German workers, however, appear to be unaware of the prior research on grinding processes done in the United States. Furthermore, they did not postulate a model for the dispersion process or for their observations.

Let us assume that the destruction of the aggregates is caused by collisions of aggregates with other aggregates. Such a mechanism is fundamentally different from the currently accepted "tearing-of-aggregates" model of dispersion presented by Patton (15) and described

by Weisberg (16). Weisberg's description of the dispersion process is reproduced below:

> "Let us examine what forces are available in a high speed disperser which may be counted on for effective dispersion work,... Two kinds of forces are generally claimed for such machine-impact and shear.
>
> It is apparent that not both of these forces can be effective under the same set of conditions. Impact will predominate as a means of momentum transfer where viscosities and solids concentrations are low. This is the "slush grind". Shear stresses of any great magnitude would be difficult to generate in such a system.
>
> At the other end of the spectrum, in a system of high viscosity liquid phase and high concentration of solid phase, high shear stresses could be generated <u>but particle-particles impact would be impeded by the protective viscous layer surrounding each particle and each cluster."</u>
> (emphasis added)

Weisberg pointed out that this theory predicted that pigment loading should not influence the fineness of grind. This theory's prediction is the opposite of what is observed.

An even more serious flaw in the model, however, is its failure to provide a mathema-

tical relationship between dispersion time and aggregate size. According to the "tearing model", all aggregates of a certain size should be destroyed simultaneously once the stress necessary to overcome attractive forces holding aggregates together is achieved. The amount of time the material spends in shear field, therefore, should not significantly influence the fineness of grind. According to the Weisberg theory, differences in the structure of the aggregates, such as are described by Crowl (17), would determine the minimum shear field necessary to destroy an aggregate. Hence, pigment structure would cause dispersion quality of an ink formula to be influenced by the type of equipment used. However, it is difficult, but not impossible, to derive the first-order rate of change in grindometer readings observed in this research and elsewhere (13, 14).

To justify the hypothesis that aggregate-aggregate collisions are responsible for the dispersion of pigments, it is necessary to determine the number of collisions occuring during dispersion. In general, there are two sources of aggregate-aggregate collisions: Brownian motion and the presence of the shear field itself. Let us first consider the number of collisions which are the result of a high shear field. A theory of collisions at high shear rates involving colloidal-sized particles was developed by von Smoluchowski (18), Tourila (19) and Muller (20). The outline of their work given below follows the description by Overbeek (21).

Let us assume that the aggregates can be considered to be spherical in shape. The rate of collisions between an aggregate, i, of radius r_i and aggregates of radius r_j must be calculated. This rate is the number

of aggregates whose centers are found within a "collision volume" of radius $R_{ij} = r_i + r_j$. Therefore, the number of collisions between aggregate i and aggregates of radius j is the number of j-sized aggregates per unit volume times the volume of material swept through the collision volume by a particle in the shear field. Following the nomenclature of Overbeek, this number of collisions is given by equation 4.

$$J = \frac{4}{3} \nu_j (R_{ij})^3 \frac{du}{dz} \qquad (4)$$

where J = the number of collisions between a particle of size r_i and particles of size r_j

ν_j = the number of aggregates of size r_j

R_{ij} = the collision radius = $r_i + r_j$

du/dz = the shear rate in the fluid.

The number of collisions per second for each pigment aggregate in a mill can be estimated by assuming that all the aggregates are the same size, (typically they are between 0.03 and 0.3 Å). Estimates of the shear rate in a roll mill range from 10^{+5} sec^{-1} (22) to 10^{+6} sec^{-1} (23). Assuming a 20% solids loading and a viscosity of 300 poise, the number of shear-induced collisions experienced by each aggregate ranges from 2 to 2,000,000 per second for monodisperse systems. Polydispersity increases the number of aggregates and changes the exact number of collisions but the order of magnitude would remain the same. Clearly, a sufficiently large number of aggregate-aggregate collisions occur in dispersion equipment to influence dispersion properties even if only a small fraction of collisions result in the destruction of an aggregate.

The ratio of shear-induced collisions to collisions caused by Brownian motion is obtainable. From von Smoluchowski's equation (13) this ratio is:

$$J/I = \mu (R_{ij})^3 (du/dz)/(2kT) \qquad (5)$$

where I = the number of collisions due to Brownian motion

μ = the viscosity of medium

k = Boltzman's constant = 1.3805×10^{-16} erg/^{o}K

T = the absolute temperature.

At 300^{o}K (27^{o}C = 81^{o}F, a low milling temperature), this ratio is $9.6 \times 10^{+8}$ to $9.6 \times 10^{+4}$. Brownian motion, therefore, can not cause a significant number of collisions, as Patton and Weisberg correctly assumed.

This work postulates that aggregate-aggregate collision cause the breaking-up of aggregates during milling. It is known, however, that such collision cause flocculation,

the opposite phenomenon. Therefore, in order to justify the assumption, it is necessary to estimate the ratio of the forces involved in shear-induced flocculation and in shear-induced dispersion. For equal-sized aggregates, this ratio is merely the ratio of the stresses involved. The example of shear-induced flocculation given by Overbeek (21) involves flocculation of an As_2S_3 sol with KCl; such an aqueous sol has a viscosity of roughly 50 cps. Agitation with a stirring rod results in a shear rate of, say, 400 sec^{-1}. The resulting stress is approximately 20 dynes/cm. A typical ink with a viscosity of 300 poise being milled at the mill conditions described earlier is subjected to a stress of $3 \times 10^{+7}$ to $3 \times 10^{+8}$ dynes/cm^2. Thus, the stress of aggregate-aggregate collisions in a roll mill is from 1,500,000 up to 15,000,000 times <u>greater</u> than the stresses encountered during floccula-

tion causing collisions. These collisions at high stress therefore, could result in vibrational motions within the aggregates which are sufficient to cause destruction of the aggregates themselves.

These processes can be illustrated by an analogy. Consider a boxcar sitting on a railroad siding. The couplers on the boxcar are open, but require a minimum impact velocity for the coupler to close, because of friction in the coupling mechanism. If another car strikes the boxcar below that velocity, the mechanism will not close, and the cars will not couple (analogous to Brownian motion-induced collisions of pigments in ink in storage). At higher impact velocities, however, the two boxcars will couple (analogous to shear-induced flocculation). However, imagine what happens when the boxcar is struck by a runaway freight going 100 miles per hour (analogous to shear-induced deagglomeration).

Therefore, a model of the dispersion process can be based on the assumptions used to derive equation 4. The number of collisions due to Brownian motion is unimportant because of the value of the ratio determined from equation 5. It is possible to extend equation 4 to determine the number of all collisions experienced by a particle os radius r_i.

$$J = \frac{4}{3} \frac{du}{dz} \sum_{j=1}^{j=n} \nu_j (r_i + r_j)^3 \qquad (6)$$

where J = the total number of collisions between a particular aggregate of radius r_i and all other aggregates.

The total number of aggregates of radius r_i undergoing collisions is therefore:

$$N_i = \nu_i (4/3) \frac{du}{dz} \sum_{j=1}^{j=n} \nu_j (r_i + r_j)^3 \qquad (7)$$

where N_i = the number of aggregates of radius r_i undergoing collisions per unit time.

The current work assumes that the rate of destruction of aggregates of radius r_i is proportional to the collision rate, N_i. N_i is the number of aggregates of radius r_i undergoing collisions, not the number of collisions involving particles of radius r_i. Therefore, each collision between two particles of radius r_i is counted twice (because both particles could disintegrate as a result of the collision). Therefore, the double counting of collisions between aggregates of equivalent size in equation 7 is valid.

The rate of destruction of aggregates of the i-th size interval may now be found to be:

$$dv(d)/dt = v_i \ (4/3) \ \frac{du}{dt} \ \sum_{j=1}^{j=n} v_j (r_i + r_j)^3 f_{i,j} \quad (8)$$

where $dv_i(d)/dt$ = the rate of loss of particles in size interval r_i through destruction of aggregates

$f_{i,j}$ = the probability that a collision between an i-th sized aggregate and a j-th sized one will result in the destruction of the i-th sized aggregate.

Crowl's analysis suggests that the difference in the structures of aggregates cause different particles of radius i to have different probabilities of destruction upon collision. One method of including this observation into the model is to postulate that: 1) a number of aggregates are "unshearable" in the shear field of the mill; and 2) that all the remaining aggregates have identical "destruction probabilities"

$j_{i,j}$. The number of "unshearable aggregates" is assumed to be a function of milling conditions. Therefore, the parameter $f_{i,j}$ is a function of the strength of the shear field. Thus, after including Crowl's observation, the rate of destruction of i-th sized aggregates becomes:

$$\frac{dv_i(t)}{dt} = (v_i - v_i^*)(4/3)\ \frac{du}{dt}$$

$$\sum_{j=1}^{j=n} v_j(r_i + r_j)^3 f_{i,j} \qquad (9)$$

where v_i^* = the number of "unshearable aggregates" for the given milling conditions.

Therefore, following the nomenclature of Austin, the complete equation describing the kinetics of the breaking-up of aggregates in dispersion equipment is given by equation 10:

$$dw_i(t)/dt = \sum_{j=1}^{i-1} S_j b_{i,j}(w_j(t) - w_j^*)$$

$$-S_i(w_i(t) - w_i^*) \qquad (10)$$

where w_i^* = the weight of material in the i-th size interval that cannot be broken down under the given milling conditions.

$w_i(t)$ = the <u>total</u> weight of material (both destructible and indestructible) in the i-th size interval

$$S_i = \frac{4}{3}\frac{du}{dt}\sum_{j=1}^{j=n} v_j(r_j(r_i + r_j)^3 f_{i,j}$$

S_i, = the destruction coefficient for the i-th interval.

It should be noted that this model of the dispersion process does predict qualitatively the relationship between pigment loading and fineness of grind mentioned by Weisberg. The dispersion coefficients, S_i, are functions of the number of aggregates present, ν_j (and hence, of pigment loading).

The rate of change of the number of i-th sized aggregates is the sum of the rate of their destruction (as given by equation 9) and the rate of formation from the destruction of larger aggregates. Of course, the weight of aggregates in the i-th size interval is related to the number of such aggregates assuming spherical aggregates, this relationship is expressed in equation 11.

$$w_i(t) = \nu_i(t)\ d\frac{4}{3}\ r_i^3 \qquad (11)$$

where d = the pigment density.

In order to illustrate the changes in particle size distribution that are predicted by this model, the system of equations described by equation 10 was integrated numerically for five size intervals. The condistions were 1) a shear rate of one million sec -1 and 2) a loading of 20% of pigment by volume equally divided among the five intervals. For purposes of calculation, it is assumed that initially equal volumes of aggregates are found in five size intervals of radii 0.011, 0.0005, 2.5×10^{-4}, 1.25×10^{-4} and 6.25×10^{-5} cm. The probability of collision ($f_{i,j}$) is assumed to be 10^{-7} and it is assumed that upon collision aggregates form eight aggregates of the next smallest size ($b_{i,i-1} = 8$, all other $b_{i,j} = 0$). The results of this integration are shown in the figure 2. Note that aggregate radius has a great influence on the rate of

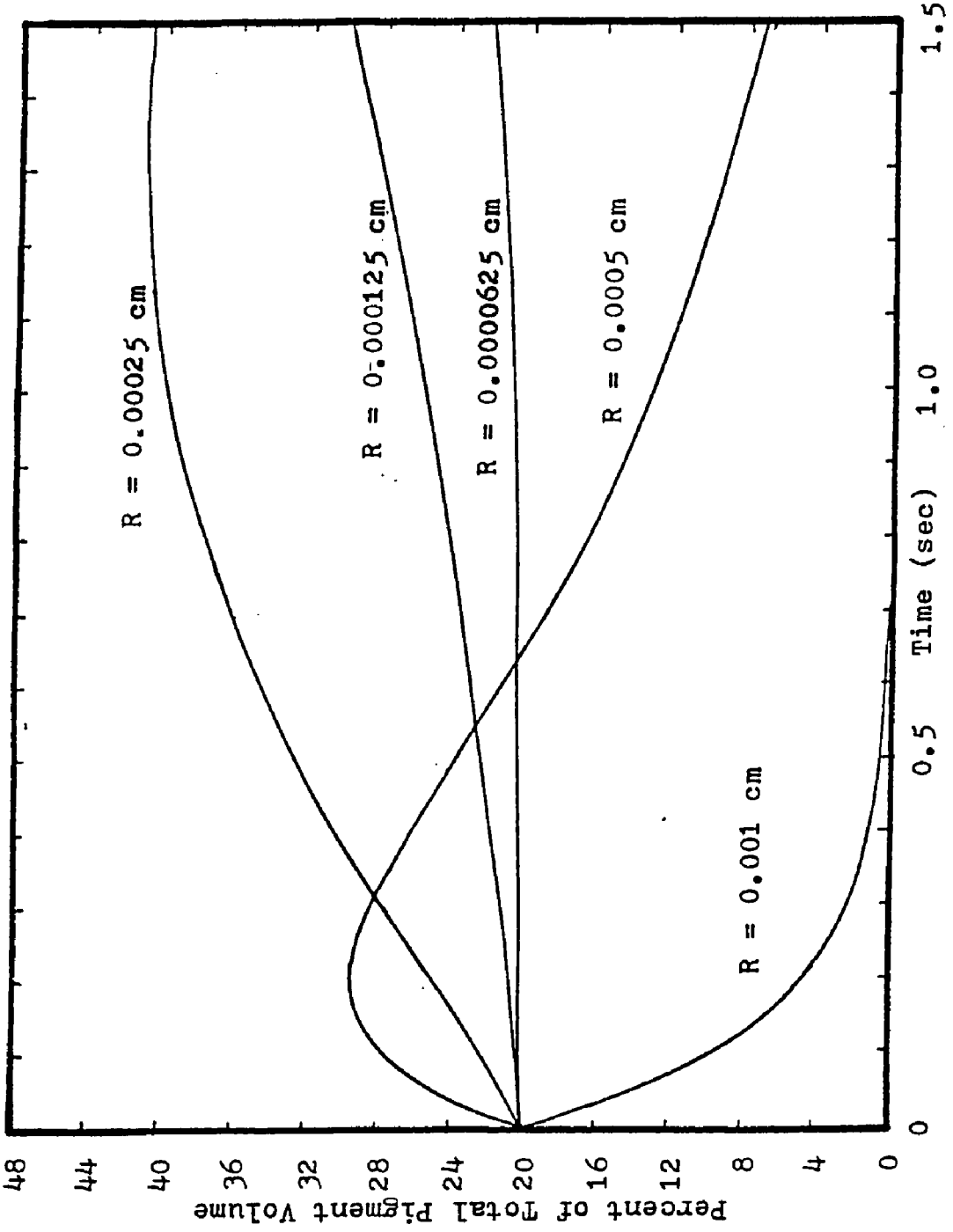

Figure 2 - Sample Calculation Showing the Change in Volume Fraction of Size Intervals As Milling Progresses

change of the percent of total pigment volume in a size interval. Large aggregates, because of their larger collision volume are broken more quickly than smaller aggregates. Note also that it is possible for some aggregate sizes to increase, although this increase is only temporary for all but the smallest aggregates.

For the current work, the rate of loss of the largest particles can be calsulated. For the largest interval, equation 12 yields:

$$w_1(t) = (w_1(0) - w_1^*)\, e^{-S_i t} + w_1^* \qquad (12)$$

Thus, the form of the equation describing the rate of a dispersion process will be similar to equation 3: however, it is theoretically possible to define S_i in terms of the surface properties of the pigment-binder system. Furthermore, equation 12 predicts that some aggregates of the largest size remain after milling for infinite times.

Relationship Between w_1 and the Grindometer Scratch Count

It should be noted that the amount of material in a given size interval is not identical to the familiar scratch count reading obtained from a grindometer (13, 14). The term $w_1(t)$ represents the amount of material of the largest size which is present after a milling time, t. The grindometer reading, on the other hand, represents the diameter (in μm) for which a given amount of material (measured by scratch count) is present. This difference is illustrated in Figure 3. The number of particles of a particular size is plotted as a continuous function of particle size. The area under the curve and bounded by the line labeled l_1 (the lower limit of size of the largest interval) is related to w_1 (more precisely, the area under the curve represents the total number of particles in

Figure 3 - Sample Calculation Showing the Change in Volume Fraction of Size Intervals as Milling Progresses

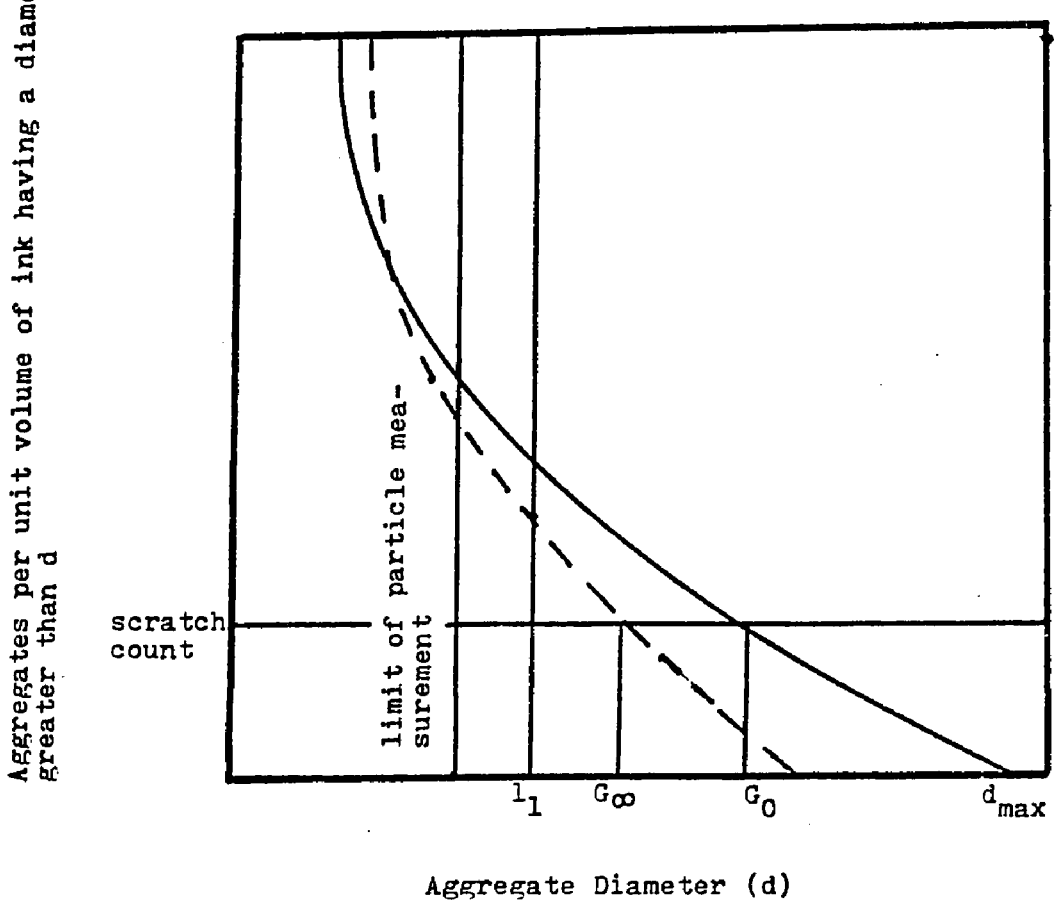

the largest interval and w_1 represents the weight of particles in the largest interval; however, these two terms are related by equation 11. The scratch count, on the other hand, corresponds to the horizontal line labeled scratch count. As the milling proceeds, the particle size distribution shifts from the solid line to the dashed line, causing the grindometer reading to fall from the initial value G_0 to a final value of G_∞ The value of w_1 changes to a final, finite non-zero value, $w_1(\infty)$ which is equivalent to w_1 and is a function of milling condition. Although the grindometer readings and the w_1 term are fundamentally different, it is true that if the term w_1 approaches zero at infinite times, then so must the grindometer reading. Furthermore, it follows that if the grindometer reading does not approach zero, then there must exist particles which are not destroyed under a particular set of milling conditions and G_∞ is not zero.

Thus, even though the previous analysis demonstrates that grindometer readings and w_1 are not identical, it is possible to assume that equation 2 implies that an exponential equation can approximate the relationship between grindometer readings and milling time, or, for a three-roll mill, between grindometer reading and the number of passes through the mill. Indeed, this relationship has been confirmed by experiment. Thus, equation 13 approximates the change in scratch count predicted from equation 12.

$$G_n = (G_0 - G_\infty)e^{-kn} + G_\infty \qquad (13)$$

where G_n = the grindometer reading after the n-th pass

G_0 = the grindometer reading after no passes (to be determined from experiment)

G_∞ = the grindometer reading after an infinite number of passes (to be

determined by experiment)

n = the number of passes

k = the rate constant; the "milling rate" (to be determined experimentally).

Experimental

Materials

Several commercial phthalo blue pigments were received from various manufacturers, as well as a sample of "crude" (i.e. non-pigmentary grade) pigment. These were used in the study and are listed in Appendix B. The dispersibility of the pigments ranged from "easily dispersible" to "difficult to disperse"; however, it is important to note that dry copper phthalocyanine is, in general, harder to disperse than most other pigments (which may account for the failure of earlier studies to observe non-zero values of G_{∞}). The binder was a commercial alkyd resin from

Superior Varnish Corp. (batch 9903). After dispersion, 1/4% of a 6% cobalt blue drier (obtained from Mooney Chemicals) was added to facilitate printing for latter tests.

Preparation of Dispersions

The first set of inks were prepared using a small (1/8 h.p.) Hermes dissolver and a Fritch 2-1/2 x 5-inch three-roll mill. Inks prepared in this equipment were subsequently used in printing tests described in other sections.

Weighed amounts of pigment and varnish were placed into a 500 x 10^{-6} m^3 (500 ml) stainless steel beaker in a 1:4 pigment-binder ratio and then "pre pre-mixed" so that no loose dry pigment would be in the beaker when the actual pre-mixing began. This procedure was followed because large amounts of dry pigment would create a cloud of pigment when the dissolver was turned on, thereby

changing the concentration of the premix, as well as creating a possible health hazard and a clean-up problem.

The impeller on the dissolver was approximately 0.05 m in diameter, and the diameter of the beaker was approximately 0.08 m. The NPIRI Color/Money Committee recommended that the ratio of beaker diameter to impeller diameter be about 2:1. The power for the dissolver and hence the control of the impeller speed was supplied by a Variac. The beaker was placed under the dissolver and the impeller of the dissolver was lowered to the bottom of the beaker, then raised about .0125 m (1/2 inch). Finally, with the Variac setting at 0, the dissolver was turned on. Then, the Variac setting was <u>slowly</u> increased to a setting of 60 (again, in order to prevent the dispersion from leaving the beaker). Increasing the setting beyond 60 caused the formation of an air pocket around the impeller, with

very little mixing. The material was premixed at the setting of 60 for 300 sec. (5 min.). The final temperature was noted.

The ink was then milled on a "2-1/2 x 5-inch" Fritch floating three-roll mill. The dimensions of the rolls are 0.0635 (2-1/2") diameter and 0.127m (5") length. The roll speeds are 1.67 rev/sec (100 rpm), 3.33 rev/sec (200 rpm) and 6.67 rev/sec (400 rpm), the fastest roll being the take-off roll. The mill is water-cooled; exit temperature of the water was controlled at $16^{o}C \pm .5^{o}$. Mill pressure was controlled by varying the compression of springs mounted on the rear of the mill. Uniform, constant mill pressure was achieved by always tightening these springs to the same location. The exact force on the rolls, however, because the spring constants were determined.

In principle, mill operation is simple,

Premixed dispersion is poured into the "bank" of a mill (see Figure 4). The premix is drawn through the "nip" by the two moving rollers that form two sides of the bank. Then, the material passes through a second nip and is removed at the take-off blade. The rolls are forced together by pressure and the nip clearances are maintained by the viscosity of fluid drawn through the nip. Premix is prevented from running out the ends of the bank by wedge plates near the ends of the rollers. These plates are made of either wood or a soft metal (such as brass) in order to prevent damage to the steel rolls. The rolls are hollow and water cooled. Mill temperature, which is critical in ink manufacture, can be regulated by controlling the amount and temperature of cooling water.

In the first dispersions produced in this series, the mill was "run dry" at the end of a

Figure 4 - Flow Pattern in a Floating Roll Mill

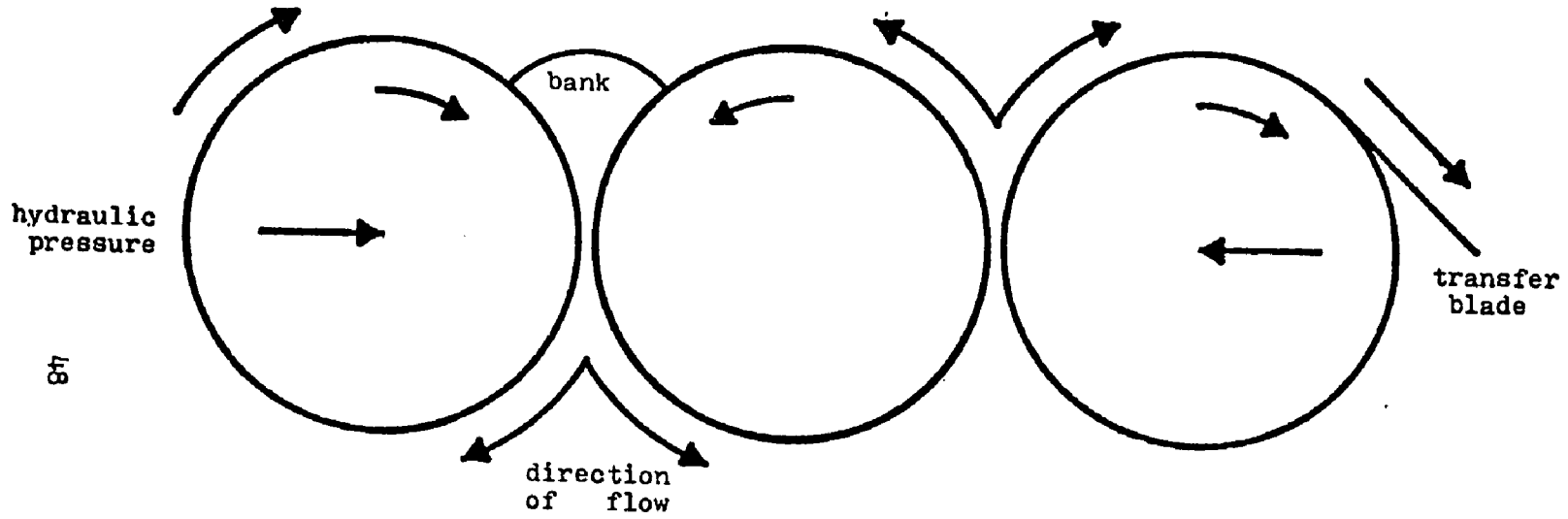

run, that is, the entire amount of ink in the bank was milled. At the suggestion of Dr. A. C. Zettlemoyer, this procedure was changed to allow some premix to remain in the bank at the end of the first pass. It is thought that the ink which remains on the mill as a result of this procedure contains very large aggregates that cannot pass through the nip. However, no noticeable difference in the properties at the finished dispersions could be attributed to this change in procedure.

After milling, the ink was tested by making two grindometer drawdowns following standard procedures and two- and four-scratch readings were made (3,24). In the later batches, the "mottle point" (defined in Chapter 2) was also determined (25). 70^{o} gloss was also measured at 6 points on each drawdown using a Hunter glossmeter. Lastly, about 0.2% by weight of 6% Cobalt blue dryer was

stirred into the ink with a spatula. Successive inks were then made at 3, 5, 10, 25 and 50 passes starting with the single-pass batch.

A second series of inks was prepared using a Hoover Automatic Muller. A muller, which consists of two glass plates, one of which is rotated by an electric motor, was operated as follows: Ink is placed in an annulus of about half the radius of a plate. The two plates are then forced together by weights. The motor is turned on. The number of revolutions of the rotating plate can be controlled. In practice, after 50 revolutions of the plate, the ink has spread to the edges of the plate and must be returned to an area about 5 cm from the center of the plate.

The above process was followed until the desired number of revolutions was reached. At the end of the process, grindometer scratch

count readings and gloss measurements of the ink on the grindometer were determined. Details of the use of grindometer and glossmeters and further analysis of the measurements are provided in the next chapter.

Results

The grindometer readings for dispersions produced on the three-roll mill are shown in Figure 5 and readings for those produced on the muller are shown in Figure 6. The grindometer readings approach a nonzero limit at increased dispersion times. A sophisticated statistical analysis is of dubious value for these data because of the sizable errors associated with the grindometer reading. However, it is evident on visual inspection that at least two of the dispersions produced in the Muller have reached a grindometer limit after about 300 revolutions. The results for the roll mill

Figure 5 - Grindometer Scratch Readings for Inks Prepared on Three-Roll Mill (four-scratch readings)

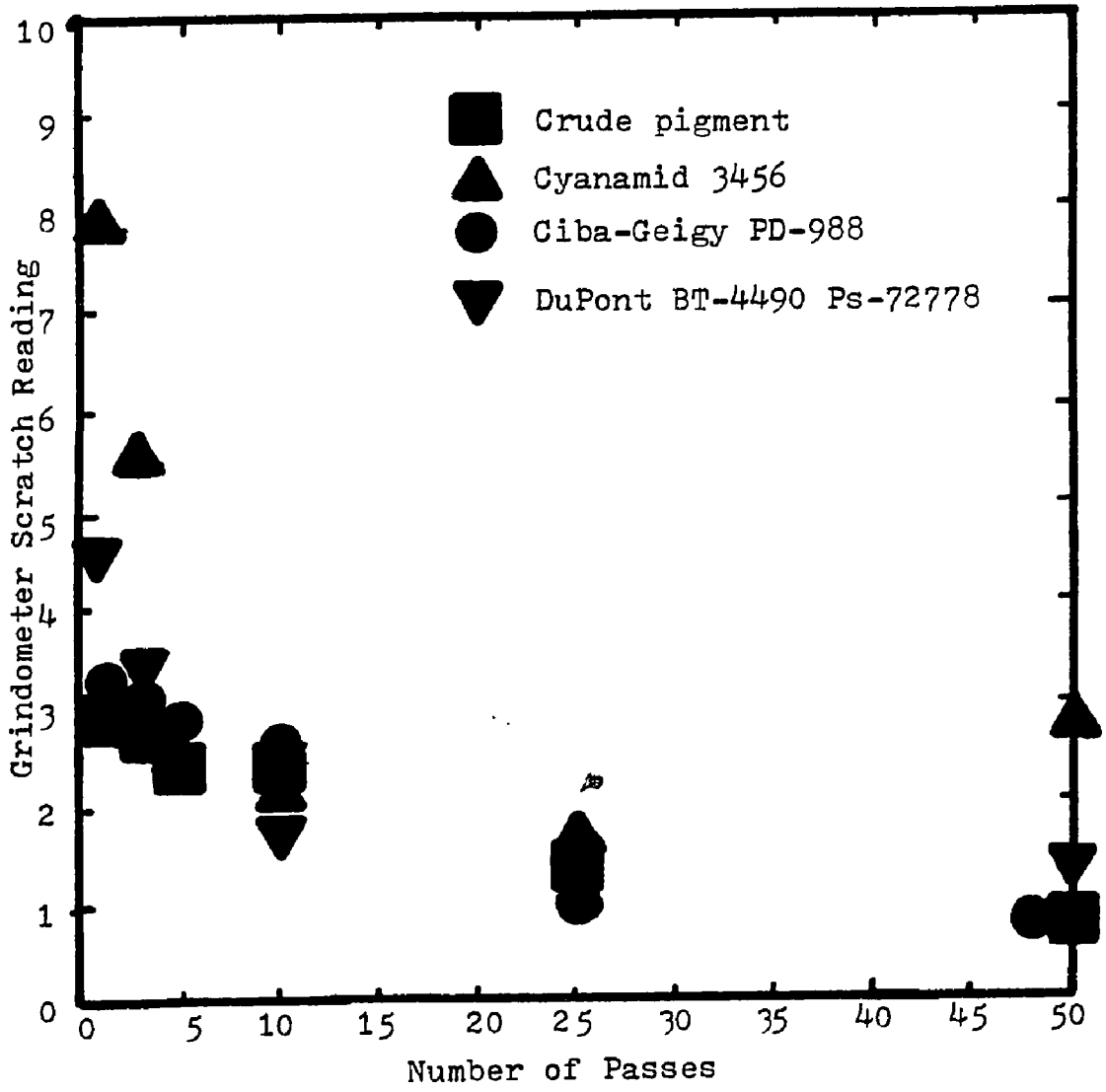

Figure 6 - Grindometer Scratch Readings for Inks Prepared on a Muller

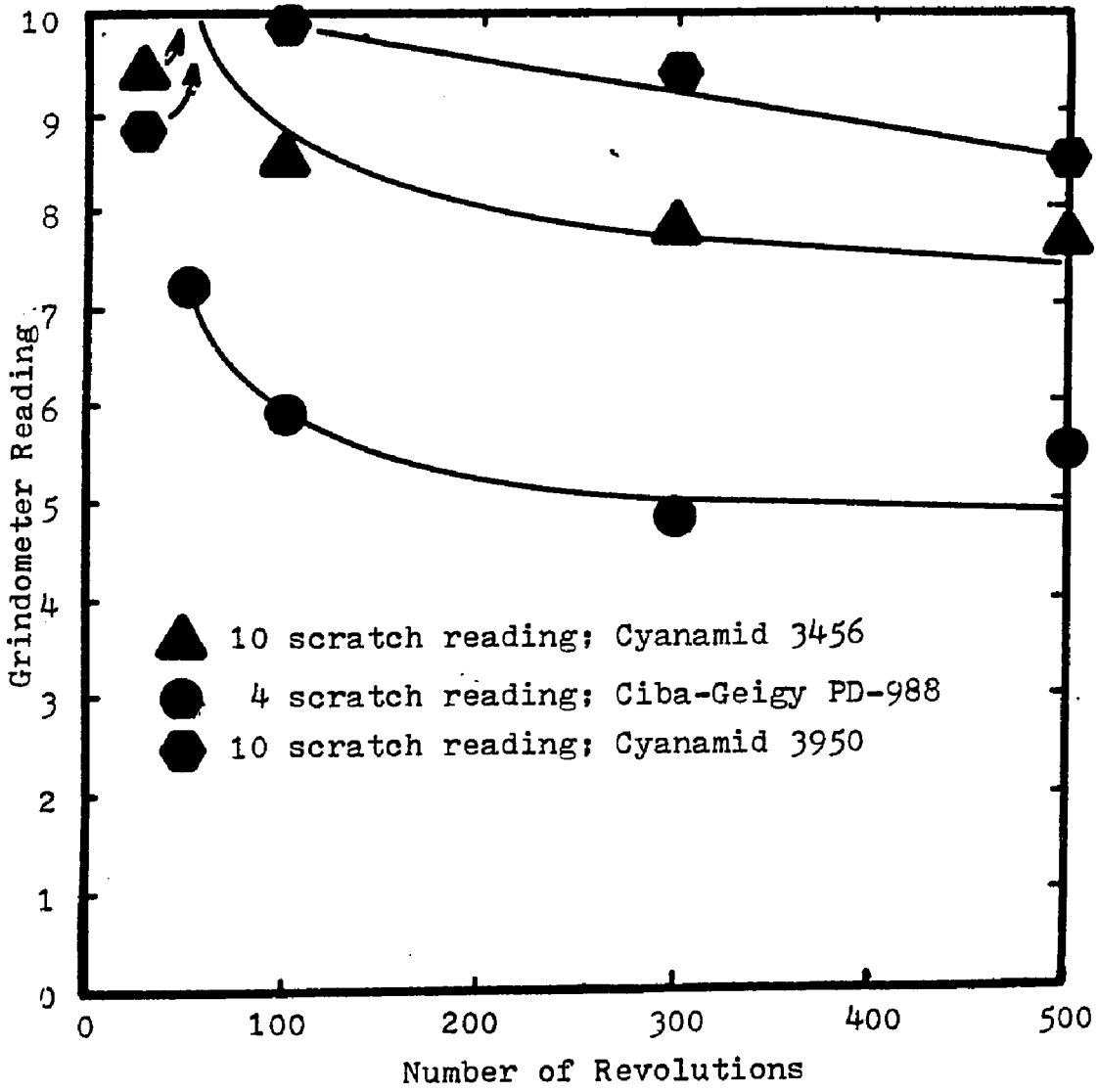

reveal a similar trend. Also,note that the value of the final limit of the grindometer reading depends, in part, upon the dispersion equipment used to make ink as well as the pigment and the binder.

There are several alternative models for dispersion kinetics which might explain the results shown in Figures 5 and 6; however, none appear to describe these observations as well as the rate theory presented in the previous section. It is possible, for instance, that the value of G_{∞} represents large primary particles rather than aggregates. This possibility seems unlikely, however, because the experimental evidence indicates that the final value of G_{∞} is dependent upon the piece of equipment used in preparing the dispersion. Such an observation would be unlikely if G_{∞} represented crystals.

Another suggested theory is that the primary particles may not have time to separate in the roll mill because fluid in roll mills is subjected to high stress for brief periods of time only. Therefore, the limitation on aggregate size is a dynamic constraint that for deagglomeration the primary particles must be separated by some distance greater than that of the surface energy repulsive barrier before the shear stress if removed. According to this explanation, the difference in values of G_{∞} for different pieces of equipment can be accounted for by the difference in residence times in the areas of highest shear. This theory fails, however, because it predicts that the Muller, which continuously shears material at low shear, should produce better dispersions than the roll mill which subjects material to very high shear for very brief periods of time. The experimental

results show the reverse to be true.

Herbst's Experiments

Experiments by Herbst (6) also appear to confirm the presence of unshearable aggregates that cause non-zero values of w_1^*. Herbst measured various ink properties ((1) gloss of prints, (2) depth of shade of inks, and (3) viscosity of inks) at various dispersion times and milling conditions. Part of his results are shown in Figure 7. For a given dispersion, Herbst prepared ink on a three-roll mill at a constant pressure for extended times. The viscosity and depth of shade clearly reach a limiting value. At that point, he increased the mill pressure, making the milling conditions more severe. The gloss of the prints then improved until a new, higher level of gloss was achieved. Mill pressure was then increased and the gloss value increased to a higher limit.

Figure 7a - Influence of Dispersing Conditions for Letter Press Inks on Ink Viscosity (Reproduced from Herbst, Figure 9 in ref. 6)

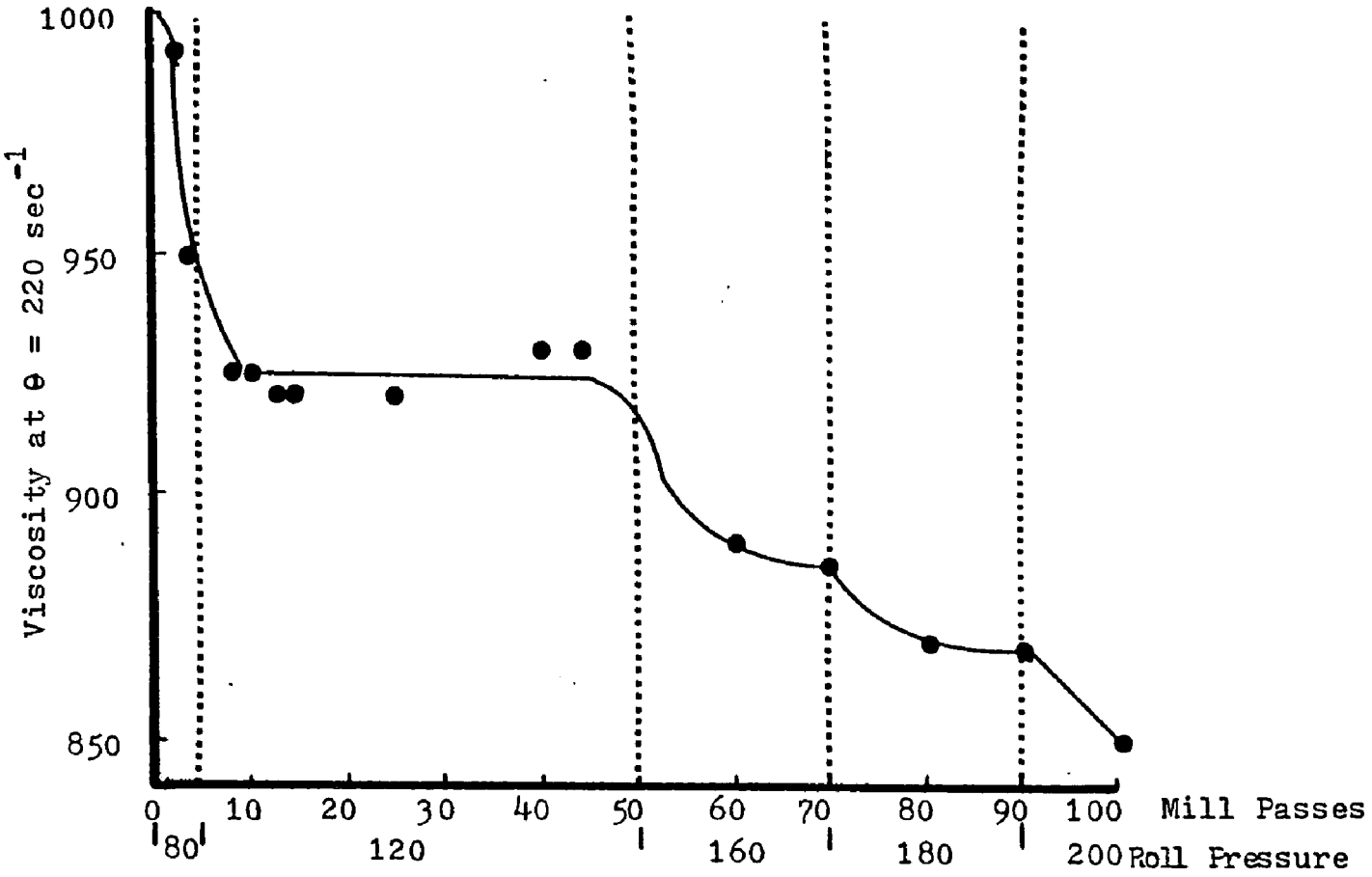

Figure 7b - Influence of Dispersing Conditions for Letter Press Inks on Depth of Shade (Reproduced from Herbst, Figure 9 in ref. 6)

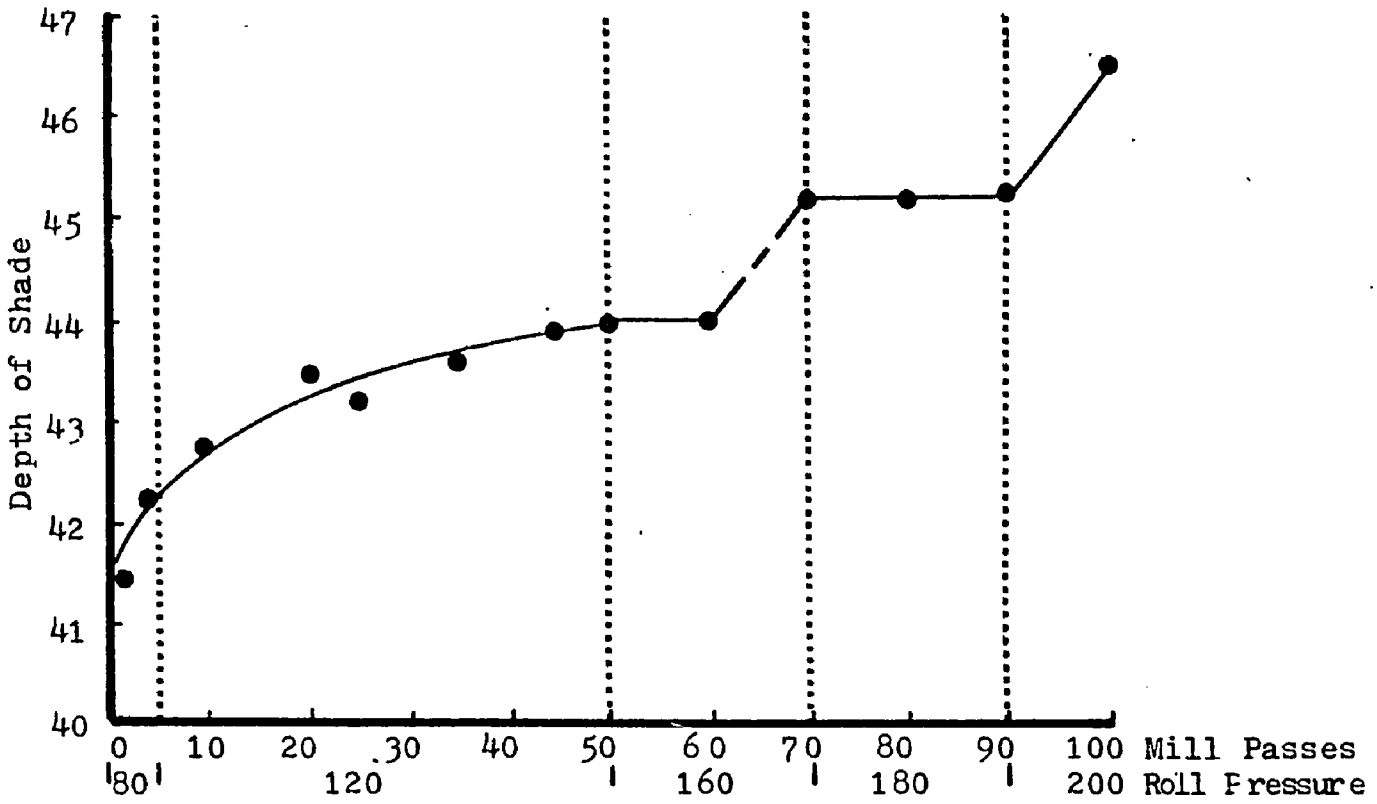

Figure 7c - Influence of the Dispersing Conditions for Letter Press Inks on the Gloss of the Prints
(Reproduced from Herbst Fig. 10 Ref. 6)

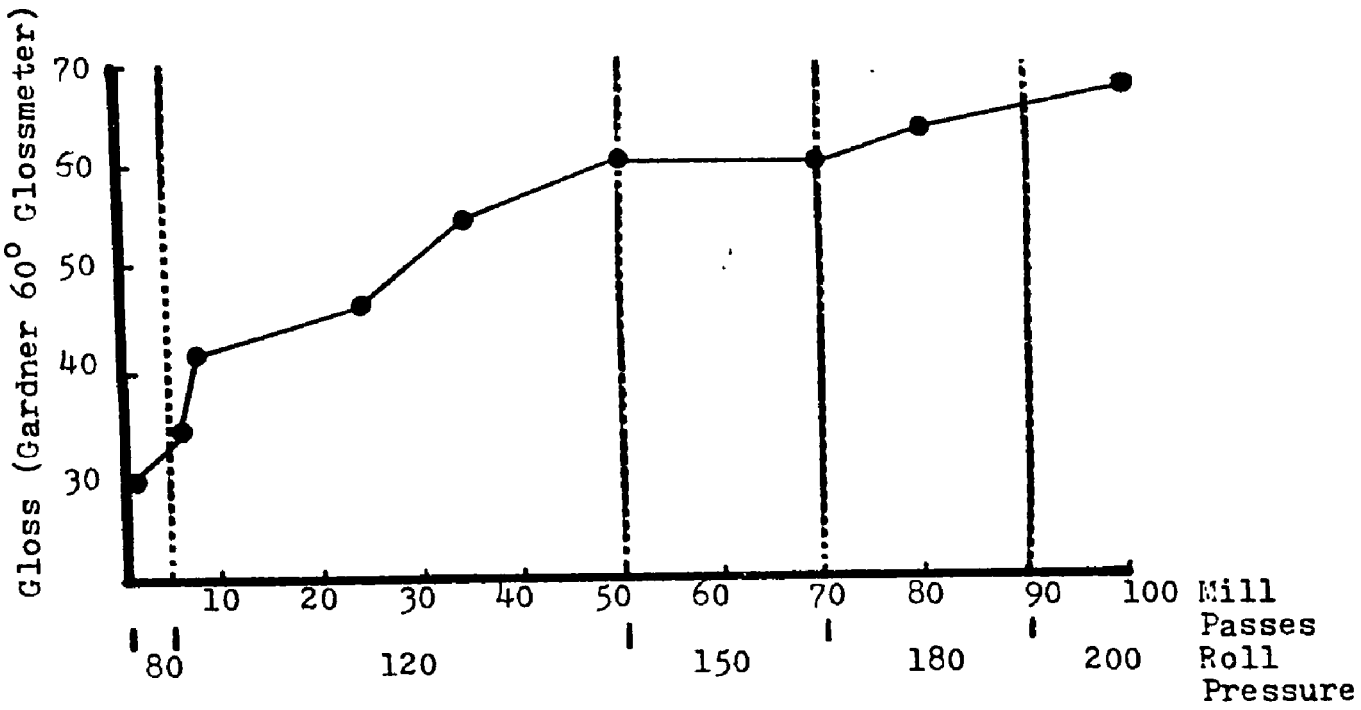

Each increase in mill pressure meant that "harder" aggregates could be destroyed, indicating a value of w_1^*. Once all the aggregates between the old value of w_1^* (associated with the lower pressure) were destroyed, additional milling proved fruitless. Therefore, Herbst's measurements appear to confirm that there exists a broad range of critical stresses necessary to destroy equal-sized aggregates.

Conclusion

The kinetic model of the dispersion process predicts that the final degree of dispersion depends on pigment and binder properties and also the shear rate. This rate determines the maximum stress achieved in the milling operation thereby affecting G_∞. This prediction differs from the model of Schmitz (13) in which all particles are assumed breakable. According to his model, the ultimate grindometer reading (G_∞) is

zero. The model can serve as the basis for analyses of grindometer readings.

Unlike grinding, in which the properties of the material tend to be uniform for a given size, dispersion involves material with a wide range of strength characteristics. Dispersion conditions influence both the rate at which large aggregates are destroyed and also the number of large aggregates which can be destroyed. Therefore, the importance of maintaining proper milling conditions cannot be overemphasized. Further, the disappearance of the largest aggregates does not imply that the "ultimate dispersion" has been achieved with the given equipment; material which is capable of being broken up can remain in intermediate size intervals. In conclusion, the collision model of dispersion which has been presented and confirmed by

experiments can be used to ezplain a) the differences among types of dispersion equipment, and b) the effect of increased milling time.

CHAPTER 2

Using the Gloss of Wet Grindometer Drawdowns to Measure the Degree of Dispersion

Introduction and Background

Currently, there are two accepted ways of analyzing grindometer drawdowns: 1) the scratch count method recommended by NPIRI Test Methods (26), and ASTM (27); and 2) the mottle point method recommended by DIN (22) and an alternate ASTM procedure (23). The work presented in this chapter indicates that the gloss of wet grindometer drawdowns may be used as another means of determining the fineness of grind. The advantages of using gloss are the rapidity, simplicity and reproducibility of the method.

The measurement of fineness-of-grind degree of dispersion is of great importance to the ink, paint and coatings industries because this property of the final dispersion

greatly influences the effectiveness of the finished product. Therefore, quick and accurate measurement of dispersion "quality" is an important goal in this field of research. However, since the initial work in the late 40's and early 50's which developed grind gages, (3, 29-32) little has been reported on new methods of using this tool to measure dispersion "quality", yet work is often reported in which grindometers have been used as measurement tools.

The NPIRI Production Gridometer is a machined block of metal with twin drawdown paths (see Figure 8). The depth of each path decreases uniformly from a maximum of 25×10^{-5} m (1 mil) at the "10" tick mark to a depth of zero at the zero tick. Tick marks at the side of the path indicate the depth at that point. A drawdown is made by placing an amount of ink at the

Figure 8
NPIRI Production Grindometer Showing
Methods of Reading Grindometers

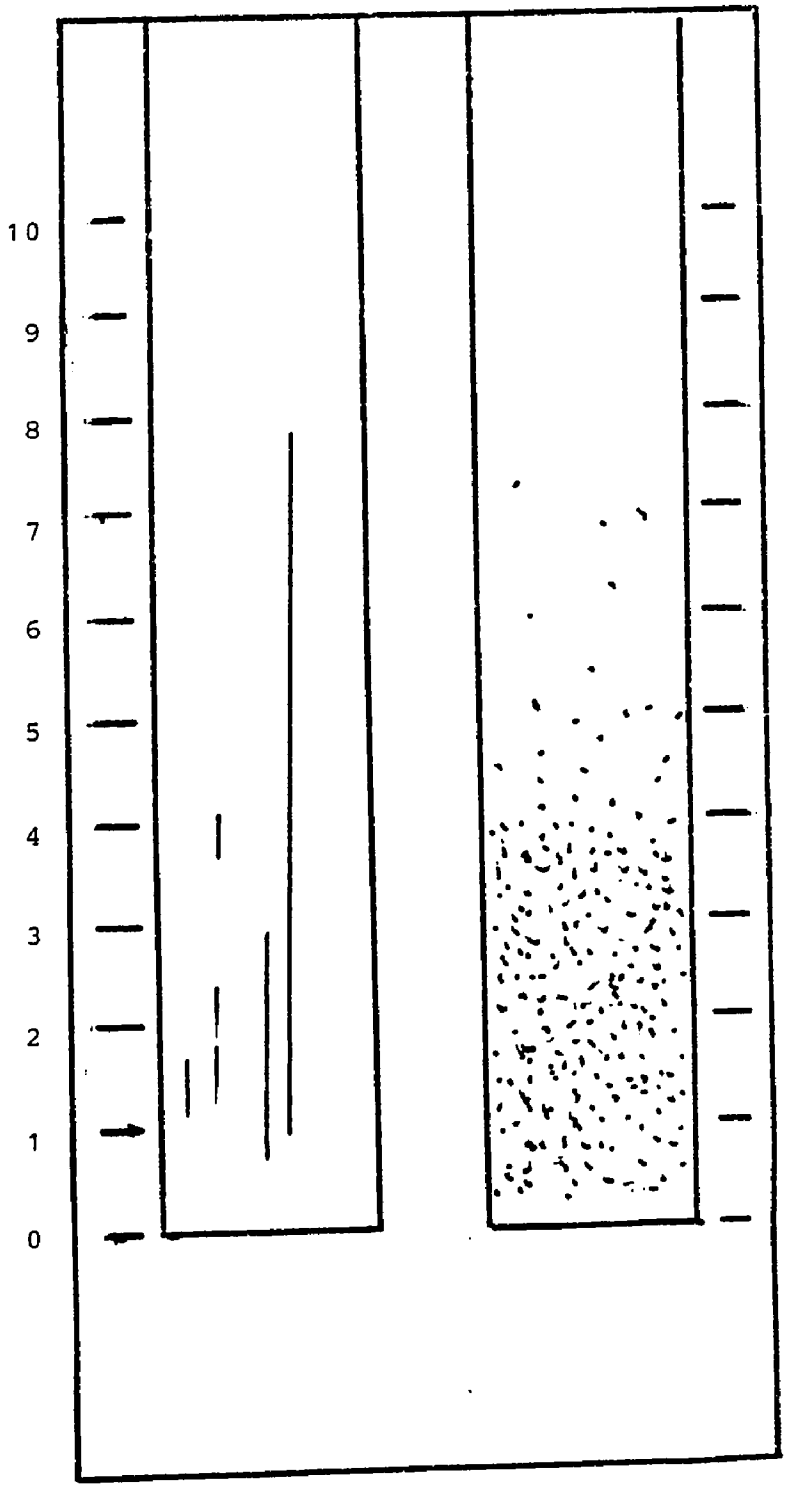

deep end of each trough. Holding the drawdown knife vertical and behind the ink, an operator slowly draws the blade (and the ink) down the path (and toward him). The surface of the remaining ink in the trough can then be examined for fineness-of-grind measurements.

Although the method of making drawdowns is standard, the dimensions of the grind gage and the techniquies of analyzing the ink in the trough do vary. As has already been mentioned, NPIRI and ASTM recommend counting the number of scratches formed by aggregates trapped between the drawdown blade and the path. The depth of the path where N scratches occur is the N-scratch grindometer reading. Therefore, the first path in Figure 8 would have a two-scratch reading of 4 and a four-scratch reading of 2.5 corresponding to path depths of 1.02×10^{-5} m (0.5 mil) and 0.635×10^{-5} m (0.25 mil) respectively (it is recommended that scratch readings be taken

for four and ten scratches). Mottle, which is caused by smaller aggregates that disrupt the smooth surface of the ink, increases as the path depth decreases. DIN and others (25, 29) define the "mottle point" as the depth of the grindometer path at which the mottle becomes pronounced. The second path in Figure 8 has a mottle point of about 5. Corresponding to a path depth of 1.27×10^{-5} m (0.5 mil). Of course, in practice, mottle and scratches occur together, rather than as shown in the figure. The mottle reading, furthermore, is highly subjective. There is no marked change in the amount of mottle present at various depths, but rather a gradual increase in mottle occurs over the length of the grindometer path.

Procedure

Measurements were made on wet drawdowns made on a NPIRI Production Grindometer using an Adco Scraper. For each ink tested, two separate drawdowns were made on the same gage. The gage was cleaned with solvent between readings. Four- and ten-scratch readings were made for each path, along with gloss measurements at the three, five and seven tick marks corresponding to path depths of 0.762×10^{-5} m (0.3 mil), 1.27×10^{-5} m (0.5 mil) and 1.78×10^{-5} m (0.7 mil). In general, inks made on the Hoover Automatic Muller had four-scratch readings greater than ten and the inks produced on the mill did not have a ten-scratch reading so that only one of the two readings was made for each ink. Gloss measurements were made using a Gardner Multi-Angle Glossmeter and later using a Hunter 75^{o} Gloss-

meter (the change in equipment was forced by the mechanical failure of the first instrument). The average of the four four-scratch readings and the average of gloss readings at all three depths were computed. The gloss of an ink was based upon the average of all twelve gloss readings.

Results

Plots of gloss versus dispersion time for the inks described in Chapter 1 are shown in Figures 9 and 10. The overall gloss measurement of wet drawdowns increases with increasing dispersion times for this series of copper phthalocyanine-based pigmented dispersions. This result indicates that the number of aggregates causing loss of gloss was reduced as dispersion proceeded.

Unusual results were achieved when crude (non-pigmentary grade) copper

Figure 9 - Influence of the Number of Mill Passes on the Gloss of Wet Grindometer Drawdowns of Dispersions Made From Three Commercial Copper Phthalocyanine Pigments

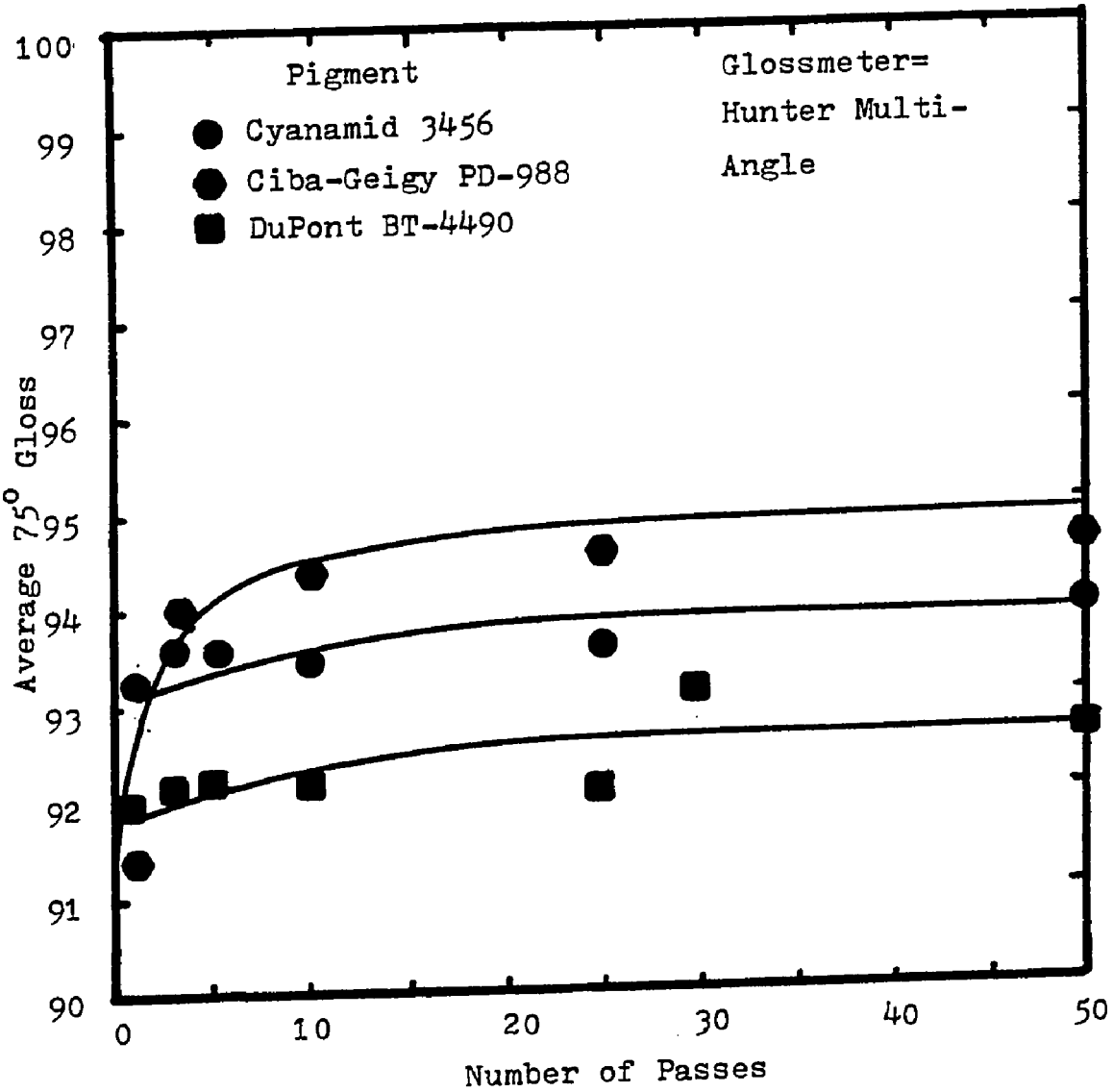

Figure 10- Influence of Muller Revolutions on the Gloss of Wet Grindometer Drawdowns of Three Dispersions Made from Commercial Copper Phthalocyanine Pigments

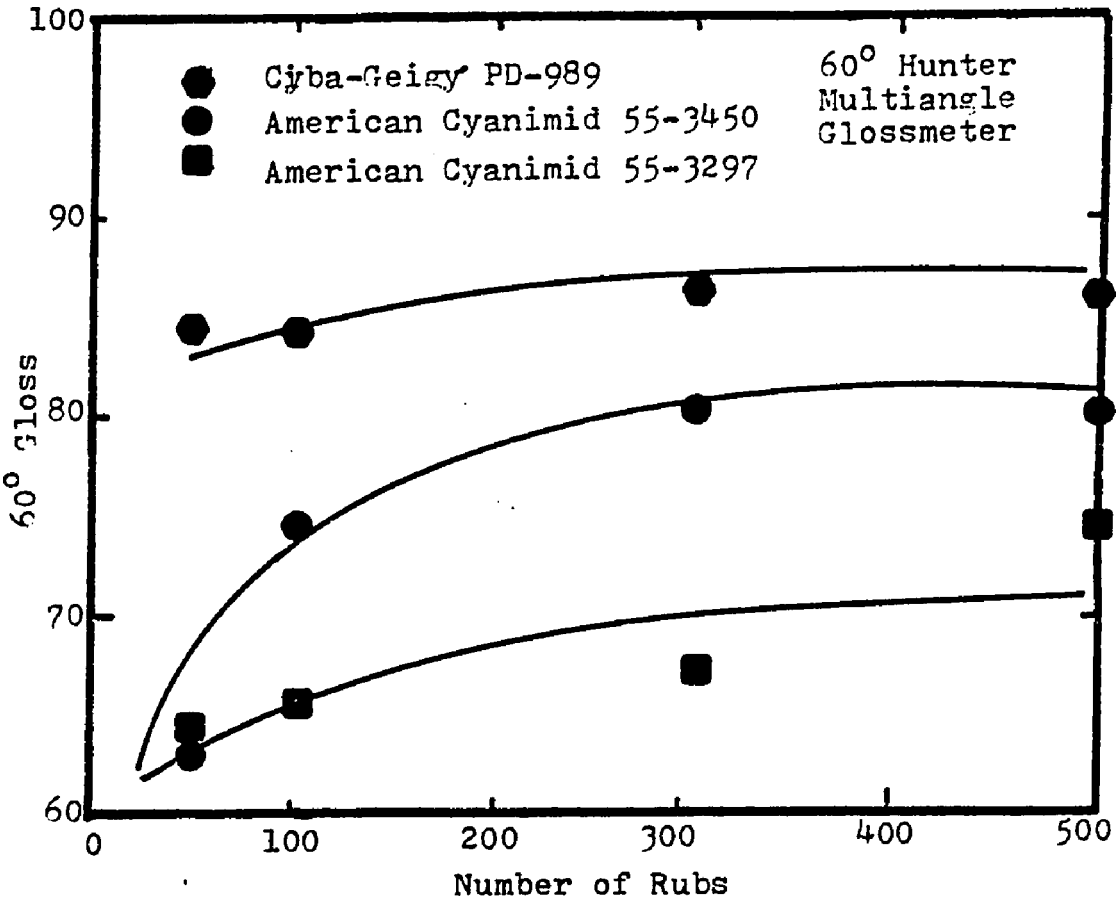

phthalocyanine was dispersed in the alkyd varnish using the three-roll mill. As can be seen from the graph (Figure 11), gloss actually declined as dispersion time increased. This result must be interpreted in light of the extremely weak tinting strength of the poorly milled dispersions. After short milling times, the ink was too weak to hide the metal underneath it. After longer milling times, the ink became stronger, and, consequently, the color of the path became darker. Therefore, the apparent gloss decreased at longer milling times for this pigmented dispersion.

Indication that the gloss-reducing aggregates are of different size than those aggregates which cause scratches is that gloss measurements made on dispersions of different pigments did not correlate with grindometer readings (Figure 12). Plotted

Figure 11 - Influence of the Number of Mill Passes on the Gloss of Drawdowns of "Crude" (non-pigmentary) Copper Phthalocyanine Dispersions

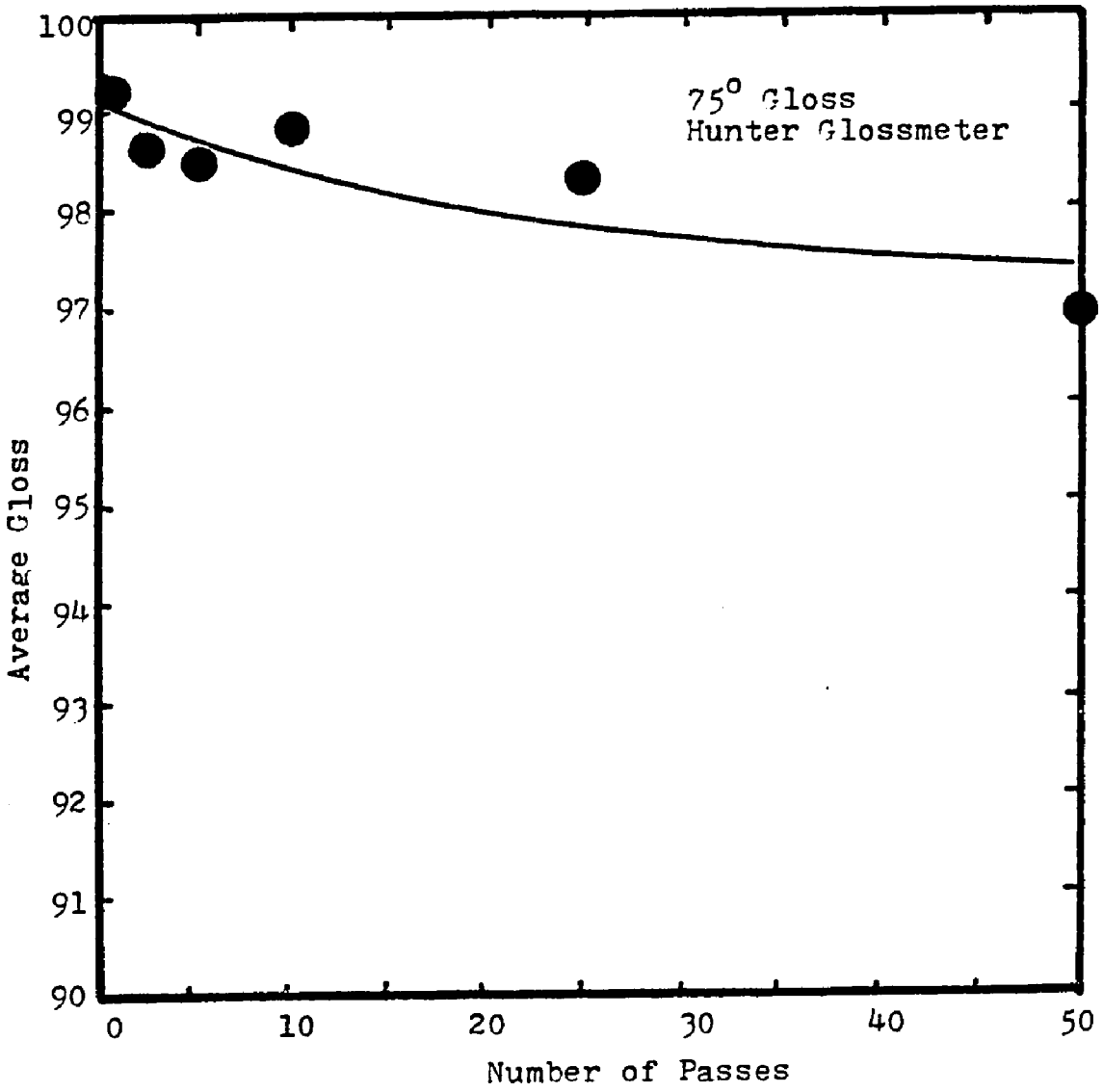

Figure 12 - Lack of Correlation Between Grindometer Wet Gloss and Grindometer Scratch Reading for Dispersions of Commercial Pigments

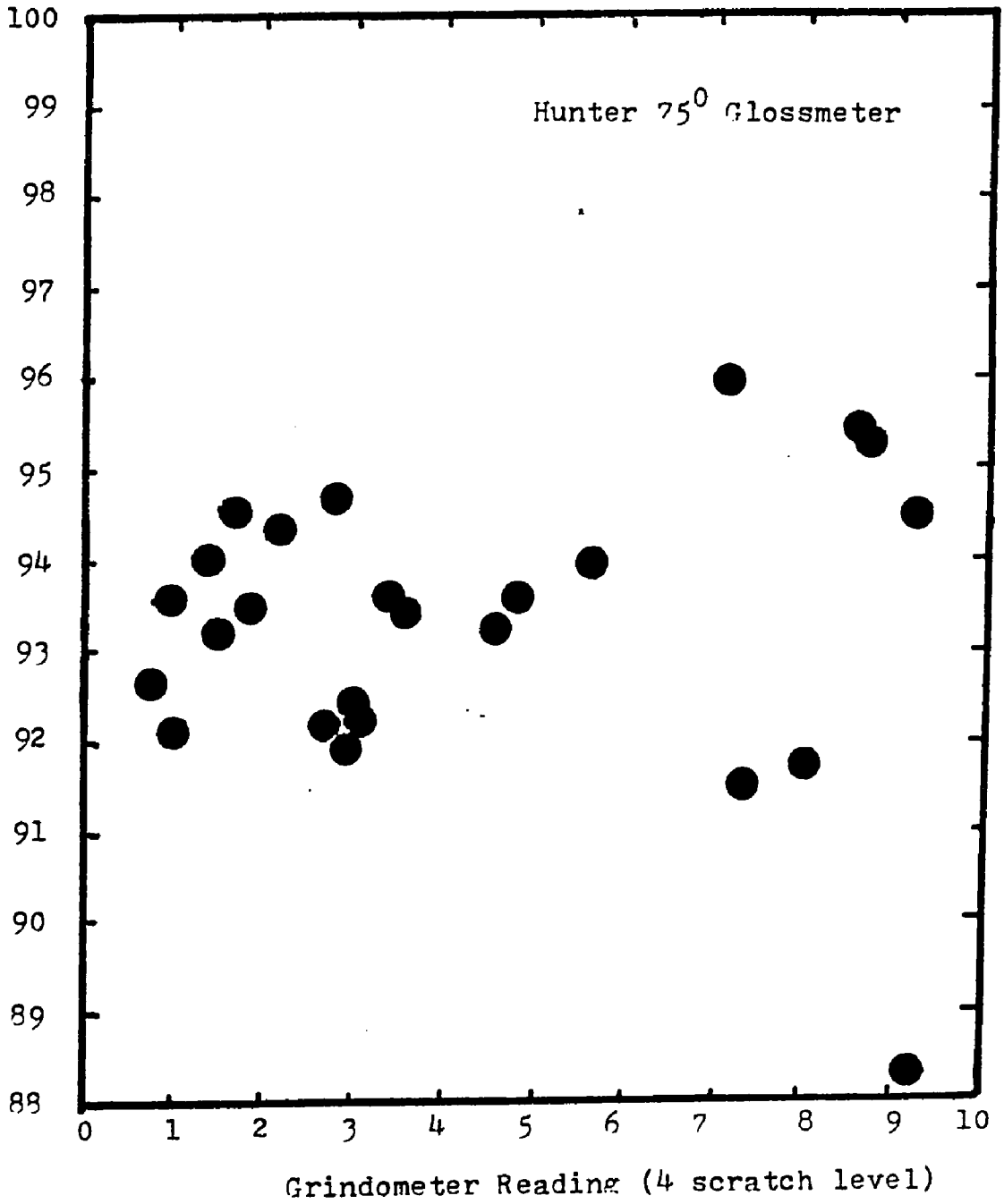

in Figure 12 are the scratch readings and overall gloss readings for several dispersions. As can be seen from the figure, there exists very little relationship between the two measurements, indicating that, the number of very large (scratch-causing) aggregates is not necessarily related to the number of smaller (gloss-reducing) aggregates. This result should not be surprising because the original aggregate size distributions were probably not identical. Using the terminology adopted in Chapter 1, the scratch-causing aggregates must be considered as a different size interval from the gloss-reducing aggregates.

Forty gloss measurements of inks made with different pigments and the same binder milled from 1 to 50 passes were subjected to student's t test (33). These measurements are shown in Appendix A. Anal-

ysis of the differences between an ink's gloss at the grindometer levels indicated that there was no statistically meaningful difference between the 5 and 7 grindometer level gloss readings; however, the gloss at the 3 level averaged 0.7% higher than the other readings, as shown in Table 1. This difference was significant at the 99% level. It is believed that, at this thinner path thickness, the films were not sufficiently thick to completely hide glossy metal at the bottom of the path.

TABLE 1

Student's Values for Gloss Measurements of Drawdowns of 40 Dispersions

Testing the Significance of the Differences Between Gloss Levels	t	t Need for Significance
3 and 5	7.16	±2.02
3 and 7	4.54	±2.02
5 and 7	.22	±2.02

The gloss measurements further confirm the presence of hard-to-disperse aggregates that were postulated in the previous chapter and whose presence was indicated by grindometer scratch readings. The difference in final values of gloss of the inks made from commercial pigments provides this confirmation. If there were no hard-to-disperse aggregates, then the amount of gloss-reducing aggregates would approach the same value (zero) for all commercial pigments, and the final gloss at long dispersion times would

approach the same value (zero) for all commercial pigments, and the final gloss at long dispersion times would approach a value corresponding to the complete absence of aggregates and dependent only on the vehicle's gloss.

Influence of Mill Temperature on Gloss

As can be seen from the experimental results (Figures 13a, 13b and 14), increasing the milling temperature improved the dispersibility of pigments, confirming the earlier results of Herbst (7). (Mill temperature can be controlled by controlling the temperature of the cooling water).

This result is especially marked for crude copper phthalocyanine dispersions (Figure 14). Mill temperature increases cause decreases in the rate of loss of gloss and the final gloss value. For this dispersion lower gloss readings are indicative of better

Figure 13 a - Influence of Mill Temperature On The Gloss of Drawdowns of Commercial Pigments After One Pass Through a 3 Roll Mill

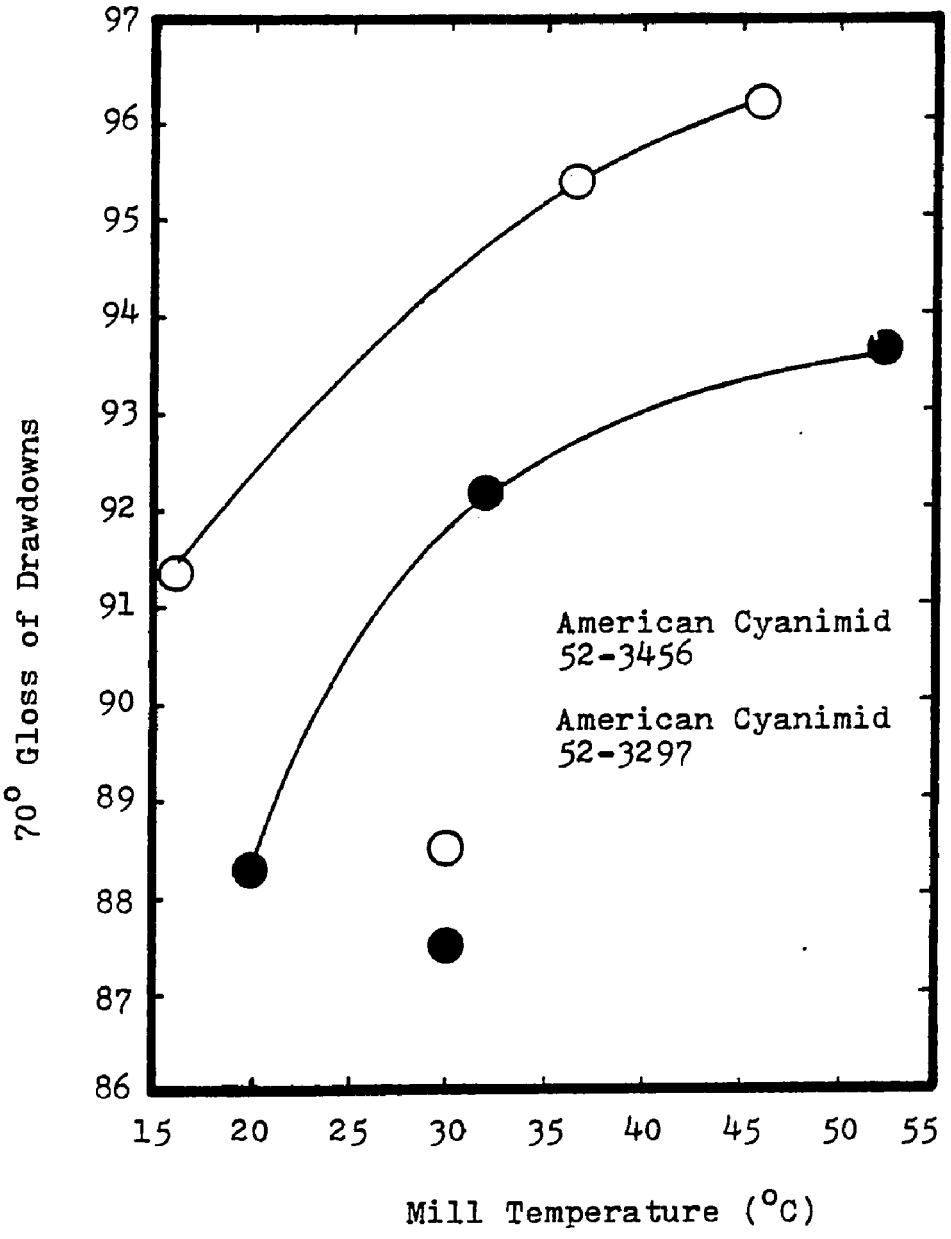

Figure 13-b - Influence of the Number of Mill Passes on the 70° Gloss of Drawdowns of Dispersions Prepared from Commercial Pigments

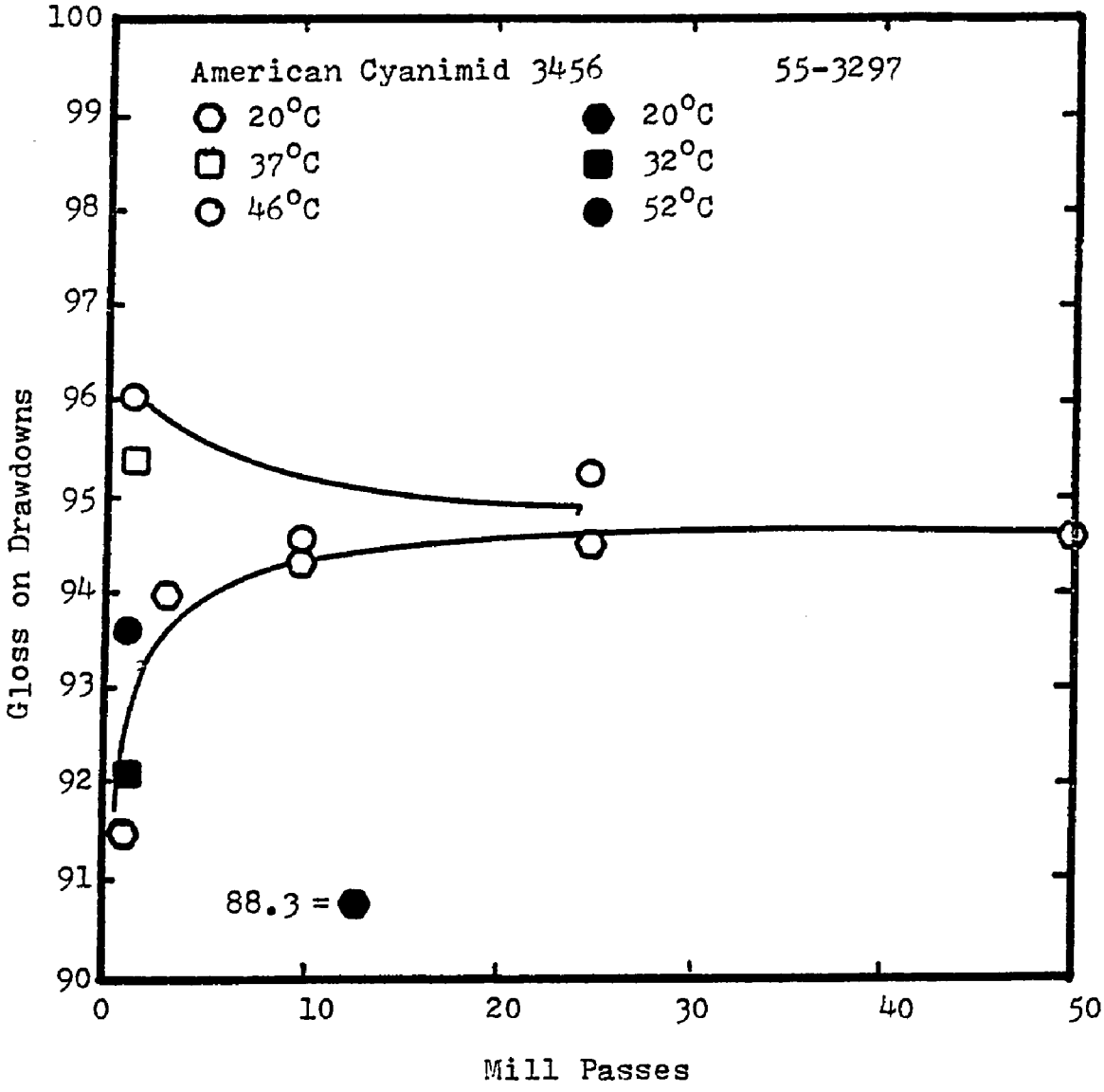

Figure 14 - Influence of Mill Temperature on the Gloss of Dispersions of Crude (non-pigmentary) Copper Phthalocyanine

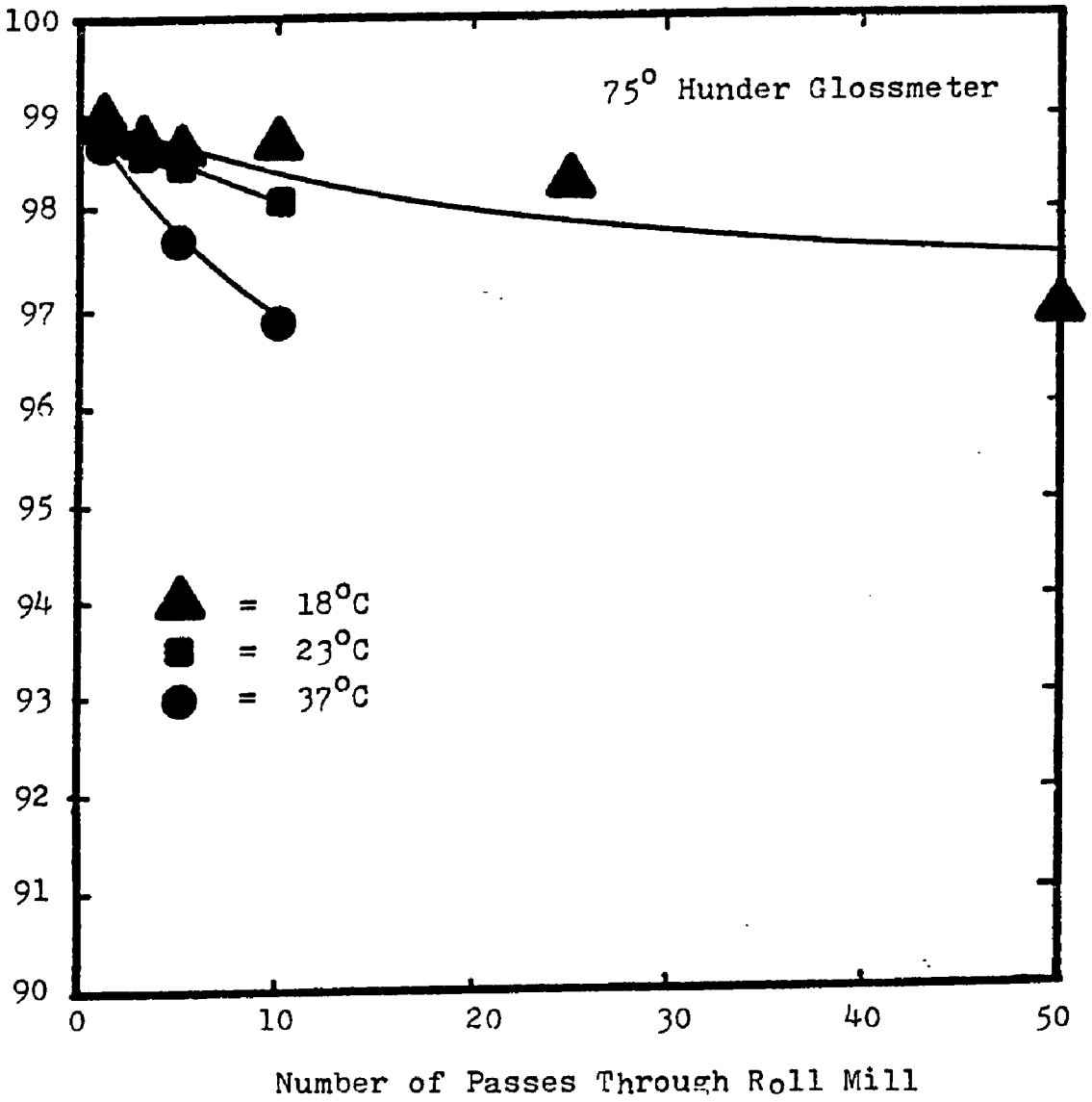

dispersions. For dispersions prepared from commercial pigments, the relationship is less clear. After one pass, the glosses of both pigments tested clearly increases at increasing temperature. However, the gloss of dispersions milled at 46°C reveal a slight loss, or possibly pass through a minimum gloss value. This result can be explained as the combination of an increase in hiding power (as with the crude dispersions) at better pigment qualities and an increase in gloss itself. This result as well as the gloss of the "crude" dispersion indicates that gloss readings must be interpreted with care and comparisons between dispersions must also include a measure of the inks' color strength.

Mill temperature affects two factors that influence gloss. As the mill temperature increases, the viscosity decreases

(which tends to give poorer dispersions) and the surface energy decreases (which tends to give better dispersions). One possible explanation for the overriding importance of the surface effect (which works to improve dispersibility at higher temperatures by lowering the energy barrier) over the viscous effect (which works to improve dispersibility at lower temperatures by increasing viscosity) lies in the nature of the floating roll mill used both in this study and in Herbst's. Mill pressure is balanced by the forces generated as the dispersion passes through the nip (22). As viscosity drops, the gap is reduced until the forces are again in balance. The reduction in the size of the mill gap causes somewhat higher stresses to be encountered, than would be found if the gap did not change, thereby, partially compensating for the loss in viscosity.

Recommended Procedure for Determining Gloss of Wet Grindometer Drawdowns

Based upon the work presented here, the following procedure is recommended for obtaining gloss measurements:

1. Prepare a grindometer drawdown in the usual manner using a NPIRI Production grindometer.
2. Measure the gloss in both paths at least two depths greater than 3.
3. Repeat steps one and two at least once for each dispersion and average the gloss readings. Report the average.

It should be noted that these experiments were performed on inks prepared with the same vehicle. Care should be taken when interpreting gloss measurements of inks prepared from different vehicles or with markedly different color strengths.

Conclusion

Measurement of the wet grindometer

drawdowns if a valid technique of obtaining fast measurements which can be related to the number of aggregates too small to be detected by scratch count methods. Analysis of gloss measurements indicates, however, that the amount of material present in the form of such aggregates need not be related to the number of larger (scratch-causing) aggregates.

Gloss measurements, furthermore, have been related to dispersion times and mill temperature confirming both earlier work and the usefulness of the measurement of gloss of grindometer drawdowns. Gloss measurements, however, have been shown to be influenced by color strength in at least one case. Therefore, care should be taken when comparing wet gloss measurements of inks having different color strengths.

PART II

Modification of the Walker-Fetsko Ink Transfer Equation

ABSTRACT

Dispersions made during the experimental work described in Part I were printed using a Fogra Printability Tester. Analysis of the transfer properties of these inks indicated that modifying of the Walker-Fetsko transfer equation would provide a closer approximation of the experimental data. The modified equation more accurately represents the influence of surface roughness on transfer than does the original.

The values of the transfer coefficients obtained using the modified Walker-Fetsko equation were used to examine the potential influence of milling time (and hence degree of dispersion) on ink transfer and were also used in the colorimetric analysis discussed in Part III.

Introduction

Because printers desire to have the minimum amount of ink on their press rolls, the transfer properties of ink to a substrate are of great importance to them and the ink makers who supply them. Clearly, the fraction of ink transferred to the stock is a function of factors other than the properties of the ink alone. Specifically, the substrate's properties (i.e., its roughness, moisture content, coating, and surface properties) and the press conditions (especially the press speed and pressure) can influence the printability of the ink. Obviously, these properties must be held constant in order to determine the effects of ink properties on printability. Furthermore, printability studies require an accurate model of the transfer of ink from the printing surface to the substrate. The purpose of this section is to discuss an

improved transfer equation and to use it to analyze the influence of milling time (and hence, degree of dispersion) on ink transfer.

A general model of ink transfer was proposed by Walker and Fetsko (34) in 1955, and since then has been used extensively in the investigation of inks and coatings (35, 36, 37). Use of this equation requires the determination of the weight of ink per unit area transferred to the substrate and the amount of ink on the printing cylinder before printing.

These values are easily obtained when using a proof press such as the FOGRA printability tester. The Walker-Fetsko equation assumes that the relationship between these two values can be completely described by three parameters, k, a function of the coverage of the ink on the paper, b, a function

of the instantaneous penetration of ink into the substrate, and f, the fraction of ink uneffected by penetration which is transferred to the substrate.

Classical Derivation of the Walker-Fetsko Equation

The derivation of the Walker-Fetsko equation, assumes that only a fraction of the substrate actually contacts the ink. This partial contact arises because of the roughness of the stock and is assumed to vary with the amount of ink on the printing surface following an exponential relationship.

$$F = (1 - e^{-kx}) \tag{14}$$

where F = the fraction of the ink in contact with the stock

x = the weight of ink on the printing surface

k = the Walker-Fetsko coverage parameter.

Next, it is assumed that the relationship between the amount of ink on the printing cylinder and the amount of ink which penetrates the stock can be described by an exponential function:

$$p = (1 - e^{-kx})\, b(1 - e^{-x/b}) \qquad (15)$$

where p = the amount of ink instantaneously immobilized during printing

b = the immobilization capacity of the stock.

Walker and Fetsko found that equation 15 adequately fitted experimental data.

Lastly, the difference between the amount of ink originally on the cylinder and contacting the stock ($x-b(1 - e^{-kx})$) and the amount of ink immediately immobilized (p) is the amount of "free ink". A fraction (f) of this free ink remains on the paper

Next, it is assumed that the relationship between the amount of ink on the printing cylinder and the amount of ink which penetrates the stock can be described by an exponential function:

$$p = (1 - e^{-kx})\, b(1 - e^{-x/b}) \qquad (15)$$

where p = the amount of ink instantaneously immobilized during printing

b = the immobilization capacity of the stock.

Walker and Fetsko found that equation 15 adequately fitted experimental data.

Lastly, the difference between the amount of ink originally on the cylinder and contacting the stock ($x-b(1 - e^{-kx})$) and the amount of ink immediately immobilized (p) is the amount of "free ink". A fraction (f) of this free ink remains on the paper

when the "free ink" film splits at the end of the transfer process. Thus the classical Walker-Fetsko equation for the total amount of ink on the substrate is given by:

$$y = (1 - e^{-kx})(b(1 - e^{-x/b}) + f(x - b(1 - e^{-x/b}))) \quad (16)$$

where y = the amount of ink transferred to the substrate per unit area

f = the fraction of "free ink" transferred to the stock.

Modification of the Classiclal Walker-Fetsko Equation

Gate, Windle and Hine (38) established that the surface irregularities of paper have a normal distribution of heights. At very low values of kx, a normal distribution cannot be approximated by the exponential relationship between F and x that is assumed by the classical Walker-Fetsko

equation. An alternative transfer equation, using normal logarithmic functions, has been proposed by Ichiakawa, Sato and Ito (39); however, Cropper (40), in his review of several transfer equations, has pointed out that such functions are mathematically more complex, involving numerical integration from + infinity to - infinity, and, consequently, are more difficult to use in analyzing experimental data. A mathematically simpler approach is to replace the exponential function $(1 - e^{-kx})$ with an analytical function that approximates it at large values of kx and also has a general shape that approximates the cumulative log-normal distribution.

The hyperbolic tangent (tanh) meets these criteria and preserves the desired mathematical simplicity. Consequently, the modified Walker-Fetsko

transfer equation (equation 17) can be expected to fit experimental data better than the original Walker-Fetsko equation (equation 16):

$$y = b(\tanh(k'x))(1 - e^{-x/b}) + f\,(x - b(1 - e^{-x/b})) \qquad (17)$$

where k' = the modified Walker-Fetsko coverage parameter

Experimental

Five premixes were made at 20 weight precent concentration using three commercial copper phthalocyanine blue (PCN) pigments and one crude (i.e., non-pigmentary) PCN blue as described in Part I. Four of these dispersions were premixed for five minutes on a Hermes dissolver with a Variac setting of 60. The other premix was prepared by mixing by hand for five minutes with a spatula. All the premixed were then finished on a Fritch (2-1/2" by 5") three-roll mill for various numbers of passes (usually for

one, three, five, then, twenty-five or fifty passes). 1/4% (by weight) of 6% Cobalt drier was added to these dispersions. The dispersions were aged at least one week, then printed on two stocks (an uncoated and a coated stock) using a Fogra proof press at 1.5 m/sec and a pressure of 20 kg/m^2. Both the press and the stock were kept in a constant-humidity room where the dry-bulb temperature was maintained at $72^{o}F \pm 1$ and the wet-bulb temperature was maintained at $62^{o}F \pm 1$ prior to printing. The weight of the ink on the printing cylinder was determined both before and after printing by weighing to 0.00001 gm on a five-place balance. From these weights, and the area of the printed surface, the value of x and y were determined for each print. From 12 to 18 prints at various weights were made from each dispersion.

The FOGRA printability tester presents several advantages to the ink maker over conventional flat-bed proof presses (e.g. The Little Joe). First, it can be made to simulate more closely actual printing conditions on a lithographic or letterpress press. The printing pressure and speed can be held to closer tolerance, prints can be made faster, and weighed prints are easily and rapidly made.

The following is a description of the manner in which the FOGRA is operated:

1. Ink to be printed is placed on a distribution system. The distribution system is a series of rubber and steel rollers running at a constant rate of speed (about 50 rpm). The ink is allowed to spread uniformly over the distribution system.
2. The printing cylinder is cleaned, dried,

weighed, and then put onto the distribution system. The printing cylinder contacts a rubber roller, uniformly picking up ink.

3. The printing cylinder is removed from the distribution system by means of mechanical levers so that the ink film is uniform over the entire cylinder (including the spot at which contact between the cylinder and the distribution system is broken).
4. The printing cylinder is weighed and put on the press.
5. The printing pressure and speed are set on the press.
6. The print is made on a paper strip about 1/2" x 8" mounted on fiber board.
7. The cylinder is reweighed and the process is repeated starting at Step 2.

Because the distribution system does not have to be re-inked (except for fast-drying inks), the process is fast. Furthermore, since the amount of ink on the printing cylinder is determined by the amount of ink on the distribution system, and the amount of ink in the distribution system is steadily depleted, one can easily make a series of prints in which all conditions are constant except the amount of ink on the print. Such a series is necessary for the transfer model.

The values of the transfer parameters, k', and b and f, for the modified Walker Fetsko equation, and k, b and f for the classical Walker-Fetsko equation were then determined by computer. The calculation proceeded by minimizing the sum of the squares of difference between the print weight predicted from the transfer equation using the

weight of ink on the cylinder and the experimentally measured value. The results are shown in Appendix A. The computer program found the minimum of this value using a simplex algorithm written by Greene (41).

Results of the Calculations

The values of the sums of the errors (S_e^2 in the Appendix) for both transfer equations were computed for 31 sets of data obtained from measuring the transfer properties of dispersions to the two stocks using the Fogra printability tester. The computed value for the difference in S_e^2 was -2.922; the value needed for significance at the 99.75% confidence level is -2.81. Therefore, the improvement is significant to a high degree of confidence. A typical transfer curve, showing plots of both the modified and classical Walker-Fetsko equations and the experimental points, is shown in Figure 15a and b. Note

Figure 15a - Comparison of Best Fits of Transfer Equations
To a Typical Experimental Transfer Curve

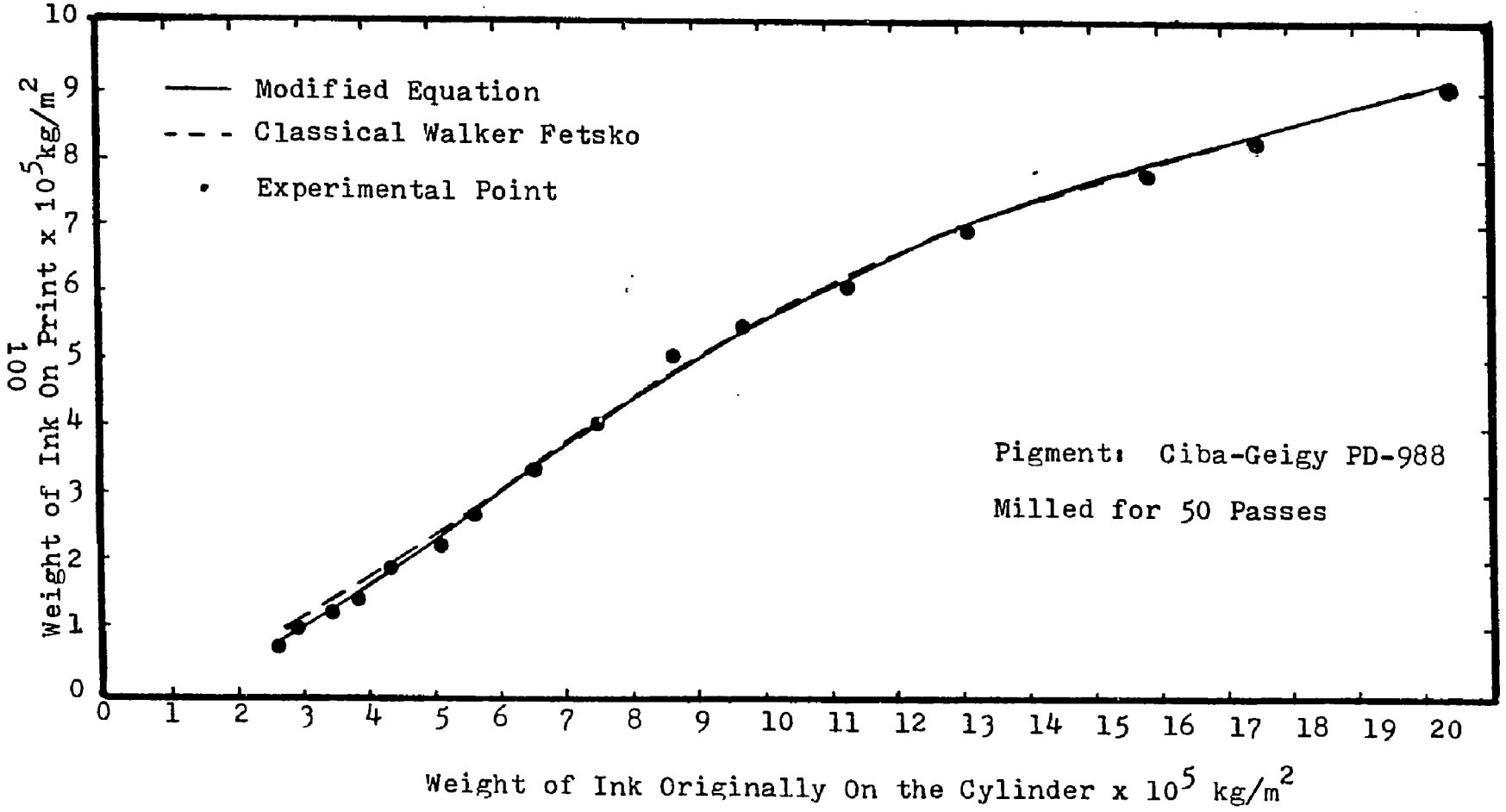

Figure 15b Comparison of Best Fits of Transfer Equations For Small Print Weights

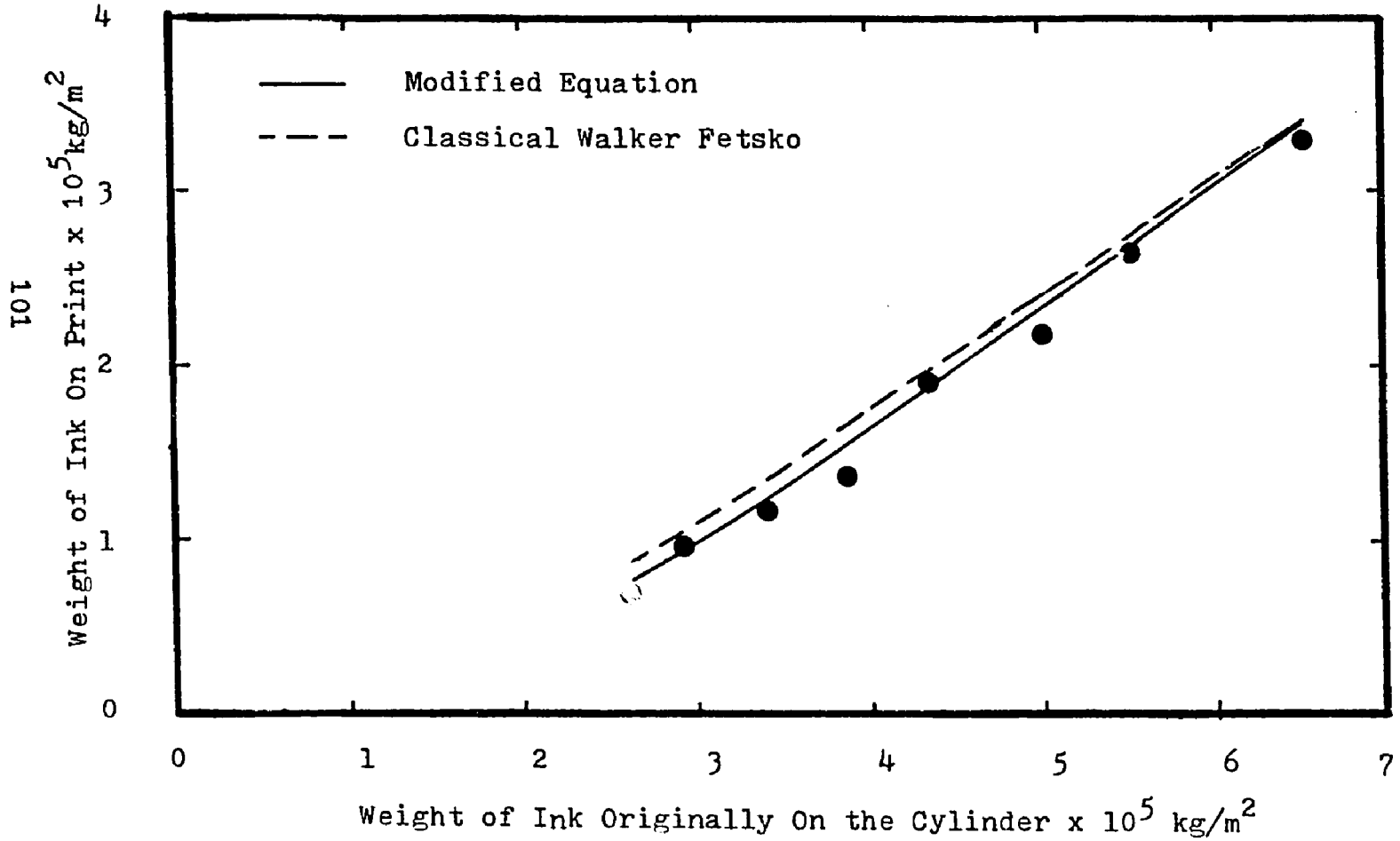

that, as expected, both functions fit the experimental data very well. The modified equation, however, more accurately describes the shape of the transfer curve for small amounts of ink on the printing cylinder than does the original equation. This observation is in accordance with the derivation of the modified equation because the greatest deviation between the exponential function in the original equation and the normal distribution occurs at these low amounts of ink on the roll.

Influence of Degree of Dispersion Upon Printing Properties

In general, the influence of milling times on the transfer coefficients was negligible as shown in Figure 16. This confirms earlier work that showed that there was little difference between two inks having the same loading and made from the same vehicle (35).

Figure 16 - Modified Walker-Fetsko Transfer Coefficients as a Function of Milling Time

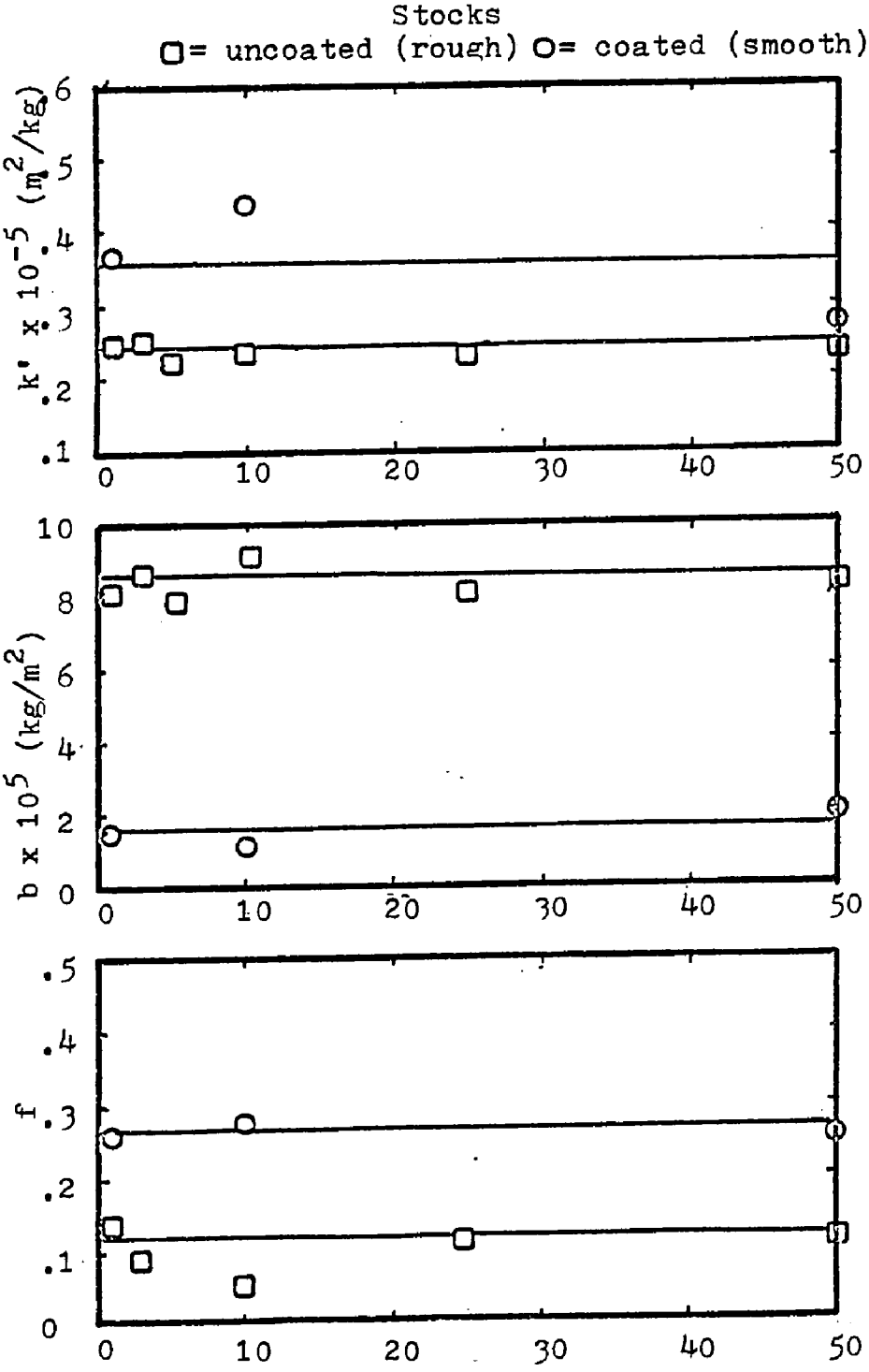

Exceptions to these observations were the dispersions made with crude PCN blue. These dispersions had immobilization coefficients of 0, indicating that little of the ink was completely immobilized, and it did not penetrate well, possibly because the exceptionally large pigment particles (around 3 μm) blocked the pores of the paper and prevented penetration.

Differences between stocks, on the other hand, were very noticible, and more predictable (Table 2). Coates stocks (which are smoother and less porous than uncoated stocks) have higher coverage coefficients (k'), indicating better coverage, but smaller immobilization coefficients, indicating less penetration.

Conclusions

As a result of this work, it may be concluded that the modified Walker-Fetsko equation

Table 2
Comparison of Transfer Coefficients
on Coated and Uncoated Stocks

Dispersion	No. of Passes	Transfer Properties on Coated Stock $k' \times 10^{-5}$ (m^2/kg)	$b \times 10^{5}$ (kg/m^2)	f	Transfer Properties on Uncoated Stock $k' \times 10^{-5}$ (m^2/kg)	$b \times 10^{5}$ (kg/m^2)	f
DuPont BT-4490 PS-92778	1	0.36	1.2	0.30	0.13	8.8	0.05
	10	0.40	1.2	0.29	0.16	6.0	0.27
	50	0.28	1.6	0.27	0.15	7.0	0.17
Ciba-Geigy PD-988	1	0.27	1.6	0.26	0.15	8.3	0.13
	10	0.35	1.2	0.28	0.14	9.1	0.04
	50	0.16	2.1	0.24	0.14	8.4	0.11

provides a better description of ink transfer than does the classical Walker-Fetsko equation.

PART III

ABSTRACT

The series of prints described in Parts I and II were examined colorimetrically in order to establish useful methods of measuring color strength of dried ink films and to use that method to study the influence of the numbers of mill passes on color of prints. A brief review of color theory is presented. Two colorimetric models of ink films are derived and tested for goodness of fit against plots of the prints' minimum reflectance versus print weight. The results indicate that a simple method of evaluating color strength is possible. Furthermore, it is demonstrated that a simple method of evaluating color strength is possible. It is also demonstrated that existing bleach tests do not provide good indications of the final color strength of prints.

Chapter 1

Mathematical Simulation of the Perception of Color

A mathematical simulation of "color" must describe the three factors that contribute to human perception of the color of an object (such as a page of printed matter) that is not itself a source of light. These factors are: 1) the light source illuminating the object: 2) the object itself; and 3) the manner in which the human eye and brain process light. Detailed treatments of each of these items is provided in several general texts (42, 43, 44). A brief review of the development of the mathematical formulism necessary for the discussion of the color of printed matter is provided in this review chapter.

In color science, the most important property of a light source is the electromagnetic energy being emitted within the range

of visible wavelengths (from about 380 nm to about 720 nm). The amount of energy for most sources varies considerably over this range. Therefore, mathematically, the energy must be considered to be a function of wavelength. Polarization of light can be neglected, however, because the sensitivity of the human eye to light is independent of its polarization.

Light can be reflected by an object as the result of two types of reflection: 1) light can be reflected at the object's surface as the result of a change in the index of refraction (called specular reflection) and 2) light that has entered the object can be re-emitted as the result of internal scattering redirecting the light toward the surface. Specular reflection from a smooth surface causes a mirror-like or "glossy" appearance. The energy spectrum of internally

scattered light can be different than that of the light striking the surface because the light at certain wavelengths can be absorbed and converted to heat. Thus, the light reaching the eye of a viewer is the product of the energy spectrum of the source and the reflecting properties of the material. In general, the distances between the source, object and eye can be neglected.

"Color" perceived by a viewer is the result of a human eye (or eyes) working together as a system for receiving and processing the energy spectrum received by the eye. The development of a mathematical model of this system is extremely complex and based on extensive experimental work and, therefore, will be presented ad hoc. This chapter will discuss the mathematical formalism and nomenclature used when determining if two colors constitute a "match", that is, whether

two objects will have the same color when viewed under the same light.

Returning to the reflecting material (a printed page, for instance) both surface reflection and internal scattering contribute to the appearance of the final print. As light impinges upon the surface of a material, a certain amount is reflected at an angle equal to, but opposite in sign, from the angle of incidence (the specular angle). The exact amount of light thus reflected can be calculated from the laws of classical optics (45, 46, 47) knowing the angle of incidence and the refractive index ratio of the reflecting material to the surrounding medium (typically air).

Saunderson (48) attempted to calculate the effect of specular reflection on reflectance measurements by calculating the theoretical reflectance of an object immersed in

a clear material of identical real refractive index. Surface reflections caused by light refraction would be absent under such conditions. Saunderson assumed that the light's path is normal to the material, thereby obtaining equation 17.

$$R' = \frac{k_1}{2} + (1-k_1)(1-k_2)\frac{R}{1-k_2R} \qquad (17)$$

where $k_1 = \left(\frac{n-1}{n+1}\right)^2$

n = refractive index ratio for the material

k_2 = the fraction of light which is diffuse (k_2 = 0.4 although this value often varies depending on the material and the colorimetric equipment used).

R = measured reflectance

R' = reflectance which would be observed if surface effects were absent.

Tunstall (49) performed experiments which indicate that this equation can be improved and, therefore, offered an empirical relation. His findings, however, did not indicate whether this discrepancy is due to surface roughness. Nonetheless, Saunderson's equation often is used when performing calculations describing glossy surfaces such as rotogravure prints. It is not however, used for "flat" (non-glossy) prints.

For smooth surfaces, specular reflection causes a glossy appearance which influences the aesthetic appearance of the finished print and, therefore, is an important consideration in ink making. The desirability of gloss depends on the nature of the product. High gloss may very desirable in magazines, for instance, but may be unwanted in other applications such as greeting cards of invitations.

Gloss (as distinguished from specular reflection) is measured in a glossmeter, illustrated schematically in Figure 17. The glossmeter consists of a collimated light source mounted at an angle to the surface of the test material and a photocell that measures the amount of light reflected at the specular angle. Typically, gloss measurements are expressed as a percent of gloss relative to a standard surface which may be "flat" (i.e. not glossy) or glossy, white, grey, or black depending upon the type of material to be measured. The reference is normally as similar in gloss and darkness to the unknown as possible.

Surface roughness causes the light refracted at the object's surface to be scattered, influencing its visual appearance. For example, a glossy black print will appear darker than a "flat" (i.e., non-glossy) black

Figure 17 - Principle of Glossmeter Operation

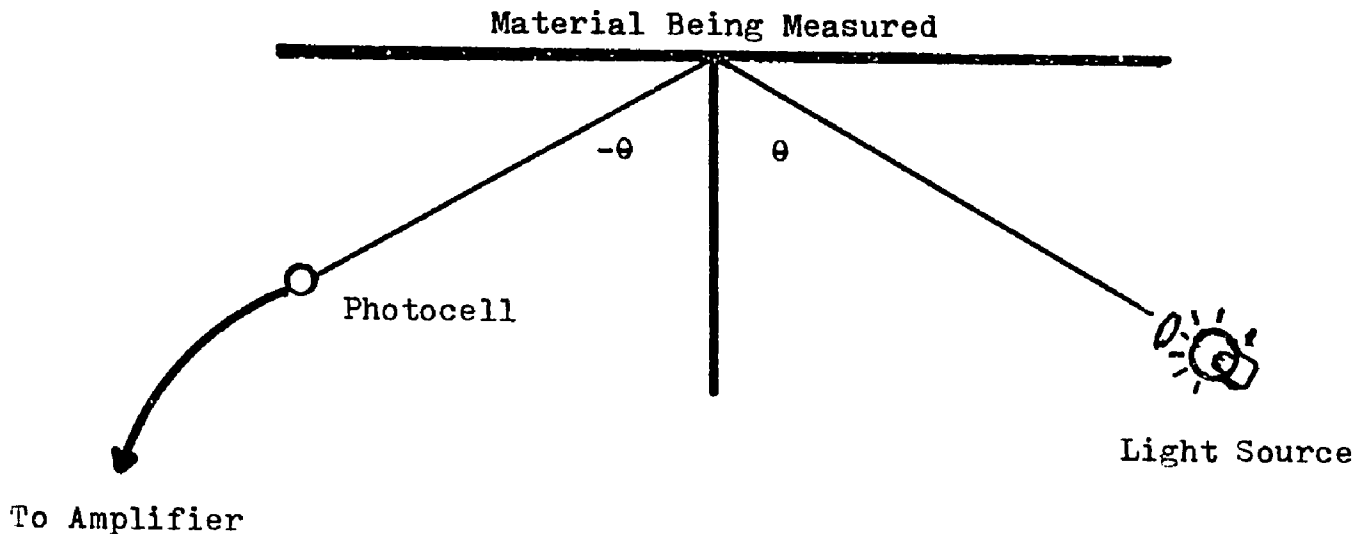

print at most viewing angles because the glossy surface reflects most incident light at the specular angle and very little light at other angles. "Flat" prints on the other hand diffuse incident light over a range of angles. Therefore, at an angle other than the specular angle, more light will strike the eye from a "flat" surface than from a glossy surface when viewed in the same light. However, when flat and glossy prints are viewed at the specular angle with the light source, more light will be seen being reflected from the glossy print. Gate, Windle and Hine (50) have related the gloss of stocks of various roughness as measured by a mechanical contact-probe which consists of a lightly loaded stylus moving across the surface. Measurements of roughness obtained by this method correlated well with standard gloss measurements (TAPPI 75^{o} gloss (51)). Witherell (52) attempted to predict the

relationship between gloss and surface roughness using a simplified model of a surface which consisted of reflecting surfaces composed of small facets tilted at various angles to the plane of the surface.

Light that passes through the front surface of an ink film into a print is scattered and absorbed by the ink and the fibers of the paper. Two mathematical analyses have been used to describe light scattering; 1) complete solutions of Maxwell's equations for the propagation of light through space; and 2) less rigorous analyses based on easily measured empirical parameters which are not directly related to fundamental properties such as refractive index.

Complete solutions of Maxwell's equations have been obtained for a few simple shapes only and are used in astrophysics and meteorology, but are difficult to apply to

the problem of the reflectance properties of printed matter. Mie (53) solved Maxwell's equations for the case of a plane wave striking a sphere. The resulting equations describe the scattering pattern of the reflected light (i.e. the amount of light reflected as a function of angle) as a function of two properties of the sphere: 1) the ratio of the sphere's diameter to the wavelength of the incident light; and 2) the refractive index ratio of the sphere to the surrounding medium. This refractive index ratio is a complex number having an imaginary term which represents the material's ability to absorb radiation (whether the absorbed energy is re-emitted at another wavelength or converted to other forms of energy is irrelevant to Mie's analysis). Tabulations of the numerical results of the Mie equations have been prepared by Lowan (54) for relatively colorless spheres and extended by Dermendham,

Clasen and Viezce (55), Chromey (56) has prepared similar tables for "colored" (i.e. light absorbing) spheres.

A less rigorous analysis developed by Kubelka and Munk (57, 58, 59) and Duntley (60) is based upon the assumption that a layer of absorbing material, such as an ink or paint film, can be considered "homogeneous". It is assumed that all light within the medium can be treated as if it were traveling in one of two directions, "upward" or "downward". Such an assumption is mathematically rigorous only if the light entering the film is perfectly diffuse, that is, the intensity of the light must be independent of the angle measured normal to the surface.

The Kubelka-Munk theory also assumes that light is either scattered in the opposite direction or absorbed as it passes through

a medium. Both the amount of light scattered and absorbed from a given direction ("upward" or "downward") is proportional to the amount in that direction. Based upon these assumptions, Kubelka wrote a system of differential equations describing the flux density of light in both directions.

$$-di = -(S+K)idx - Sjdx \qquad (18\ a)$$

$$dj = (S+K)jdx + Sidx \qquad (18\ b)$$

where i = the intensity of light within a medium traveling toward its unilluminated surface

j = the intensity of light within a medium traveling toward its illuminated surface

S = the scattering coefficient of the medium

K = the absorption coefficient of the medium

x = the distance from the unilluminated surface (i.e. the "back")

The constants K and S are empirical and can be determined by experimental measurement. These equations can be solved for a variety of boundary conditions. The reflectance (neglecting front surface effects) is merely the ratio j/i at the illuminated (i.e. front) surface. The transmittance is the ratio of the value of i at the back surface to the value of i at the front surface. For a layer of material of thickness x having a reflectance at the back surface of R_g, the Kubelka-Munk equations yield:

$$R = \frac{1-R_g(a-b\ \mathrm{ctgh}\ (bSS))}{a+b\ \mathrm{ctgh}\ (bSX)-R_g} \qquad (19)$$

where $a = (K+S)/S$

$b = (a^2-1)^{\frac{1}{2}}$

R_g = reflectance at the back surface

X = thickness of the layer

Approximations of the equations resulting from the integration of equations 18 a and b have been made by Ross (61). These are based

on rearrangement of terms and various approximations; however, the complete solution given by equation 19 is more often used.

The solution of equation 18 for the special case in which $x \to \infty$ is frequently encountered and is given by equation 20.

$$R_\infty = \frac{K}{S} + 1 - \left(\frac{K}{S} + 1\right)^2 - 1 \qquad (20)$$

where R_∞ = the reflectance as $S \to \infty$

This equation is often used to describe thick films, that is, films which are thick enough so that increasing the thickness does not change R. Note that as $x \to \infty$, R approaches a limit which is not necessarily zero. This limit is not zero because the value of S is not zero, that is, some light will be scattered upward before all of it has been absorbed.

The assumptions made to achieve the mathematical simplicity of Kubelka-Munk theory also limit the accuracy of it. In reality, the phenomenon of diffuse reflectance by an

ink print is the result of scattering in all directions of electromagnetic radiation by many complex-shaped reflectors close together. Kubelka-Munk theory assumes that light is scattered uniformly, that is, that the scattering pattern of a source is a circle. Although this pattern never occurs, Kubelka-Munk theory is a good approximation if a print's surface is illuminated by totally diffuse illumination or if the film is thick enough to diffuse all light passing through it. Otherwise, the reflected light may not be perfectly diffuse (uniform over all angles). Allen (47) has mentioned that an ink film may be too thin for a collimated light beam to be diffused as it passes through the ink film. Nonetheless, Kubelka-Munk analysis is the the basis of much of the colorimetric analysis of inks and paints because of the simplicity of the equations of the accuracy

of the equations of the accuracy of the theory for predicting certain phenomena. Automated color matching (62, 63), for instance, predicts the color of an ink or paint made from a combination of pigments, by Kubelka-Munk theory.

The absorption and scattering coefficients of a layer of material composed of a mixture of materials often are assumed to be the sums of the coefficients of the pure constituents times their respective volume fractios. This is strictly true if there is no synergistic relationship between any of the constituents. Such synergism does exist, however, between titanium dioxide pigment and microvoids (64, 65). These effects may be neglected for most colored materials (i.e., non-white). Therefore, the absorption and scattering coefficients of a layer made up of n different constituents are:

$$K = \sum_{i=1}^{n} c_i K_i \qquad (21)$$

$$S = \sum_{i=1}^{n} c_i S_i \qquad (22)$$

where K = the absorption coefficient of the layer

S = the scattering coefficient of the layer

c_i = the volume fraction of the i-th constituent

K_i = the absorption coefficient of the i-th constituent

S_i = the scattering coefficient of the i-th constituent

n = the number of constituents

Billmeyer (66, 67, 68) compared the predictions of a Kubelka-Munk model of a paint film with experimental data. The color

difference between experimental paints pigmented with titanium dioxide and a colored pigment and the predictions of Kubelka-Munk theory based upon the reflectance spectra of paints made with different amounts of the same pigments were compared. The results indicated that the accuracy of Kubelka-Munk predictions of the color of paints was on the order of the smallest color difference perceived by the human eye.

It should be noted that the basic approach of the Kubelka-Munk theory can be extended to a more general analysis developed by Mudgett and Richards (69, 70, 71) and called multi-channel analysis. In Kubelka-Munk theory, all of the light within a film is considered to be a part of one of two fluxes, either the "upward flux" or the "downward flux". In reality, light is reflected in many directions and the number of

directions of travel need not be limited to "upwards" or "downwards". Therefore, it is possible to generalize by saying the light may be treated as traveling in any number of "channels", each channel identified by a particular angle θ and channel width θ. This approach yields a system of equations analogous to equations 17 a and b; the i-th equation of this system is shown in equation 23.

$$\frac{d\ell_i}{dx} = - \sum_{j=1}^{n} S_{in\ i} + \sum_{\substack{j=1 \\ j \neq i}}^{n} S_{in\ j} \qquad (23)$$

where ℓ_i = the light in the i-th channel

S_{ij} = the scattering coefficient from the i-th channel into the j-th channel

n = the number of channels

S_{in} = the absorption coefficient (cor-

responding to K in Kubelka-Munk theory

The scattering coefficients S_i can be more accurately related to the scattering pattern of the scattering sites within the material than can the single Kubelka-Munk scattering coefficient S. The number of channels is limited only by the size of the computer doing the calculations, the cost of the calculations and the amount of data available. Therefore, this technique is extremely useful when considering the properties of the film in which the synergistic effects mentioned earlier are important, such as when microvoids are mixed with titanium dioxide or when considering films in which the scattering pattern is strongly a function of angle such as metal-flake paints (54). However, the extra coefficients make the experimental measurement

of the coefficients, S_{ij}, more difficult than the measurement of the Kubelka-Munk K and S values.

Light reflected by a print must be received by the eye in order for color to be perceived. The human eye is important in the consideration of color because of the manner in which the eye interprets the energy spectrum it receives. The eye is sensitive to light over a range from roughly 380 nm to 720 nm. However, two objects having different reflectance properties over this range may appear to have the same color when viewed under identical conditions. This phenomenon, known as metamerism, is responsible for much of the complexity of color science.

Let us now discuss the mathematical simulation of color vision in order to demonstrate how metamerism can occur and to complete the mathematical description of the

perception of color from prints. Many systems have been proposed to describe color vision. All of these define three dimensions necessary to characterize the phenomenon.

One such system is the tristimulus functions established by the "Commission Internationale del 'Eclairage" (CIE), an international body which has specified standard (ideal) observers. The tristimulus values, normally designated X, Y and Z are defined mathematically as shown in equation 24 a, b and c.

$$X = \int_{380}^{720} x'(\lambda)E(\lambda)R(\lambda)d \qquad (24\ a)$$

$$Y = \int_{380}^{720} y'(\lambda)E(\lambda)R(\lambda)d \qquad (24\ b)$$

$$Z = \int_{380}^{720} z'(\lambda)E(\lambda)R(\lambda)d \qquad (24\ c)$$

where S, Y and Z are the tristimulus values
$x'(\lambda)$, $y(\lambda)$ and $z'(\lambda)$ are the tristi-
functions

$E(\lambda)$ = the energy spectrum of the source

$R(\lambda)$ = the reflectance spectrum of the object.

For non-emitting objects, such as paint films, the tristimulus functions are often combined with the energy spectrum to simplify computation. In practice, the integration is frequently replaced with a summation of the reflectances at a finite number of wavelengths (typically 16 or 32).

If the object in question is a light source, then the light received by the eye is merely the energy spectrum of the source. If the object does not emit light, the energy spectrum of the light reflected from the object is the product of the energy spectrum of the light source times the reflectance of the object ($E(\lambda)R(\lambda)$). The amount of reflectance can be obtained (us-

ually from either Kubelka-Munk or Mudgett-Richards theories).

The values of the three tristimulus functions (designated x (λ), y(λ) or z (λ)) have been determined experimentally and exact functions have been defined for standard observers. Very generally, x corresponds to the amount of red present, Y to the amount of yellow (also to the brightness) and Z to the amount of blue. This correspondence is not exact and is only meant to be an approximation of the individual values.

The functions x(λ), y(λ) and z(λ) are continuous non-negative functions over the entire range of wavelengths. Therefore, it is possible for two different energy distributions to have identical values of the tristimulus values, X, Y and Z. This is equivalent to saying that two different prints having different reflectance properties could

have the same color when viewed under the same conditions. Such prints are called metameric matches.

The difference between two colors having two different sets of tristimulus values is a function of their tristimulus values. The MacAdam Unit has been defined as being the largest difference in color that is imperceptible to to human eye. Brown performed experimental work (72, 73) to measure this difference. MacAdam, Friele and Chickering (74 - 80) have analyzed these data to produce a series of functions which allow the color difference (measured in MacAdam Units) to be calculated from the tristimulus values of two colors. Billmeyer (81) has written a FORTRAN program which performs the necessary calculations.

The tristimulus are frequently represented on a two-dimensional plot called a

Chromaticity Diagram (Figure 18). The chromaticity coordinates are difined as shown below:

$$x = X/(X + Y + Z) \qquad (25\ a)$$

$$y = Y/(X + Y + Z) \qquad (25\ b)$$

$$z = Z/(X + Y + Z) \qquad (25\ c)$$

where x, y and z are the chromaticity coordinates.

The chromaticity coordinates of every wavelength of visible light is plotted on the chromaticity plot as shown in Figure 16. This horseshoe-shaped curve (called the pure spectrum locus) is joined at the bottom by a straight line. The chromaticity of any "real" color will be inside this curve. Points outside the curve represent "unreal" colors; that is, they represent chromaticities which require a negative amount of energy at some wavelength.

The "purity" and "dominant wavelength" of a color, two useful properties which will

Figure 18
Chromaticity Diagram

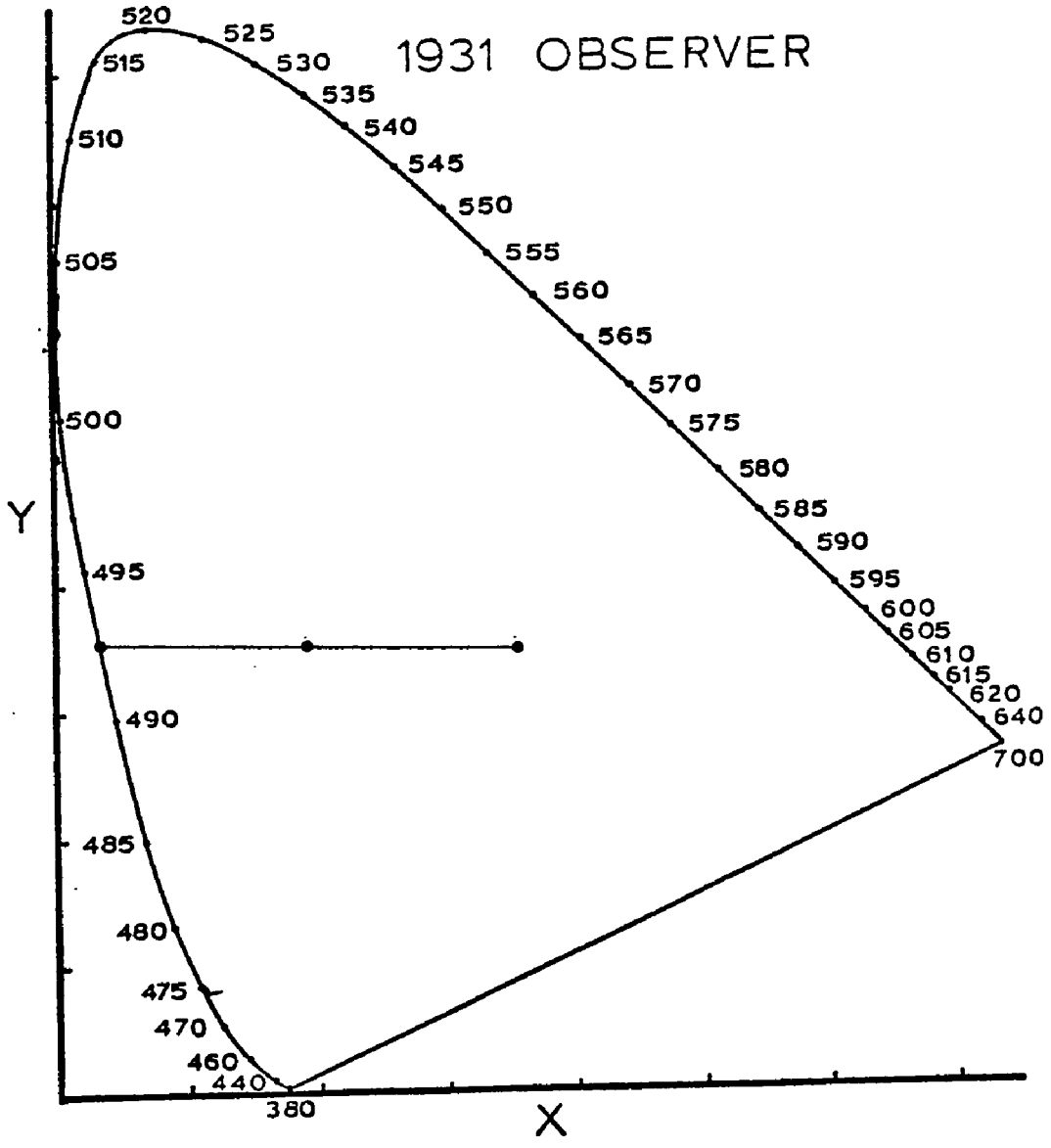

be used later, are derived from the chromaticity diagram. These values are calculated as follows:

1. On a chromaticity diagram for the standard observer, plot the x and y values for both the energy spectrum of the light source and the object when viewed under that source.
2. Draw a line from the point representing the source to spectrum locus through the point representing the color. If this line intersects the straight line drawn from 380 to 700, both terms are undefined.
3. If the line intersects the spectrum locus, the dominant wavelength is the wavelength corresponding to the point of intersection. Purity is defined as one hundred times the ratio of the distance between the light source's and the object's chromaticities to the distance between the

source's and the dominant wavelength's chromaticities. In Figure 18, if L is the light source, and A is the color, then the wavelength corresponding to point C is the dominant wavelength and 100 x ($\overline{AL}$ / $\overline{LC}$) is the purity.

The significance of the terms "dominant wavelength" and "purity" are that they constitute a recipe for reproducing a color with the same chromaticity by combining light of a single wavelength (the dominant wavelength) with the energy spectrum of the light source. The purity is the fraction of the total light from these two sources which comes from the dominant wavelength.

Thus, if $\overline{AL}$ is twice $\overline{AC}$ and if lights C and L are combined, and if C's luminosity (brightness) is twice as great as L's, then the chromaticity of the combined color will lie on $\overline{LC}$ at point A.

CHAPTER 2

Measurement of the Tinting Strength of Lithographic Inks From the Color of Weighed Prints

Introduction

The purpose of this work is to develop an alternative technique to current bleach tests that would allow the determination of a "printing strength" value from colorimetric analysis of proof prints.

There are several standard methods of measuring an ink's or a print's degree of dispersion. In general, dispersion tests detect the presence of aggregates in a certain size range by measuring properties that are strongly related to the humber of aggregates in that range, but are weakly related to the number of other ranges. A grind gage, for instance, detects the presence of the largest aggregates in an ink, but is insensitive to the number of smaller aggregates.

Bleach strength, which measures the ability of a dispersion to impart its color to a white paste, is a function of several critical properties, e.g., pigment loading and quality of dispersion, and is most sensitive to the number of smaller aggregates. "Dispersion quality" refers to the nature of the size distribution of the pigment aggregates. Poor dispersions have many large aggregates; good dispersion, on the other hand, have narrow size distributions around an optimum size that gives the best combination of printing and colorimetric properties.

It has been established theoretically and experimentally that, below a certain size, the ability of a pigment to absorb light will be reduced. However, this optimum appears to be smaller than the size of aggregates ordinarily achieved in ink manufacture. Furthermore, an ink composed of aggregates of this

optimum size might not have good printing characteristics, and therefore, might be undesirable. A literature review of the dispersion properties of colored pigments (6, 7, 17, 35, 82 - 94) found no case in which overmilling was reported to cause undersized aggregates and, therefore, a color strength loss. Indeed, only one case reported a loss of color because of excessive milling. Those measurements were performed by Herbst (6), using a copper phthalocyanine blue pigment which underwent a change in crystal morphology. In general, therefore, overmilling does not appear to be a significant problem with colored pigments.

The overall degree of dispersion at a particular ink concentration currently is best measured by the "color strength" or "tinting strength" of an ink as determined by a bleach test. There are, however, sev-

eral problems associated with conventional bleach tests. These tests, such as NPIRI TM E-2 are time-consuming (and, therefore, costly) and have great operator variability. Furthermore, most ink makers prepare proof prints to test both the printability and final appearance of their products. Therefore, it is desirable to determine the relationship between an ink's tinting strength and its final appearance on a print so that both tests can be combined into one.

Because of the possibility of computational complexity involved in developing such mathematical relationships, only one worker, Zroll (14), has attempted to develop such a method. He investigated the change in reflectance at increasing print weights for dispersions made with two different yellow pigments. His empirical work did not attempt to explain his results using color

theory, although he did find a correlation between bleach strength and printing strength.

Existing Tests

Currently, there are two slightly different types of bleach tests. The first conventional test (NPIRI E-2) (95) requires the simultaneous preparation of two bleaches at a fixed ratio of ink to bleach. One bleach is made from a reference ink and the other bleach is prepared from the test ink. The relative color strengths of the two bleaches are evaluated by preparing side-by-side drawdowns of opaque films of the two bleaches. The concentration of ink in the stronger bleach is reduced by adding white paste until the color strengths of the two bleaches are the same. The bleach strength is the ratio of the concentrations of the reference ink to the test ink multiplied by one hundred. This value approximates one hundred times the ratio

of the Kubelka-Munk absorption coefficients of the wet inks. This approximation is based on the assumption that the scattering coeffient of the bleach is independent of the ink and dependent solely on the white paste. The absorption coefficient is assume do be the product of the absorption coefficient of the ink times the volumetric concentration. If the two bleaches are a "true" (i.e. non-metameric) match, then the reflectances of the bleaches are identical at every wavelength. Therefore, according to equations 21 and 22, the ratio of ink concentrations is equivalent to the ratio of the absorption coefficients.

A simpler technique for measuring bleach strength is recommended in DIN 53234 (46) and consists of preparing a bleach at a fixed concentration, placing the bleach into a glass cell and examining its color spectro-

photometrically. The tinting strength relative to a previously prepared reference bleach can then be determined from equation 21 by calculating the value of K/S for both bleaches at a selected wavelength (typically, the wavelength having the minimum reflectance). This test defines the ratio of the values of K/S for both bleaches times one hundred as the bleach strength. Theroretically, this value is identical to the value calculated by the NPIRI method. The DIN method is somewhat faster and provides less opportunity for operator error. Consequently, it was used in the experimental determination of bleach strengths throughout this work.

Development of the Kubelka-Munk Models of Ink Films On Prints

The accuracies of curve fits of two Kubelka-Munk models of ink films were com-

pared to experimentally measured relationships between reflectance and print weight (that is, the weight of ink per unit area). The series of prints described in Parts I and II was used for this work. Additionally, a simplified graphical method of interpreting plots of reflectance versus print weight was also developed. Computations using this last method were compared to those obtained from the better Kubelka-Munk model.

The first Kubelka-Munk model, Model 1 (Figure 19) consists of the three layers of prints described in the Walker-Fetsko ink transfer equation. The second model assumed that prints could be represented by a single layer of ink in a stock. This single-layer model will be discussed later,

Model 1 (Figure 19) assumes an ink print is composed of three layers. The first layer is the deepest layer and concists of the

Figure 19 - Multi-Layer Model of Ink Films
(Model 1)

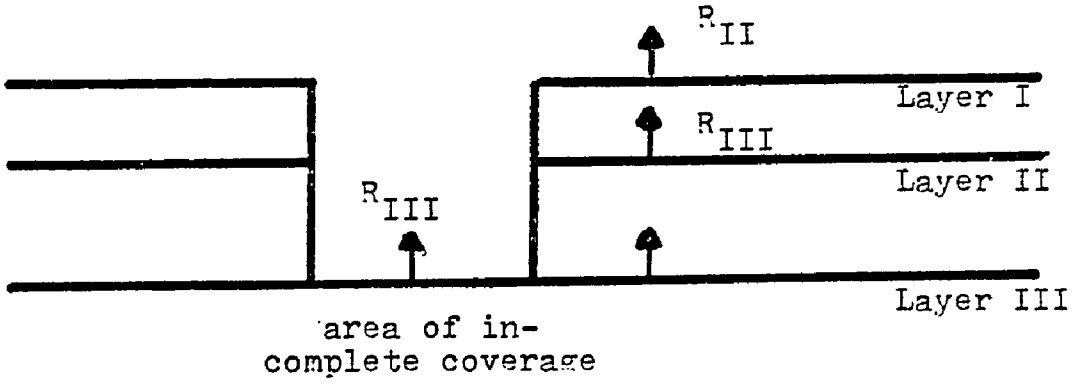

uninked paper below any ink layer. The second layer consists of paper that contains a certain volume fraction of ink (the volume fraction depending upon the stock, the vehicle, and the press conditions, but not on the pigment or the degree of dispersion). The third layer is a dried ink film on the surface of the stock. It is assumed that the top two layers containing ink do not completely cover the surface. Unprinted areas of incomplete coverage are assumed to exist as a result of the influence of surface roughness on ink transfer. The reflectance of the unprinted portions is assumed to be that of unprinted stock.

The overall reflectance for this model ink film is obtained by determining the reflectance at the top of each layer starting with the bottom layer and proceeding to the top surface. The reflectance at the top is

then combined with the reflectance of the white (uncovered) area to yield the overall reflectance of the print.

The reflectance at the bottom of the penetration layer (i.e., the top of the uninked layer) is assumed to be the reflectance of the unprinted paper. This assumption can be made for two reasons: 1) the thickness of the penetration layer is small with respect to the total thickness of the paper (as would be expected on prints on good quality stock having typical holdout properties; and 2) the scattering coefficient of the unprinted paper is large for most stocks.

The reflectance at the top of the second layer can be calculated from Kubelka-Munk theory (58, 59, 60) using equation 19. First, assume that the volume fraction of ink in the penetration layer is uniform throughout and independent of the thickness of the layer.

The thickness of the layer, then, is related to the amount of ink in the layer by equation 27.

$$t = Y_p / C_p d_i \qquad (27)$$

where t = the thickness of layer II

Y_p = the weight of the ink in layer II per unit area of paper covered with ink

C_p = the volume fraction of ink in layer II

d_i = the density of ink

The Kubelka-Munk absorption and scattering coefficients for the layer (K_{II}, S_{II}) are related to those of the ink and stock as shown in equations 28 a and b:

$$K_{II} = C_p K_i + K_p \qquad (28\ a)$$

$$S_{II} = S_p S_i + S_p \qquad (28\ b)$$

where K_i and S_i are the absorption and scattering coefficients of the ink; K_p and S are the absorption and scattering coefficients of

the inked paper. Note that S_p is not the same as the scattering coefficient of unprinted paper. These two coefficients have different values because the refractive index ratio of cellulose to air is different than the ratio of cellulose to binder, hence, the scattering ability (and Kubelka-Munk scattering coefficient) of paper covered with ink is different than that of unprinted stock.

The terms K_{II}/S_{II} and $S_{II}t$, appearing in the Kubelka-Munk equation, are given by

$$\frac{K_{II}}{S_{II}} = \frac{C_p K_i + K_p}{C_p S_i + S_p} = \frac{K_i/d_i + K_p/d_i C_p}{S_i/d_i + S_p/d_i C_p} \quad (29\ a)$$

$$S_{II}t = (C_p S_i + S_p)\ (Y_p/C/d_i) = (S_i/d_i + S_p/d_i C_p)Y_p \quad (29\ b)$$

These equations can be simplified by defining the terms K_i', S_i', K_p' and S_p' given by equations 30 a, b, c and d, which have unites of (M/L^2).

$$K_i' = K_i/d_i \qquad (30\ a)$$

$$S_i' = S_i/d_i \qquad (30\ b)$$

$$K_p' = K_p/d_i C_p \qquad (30\ c)$$

$$S_i' = S_p/D_i C_p \qquad (30\ d)$$

Using these terms, equations 29 a and b rewritten as shown by equation 31 a and b:

$$\frac{K_{II}}{S_{II}} = \frac{K_i' + K_p'}{S_i' + S_p'} \qquad (31\ a)$$

$$S_{II} t = (S_i' + S_p')\ Y_p. \qquad (31\ b)$$

This description of the second layer will be called Model 1 a.

A variation of this model (called Model 1 b) based on a model presented by Allen (62) was also considered. In Model 1 b, the volume fraction of ink, C_p, in layer II is assumed to be proportional to the amount of ink in the layer, Y_p. Therefore, the thickness of the layer is constant. This assumption produces a slightly different relationship between Y_p and the terms $S_{II} t$ and K_{II}/S_{II} as

shown in equation 32 a and b below:

$$\frac{K_{II}}{S_{II}} = \frac{K_{II}t}{S_{II}t} = \frac{Y_p K'_p}{Y_p S_i} + \frac{K''_p}{S''_p} \qquad (32\ a)$$

$$S_{II}t = Y_p S''_p \qquad (32\ b)$$

where t = a constant

$K''_p = K_p t$

$S''_p = S_p t$

The values of K_{II}, S_{II} and $S_{II}t$ calculated from either of these two assumptions can be substituted into the general Kubelka-Munk equation (equation 19) to obtain the reflectance at the top of the second layer.

$$R_{II} = \frac{1 - R_I(a - b\coth(bS_{II}t))}{a + b\coth(bS_{II}t) - R_I} \qquad (19)$$

where R_{II} = the reflectance of the surface of the second layer

R_I = the reflectance at the bottom of the penetration layer (assumed to be the reflectance of unprinted stock)

$$a = (K_{II} + S_{II})/S_{II}$$

$$b = (a^2 - 1)^{\frac{1}{2}}$$

An equation analogous to equation 19 can be written for layer III to give R_{III} in terms of K_i', S_i', Y_s (the weight of ink per unit of the surface layer) and R_{II}.

The total reflectance of the print, however, is the combination of the reflectance of the printed portion (R_I) and the reflectance of any unprinted portion (R_{III}) caused by incomplete coverage of the stock by the ink.

The overall reflectance for this model of a print can be computed using an equation developed for the relationship between reflectance and coverage for half-tone prints. A half-tone print achieves tonal variations through the combination of printed area (small half-tone dots) and unprinted area (stock). In 1936, Murray (97) presented a relationship that is summarized in equation 33

for the overall reflectance of such prints that is summarized by equation 33. Equation 33 is based on the assumption that the diffusion of light is negligible between areas of differing reflectance (i.e., between half-tone dots and the spaces between them).

$$R_p = FR_{III} + (1 - F)R_I \qquad (33)$$

where R_p = the reflectance of the print

F = the fraction of surface that is not covered.

Of course, diffusion of light between these area does occur and does influence the overall reflectance, R_p. To correct equation 33 for this cross diffusion, Yule and Neilson (98) modified it by introducing the parameter "n" as shown in equation 34:

$$R_p = ((1 - F)\, R_I + FR_{III}^{1/n})^n \qquad (34)$$

where n = an empirical value that is a function of the dot size and the type of paper used in printing.

Yule and Neilson determined experimentally the values of "n", finding that it ranged from 1.3 to 2 for several combinations of dot sizes and paper stocks. They found that high values of "n" are associated with prints on uncoated stocks made with small dots (both conditions tend to increase the amount of diffusion between printed and unprinted areas).

Thus, according to these models, a print's reflectance can be calculated from equation 34. For both Models I a and b, the calculation of the reflectance of a print at a particular wavelength can proceed in a straight forward manner when the following are known: 1) the absorption and scattering coefficients of both the ink and the paper substrate that contains ink: 2) the amount of ink in each of the various layers; and 3) the reflectance of the unprinted paper. Item 2 can be obtained from transfer data

using the modified Walker-Fetsko equation given in Part II. Therefore, from a series of proof prints using the same ink and printed following the procedure outlined earlier, it is possible to determine the remaining unknown variables. This calculation may be done by minimizing the sum of the squares of the difference between calculated and measured values of R_p using standard search techniques described earlier (41).

Model 2 (shown in Figure 20) is a single layer model in which it is assumed that all the ink penetrates the stock forming a single uniform layer that is similar to the second layer of Model 1b. Model 2 further assumes that the absorption coefficient of the stock is small compared to that of the ink and that the scattering coefficient of the ink is small compared to that of the ink bearing stock. These assumptions, which are analogous to the ones made in calculating

Figure 20 - Single Layer Model of an Ink Film Model 2

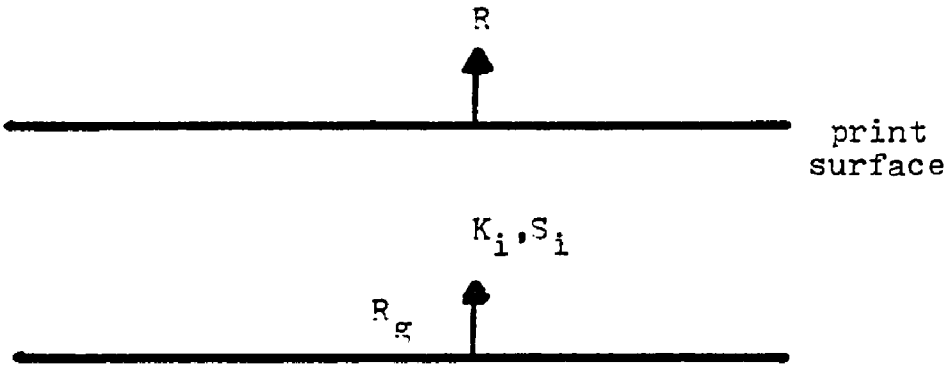

bleach strengths, yield equations 35 a and b for K/S and St for the single ink-containing layer

$$\frac{K}{S} = \frac{Y_p K''_i}{S''_p} \qquad (35\ a)$$

$$St = S''_p$$

Note that in this model the absorption parameter is the product $Y_p K''_i$. This implies that an increase in an ink's absorption coefficient due to increased pigment concentration or better milling could cause a proportional decrease in the amount of ink required to produce the same reflectance at a given wavelength. A similar proportional relationship exists between the concentration of ink in a bleach and the absorption coefficient of wet ink. The difference between the absorption coefficients measured in bleach tests and on prints, however, is unpredictable because of the problems described earlier.

Graphical Method

A practical method of approximating the relative printing strength that does not require numerical calculations was developed. The graphical procedure is given below:

1. Plot the reflectance versus print weight, preferably on semilog paper with the print weight on the log axis and the reflectance on the linear axis.
2. Determine by interpolation the print weight necessary to produce a standard reflectance well above the minimum reflectance for a reference ink. For the trial calculations this standard reflectance was set at 20% at 620 nm wavelength.
3. Repeat the above procedure at the same conditions for the test ink.
4. The relative printing strength is then the weight of the reference ink at the standard wavelength and reflectance level divided by the weight of the test ink.

This is illustrated graphically in Figure 21 which shows a typical plot of experimental data. This method of analysis is less rigorous than the Kubelka-Munk models but has the advantage of simplicity. Great care should be exercised in chosing a standard reflectance that is in the "mid-range" of the prints because this range offers the best combination of precision of measurement of print weight and of reflectances (see Figure 21). The absolute precision of the reflectance measurements is independent of reflectance, hence, the precision expressed as percent of measured reflectance is lower on the lighter prints; however, the absolute precision for print weights is also independent of print weight, hence, the precision as a precent of measured weight is higher for the lighter prints.

Experimental

The dispersions of copper phthalocya-

Figure 21 - Typical Plot of Reflectance vs. Print Weight

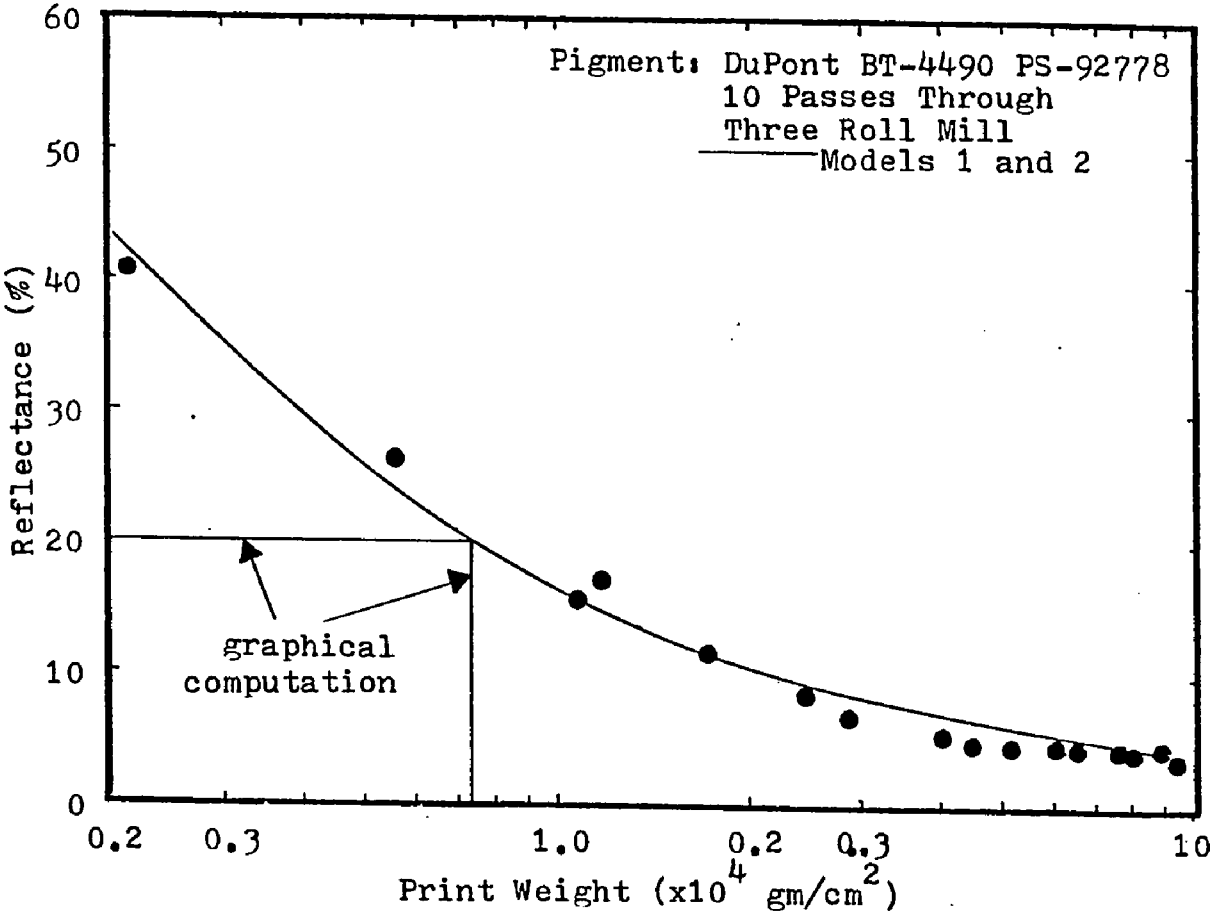

nine pigments in alkyd resin prepared in Part I were printed on two different stocks using the Fogra Printability Tester (a small proof press) described in Part II. The weight of each print was determined by weighing the printing cylinder before and after printing on a 5 place balance to ±0.00001 g. The weight of the ink on the printing cylinder before printing and the weight transferred to the paper were determined from these measurements. The parameters for the modified Walker-Fetsko equation were obtained using a simplex search program also described in Part II. The prints were allowed to dry for one day and were examined using a KCS-40 automatic spectrophotometer manufactured by Kollmorgen Corporation. The prints were made using two stocks, and uncoated stock which was readily penetrated by the ink, as indicated by the printability parameters, and a coated stock which produced prints with little penetration (good holdout).

Bleaches

Bleach tests were conducted on the inks using DIN 53-234 as described previously. In these tests, the bleaches were prepared by mixing paste and ink at a fixed ratio of 100:1. The white paste was prepared by milling 80 grams of zinc oxide with 120 grams of the alkyd resin used in preparing the phthalocyanine blue dispersions. Use of the same vehicle for both bleach and dispersion prevented false bleach measurements caused by incompatibility of vehicles. The finished bleaches were examined spectrophotometrically using a bleach holding cell which consisted of two glass slides separated by spacers, leaving a gap of approximately 2 mm.

Calculations and Results of Comparison of Prints and Bleaches

The transfer coefficients for the modified Walker-Fetsko equation were obtained for all series of inks using the sum of squares

of the error criterion described earlier. As expected, these terms (described in Part II) indicated that more complete coverage and less penetration occurred with the coated stock.

Analysis of Models 1 a and b

Models 1 a and b were used to fit experimental data using five unknowns, K_i, S_i, K_p, S_p and n. These fits were very poor. Consequently, Models 1 a and b were modified to calculate a pseudo-Walker-Fetsko transfer coefficient, K, from the colorimetric data assuming a value of two for the Yule-Neilson constant. A typical curve fit for these modified models is shown in Figure 21. Note that the fit is extremely good for this model. The values for the optimized parameters are shown in Table 3. The calculated absorption coefficient of the ink is roughtly 10,000 times greater than that of the paper. Furthermore, the scattering coefficient of the ink multiplied by the weight of ink on the paper is

Table 3

Typical Results of a Least Squares Fit of Reflectance vs. Print Weight

(Pigment: Ciba-Geigy PD-989)

(1 Mill Pass)

(Model 1 a)

(Yule-Neilson Constant Assumed Equal to 2)

Ink Properties	K_i'	1.796
	S_i'	0.05373
Paper Properties	K_p'	0.0001295
	S_p'	0.7622

Modified Transfer Coefficient K=5.157

(based on reflectance data)

roughly 10 times that of the paper. Furthermore, the calculated value of the modified Walker-Fetsko coverage parameter is large enough to eliminate the influence of un-inked areas. Therefore, it appears that the attempt to include the effect of incomplete coverage produces a negligible increase in the accuracy of the prediction of variation of reflectance with print weight. Furthermore, these results indicate that the relationship between reflectance and print weight may be adequately described by two numbers: an absorption coefficient for the ink and a scattering coefficient for the paper. This conclusion is confirmed by the accuracy of fit for the two-constant model (Figure 21). Note that, mathematically, model 2 is not identical to models 1 a and b because the scattering coefficient of the ink is not included in the calculation of R_{III}, the reflectance at the top of surface layer.

Nonetheless, model 2 and the modified version of models 1 a and 1 b produced equally accurate fits. Note that model 2 also presents the advantage of eliminating the use of the Walker-Fetsko transfer equation, thereby eliminating a potential source of error as well as a computationally time-consuming step. Therefore, model 2, the simpler model, was used for the remaining analyses.

Comparison of Model 2, Bleach Test and Graphical Calculations

Computation of absorption coefficients obtained using model 2 were compared with bleach measurements and the results of the simplified graphical analysis. In order to calculate a single value that could be compared to the single value obtained from bleach strength measurements or the graphical method, absorption coefficients (K_i) were calculated from model 2 by holding the scattering coefficient constant for all prints made on the

same stock. Thus, any difference in ink properties would be reflected in the absorption coefficient. The scattering coefficient used was 0.6273, the value obtained from the best fit of reflectance versus print weight for Ciba-Geigy Pigment subjected to 10 passes through the three-roll mill.

Computed values of the absorption coefficients obtained using Model 2 are shown in Figure 22 as a function of dispersion time. Bleach test results are shown in Figure 23. Appendix E summarizes these values. The units on the x axis are arbitrary. On Figure 23, as with bleach measurements of earlier workers (6), the absorption coefficients, in general, show modest increases in strengths as dispersion times increase.

It should be also noted, however, that one set of dispersions (those made from CIBA-GEIGY pigments) produced prints which were significantly lighter than would be predicted

Figure 22 - Relationship Between K_i Calculated From Model 2 at 620 nm and Mill Passes

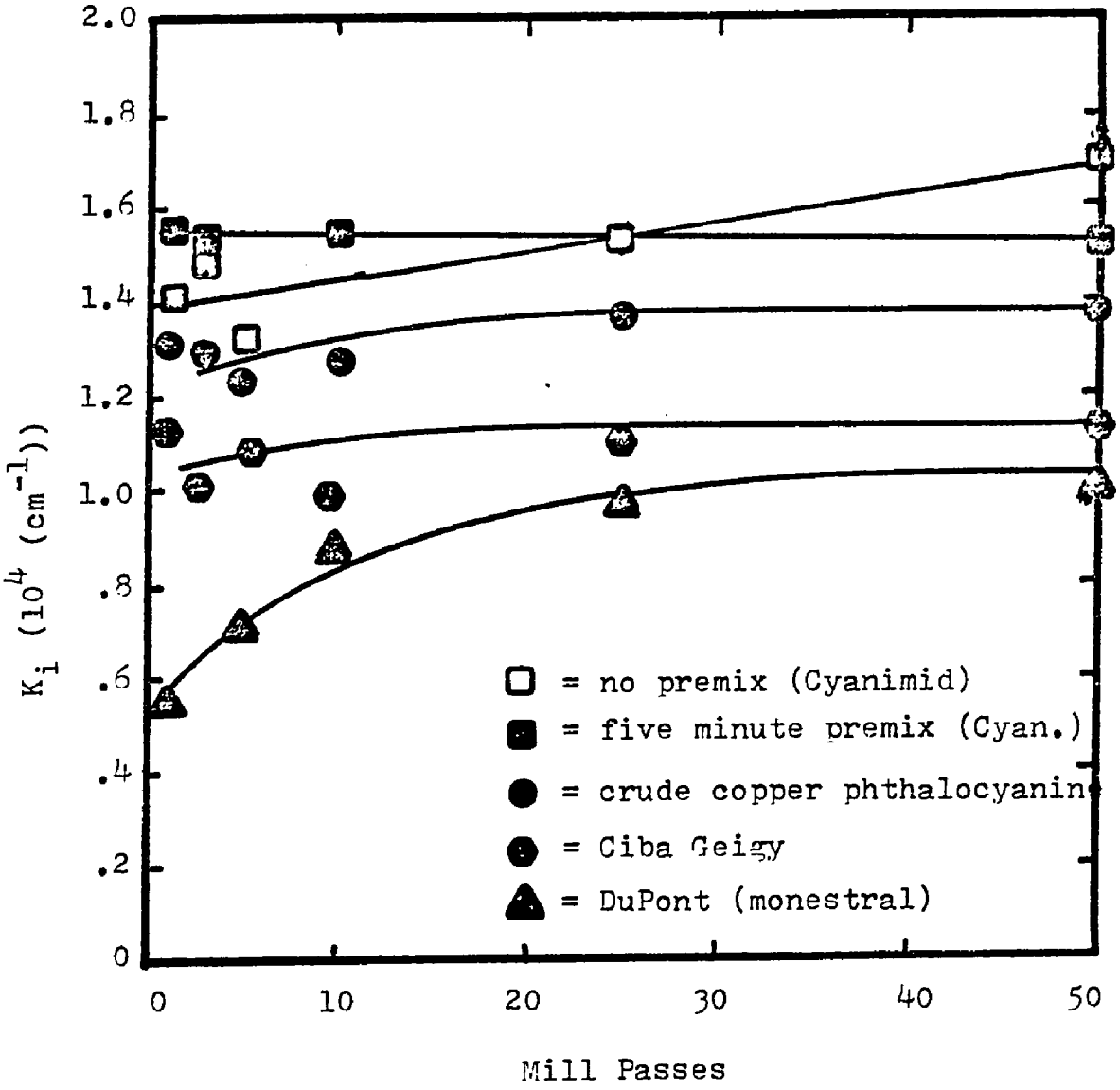

Figure 23 - Relationship Between Bleach Strength (prepared at 100:1 Bleach to Ink Ratio) and the Number of Passes Through the Three-Roll Mill

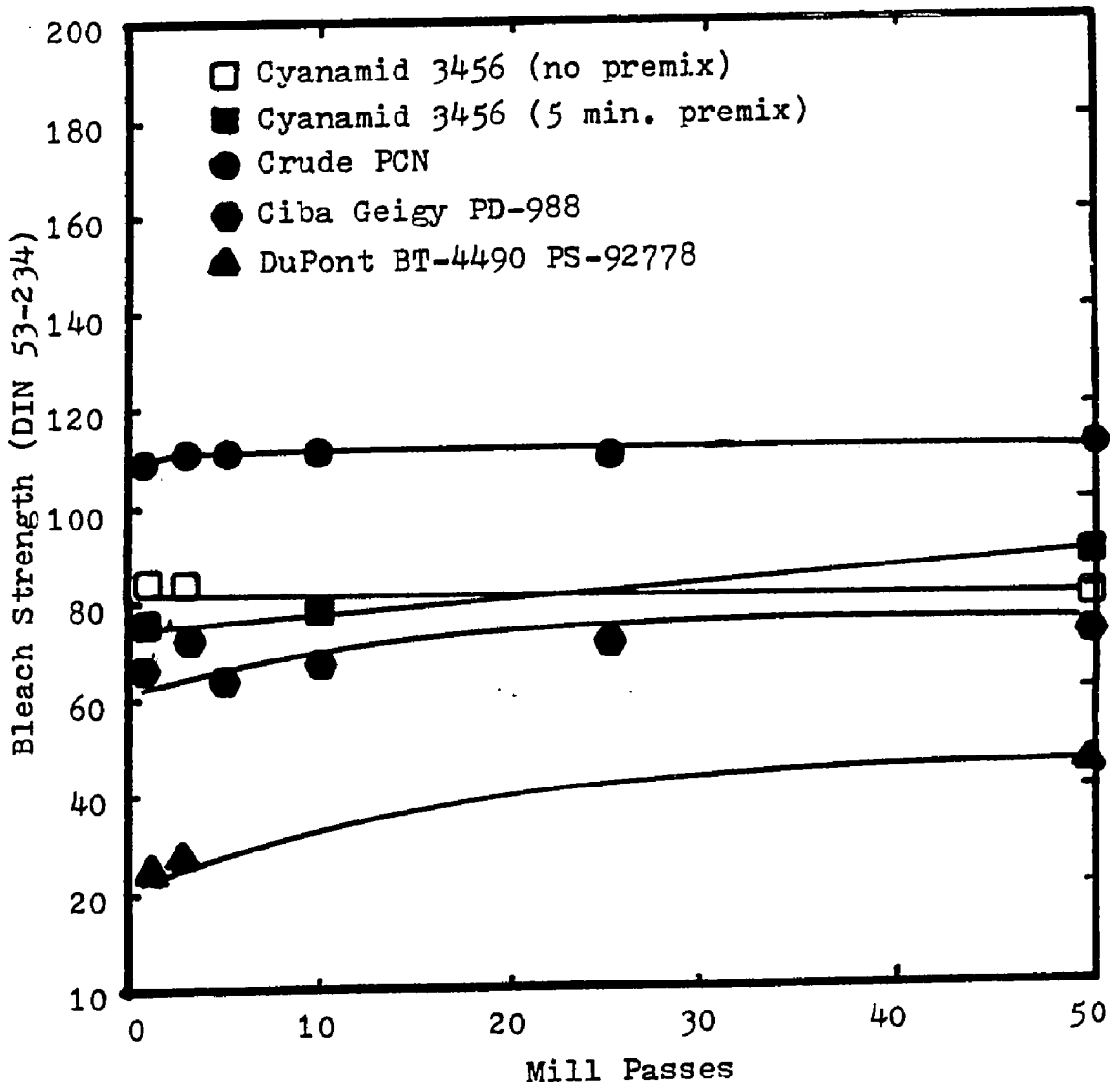

by the bleach test. In other words, although the bleaches made from CIBA-GEIGY dispersion were very much darker than those made from other pigment dispersions, the prints were not darker.

These figures indicate that bleach measurements are not related to color strengths of prints made from different pigments and confirms the practical importance of using print strength tests.

A comparison was made of the absorption coefficients with the print weights to give a 20 % reflectance at 620 nm. The purpose of this comparison was to serve as a measure of the agreement between the Kubelka-Munk model and the graphical method. Lack of a good correlation would cast doubt on the validity of the computational method used to obtain the absorption coefficient. As can be seen in Figure 24, a strong relationship does exist. Furthermore, the values

Figure 24 - Relationship Between Computed Absorption Coefficient and Print Weight at a Standard Reflectance (20%)

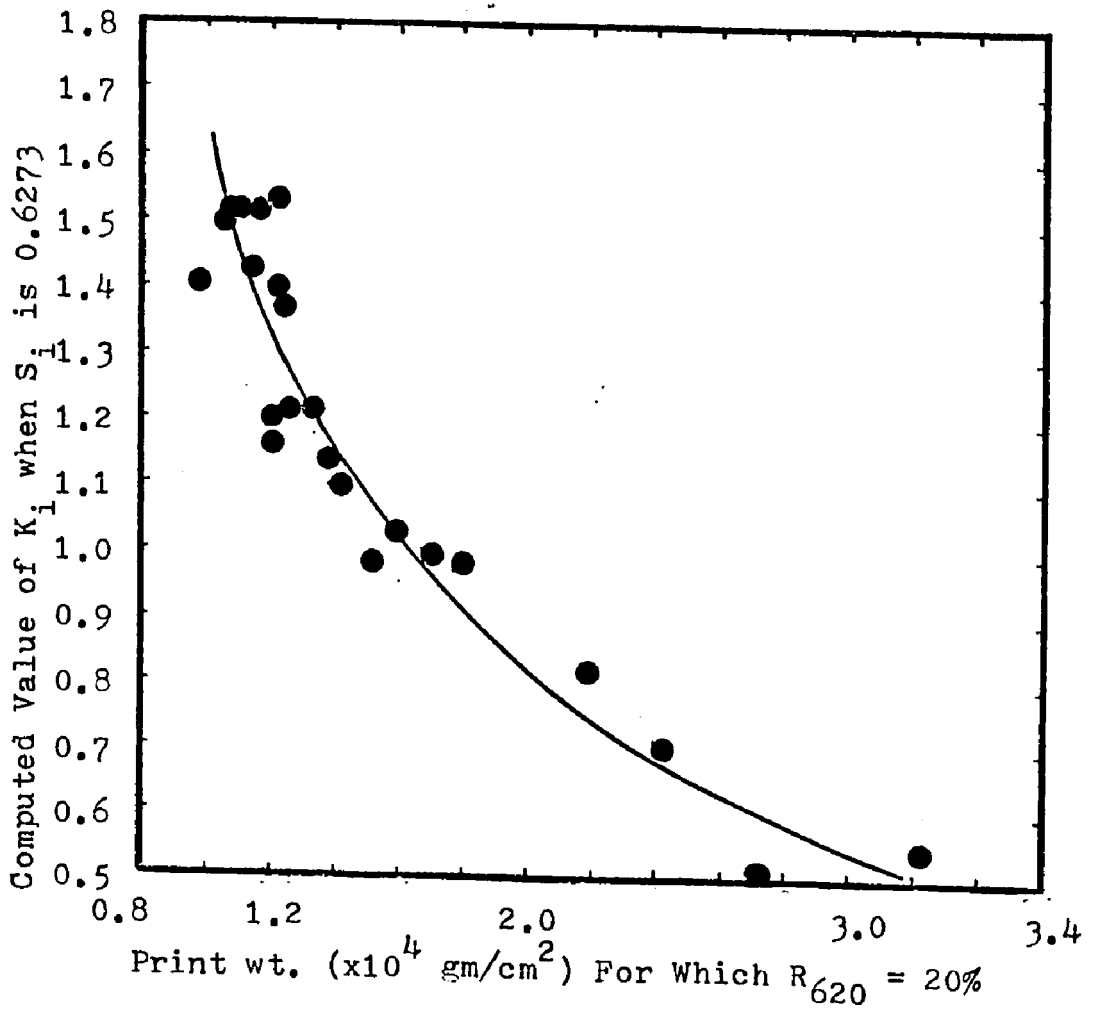

of K predicted from the fit of all the prints lie very close to the value predicted for the print using model 2 (the curved line) with S= 0.6273, Rg = 81.19%.

Influence of Stock on Reflectance

In general, the two stocks have similar reflectances at equal print weights as shown in Figure 25. Obviously, for heavy prints, the reflectance approaches the mass tone, which is independent of stock; however, it should also be noted that lighter weights as well have similar reflectances. "Medium weight prints", that is prints have reflectances slightly higher than the lowest, appear to be significantly influenced by stock. These "medium weights" are the weights of most commercial prints.

Influence of Print Weight on "Purity"

Model 2 may be simplified by assuming that the depth of the inked layer is "infinite" (i.e., that the layer is so thick that

Figure 25 - Influence of Stock on the Relationship Between Reflectance at 620 nm and Weight of Ink on Print

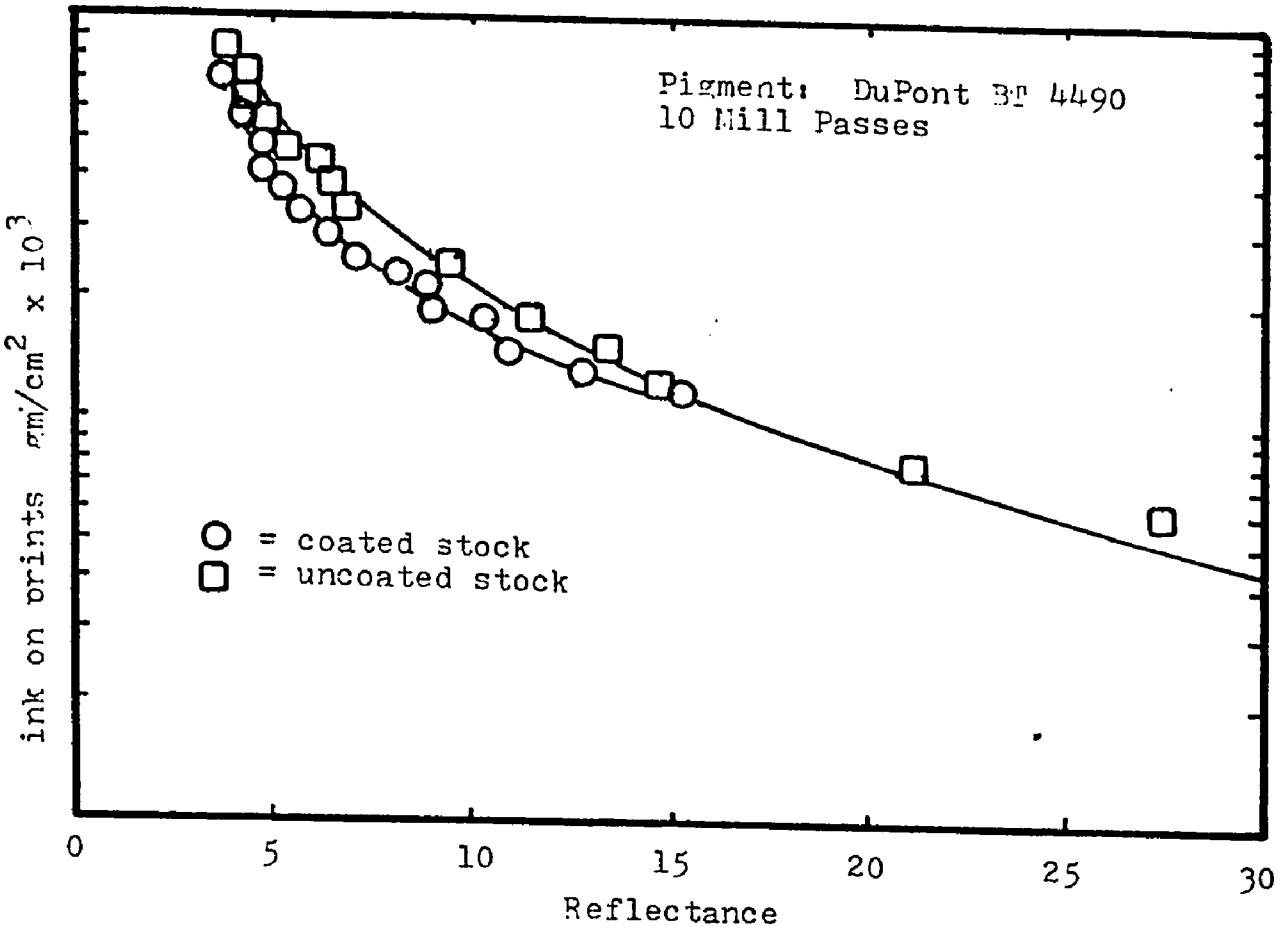

changes in thickness do not affect the reflectance). This assumption allows for the derivation of an asymptotic relationship between print weight and "purity" that had been observed by Schaeffer (99) but never explained.

The derivation begins with the general Kubelka-Munk equation for reflectance.

$$R = \frac{1 - R_g(a - b \coth(bSx))}{a + b \coth(bSx) - R_g} \qquad (19)$$

where R = reflectance at the top surface of the material

R_g = the reflectance at the bottom of the layer (here assumed to be the reflectance of unprinted paper)

$a = (K + S)/S$

$b = (a^2 - 1)^{\frac{1}{2}}$

K = the absorption coefficient of the layer

S = the scattering coefficient of the layer

x = the thickness of the layer

Note that the thickness only appears in the term bSx, When S is large (as it would be for paper), the term coth(bSx) rapidly approaches 1 as x increases. Therefore, the assumption that the film is infinitely thick is a good first approximation. For this inked layer of a print (or for any bleach), the ratio K/S has been shown to be given by equation 31 a:

$$\left(\frac{K}{S}\right)_{II} = \frac{c_p K_i + K_p}{c_p S_i + S_p} \qquad (31\ a)$$

where K_i and S_i = the absorption and scattering coefficients of the paper.

c_p = the volume fraction of ink in the layer.

For inks which have penetrated white paper (or which have been mixed with bleaches) $C_p K_i \quad K_p$ and $C_p S_i \quad S_p$; therefore, equation 31 can be approximated by equation 36.

$$\left(\frac{K}{S}\right)_{II} = \frac{c_p K_i}{S_p} \qquad (36)$$

The experimental work has already

proven that equation 36 is adequate for prints. Let us now consider the relationship between the observed reflectance, R, the amount of ink present, c_p, and the term K_i/S_p. According to Kubelka (48-50), this relationship is given by equation 37:

$$R = (c_p(K_i/S_p) + 1) - (c_p(K_iS_p) + 1)^2 - 1. \quad (37)$$

A semilog plot of reflectance versus the term c_pK_i/S_i is shown in Figure 26. As can be seen from the figure, equation 38 serves as a very good approximation for equation 37 for values of reflectance between 0.2 and 0.65:

$$R = 0.1641 \ln(0.194c_pK_i/S_p) \quad (38)$$

The form of this equation should be compared to that of the general equation relating concentration of absorbing medium, transmittance, and optical density for transmitting media:

$$T = \ln(ck) - -\ln(d) \quad (39)$$

Figure 26 - $c_p K_i/S_p$ vs. Reflectance for an Infinitely Thick Film

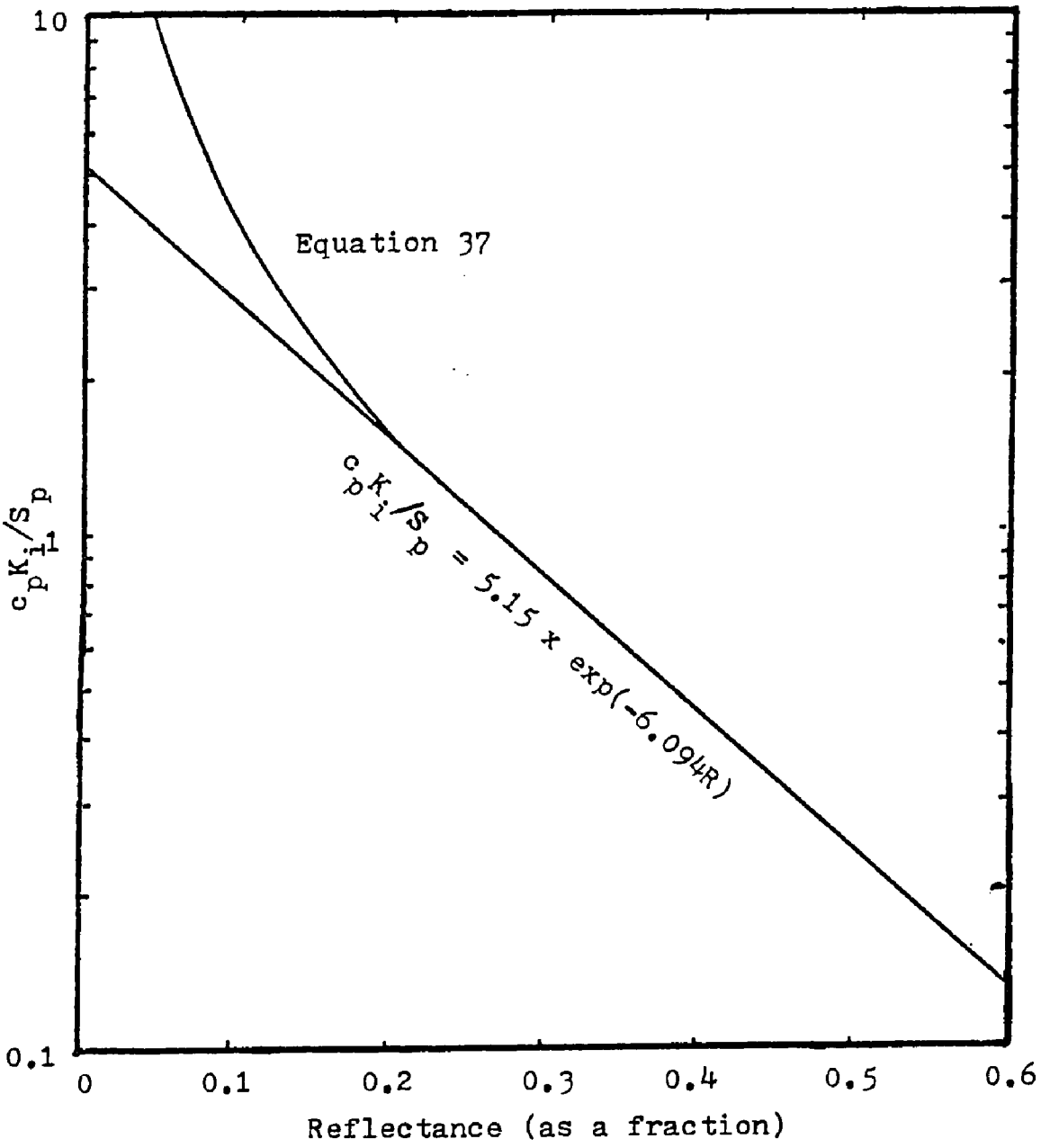

where T = transmittance = the ratio of light passing through a medium to the amount of light impinging upon the opposite surface

c = the volume concentration of absorbing material

k = a constant for a given absorbing material

D = optical density.

Although equation 38 is slightly more complex than equation 39, the exponential relationship between the reflectance and the amount of ink present is analogous to the relationship between c and T. Equation 38 is the basis for an interesting and useful property of the reflectance spectrum over the range of visible light. First, note that increasing the amount of ink present by some amount c_p result in a change in reflectance, R, which is independent of the original value of R and the value of K_i/S_i. Thus

for colored material for which equation 38 is valid, changes in the concentration of colorant will result in parallel displacement of the reflectance spectrum. Figure 27 shows a series of prints of various weights made on the same stock with the same ink. Note that the curves are approximately parallel especially for the lower, more reflective wavelengths.

Human color perception can be described mathematically by the three tristimulus values described earlier. These values are calculated from the diffuse reflectance spectrum using equations 24 a, b and c.

$$X = \int_{380}^{720} x(\lambda)R(\lambda)d \qquad (24\ a)$$

$$Y = \int_{380}^{720} y(\lambda)R(\lambda)d \qquad (24\ b)$$

$$Z = \int_{380}^{720} z(\lambda)R(\lambda)d \qquad (24\ c)$$

where X, Y and Z = the tristimulus values

Figure 27
Reflectances at Visible Wavelengths for a
Series of Weighed Prints Made from the Same Ink

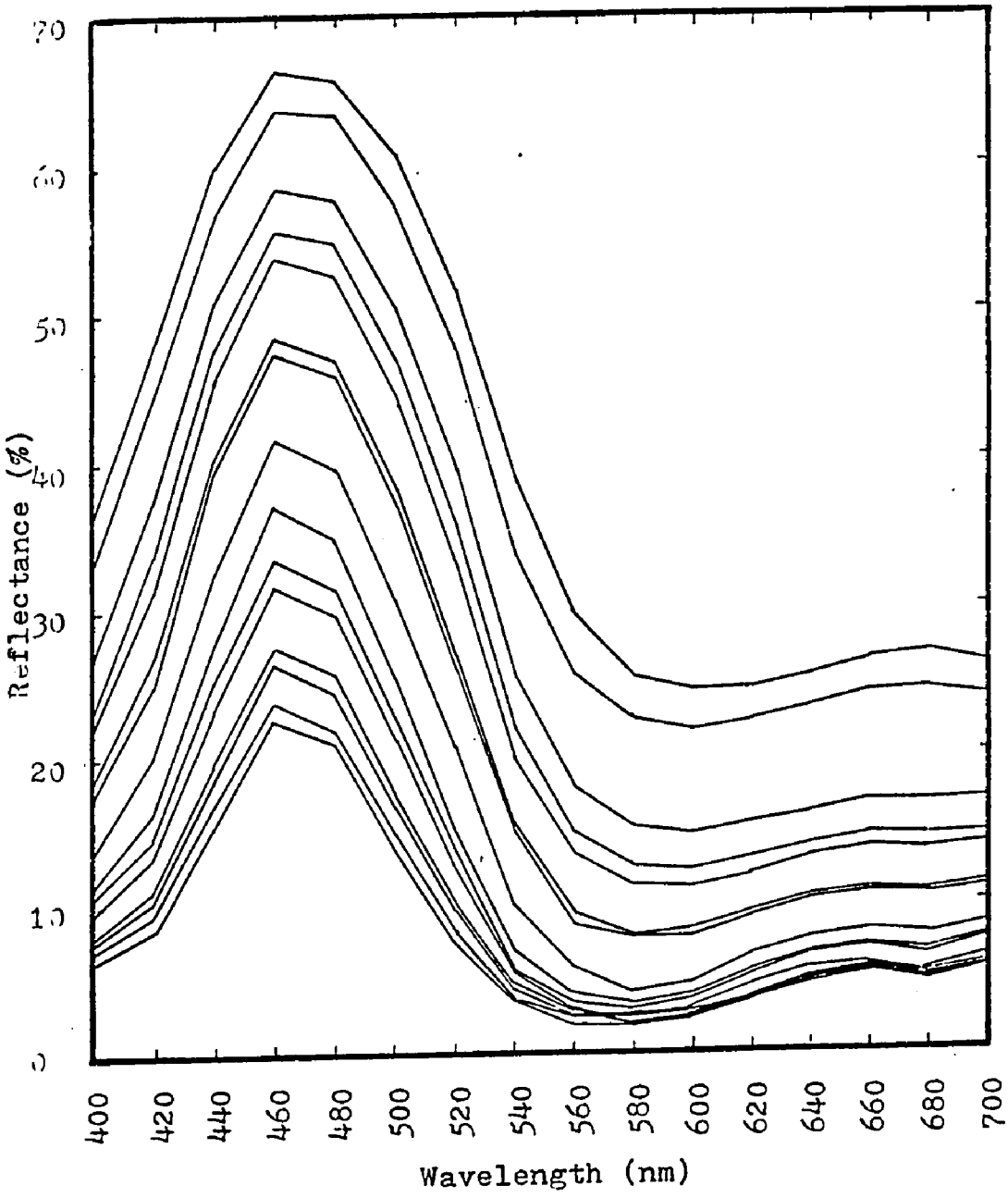

$x(\lambda)$, $y(\lambda)$ and $z(\lambda)$ = the tristimu-
functions and depend upon both the
nature of color perception and
light source

$R(\lambda)$ = the reflectance of the material
over the range of visible light

= wavelength (nm)

Substituting equation 38 into equation 34 yields, upon rearrangement, equation 40:

$$X = a_x \ln(c_p) + {}_x \tag{40}$$

where $a_x = -0.1641 \int_{380}^{720} x(\lambda)d$

$$x = 0.1641 \int_{380}^{720} x(\lambda) \ln(0.194K_i(\lambda) / S_p(\lambda))d .$$

The equations for Y and Z can be obtained also, Obviously, the tristimulus values of a series of prints made at various print weights from the same ink will be linear functions of ln(cp). The chromaticities are defined by equation 25 a, b and c:

$$x = X/(X+Y+Z) \qquad (25\ a)$$

$$y = Y/(X+Y+Z) \qquad (25\ b)$$

$$z = Z/(X+Y+Z) \qquad (25\ c)$$

The chromaticity coordinates x, y and z should not be confused with the tristimulus functions $x(\lambda)$, $y(\lambda)$ and $z(\lambda)$. Chromaticity plots of x versus y are frequently made. On such plots, the chromaticity values of a series of prints will lie along a straight line. If the "origin" of this line (i.e., the point determined by $c_p=0$) is near the point representing the light source, then the purity should follow a simple relationship with film thickness.

The above relationship had been found experimentally, but not explained by Schaeffer et al. (99). In 1961, they published the reflectances of weighed prints made from phthalocyanine blue inks. Part of their results are shown in Table 4 and Figure 28. As can be seen from the figure, the exponential

Table 4

Chromaticity Values for PCN Blue Prints

on Brush-Coated Paper

(from Schaeffer - Ref. 99)

Dispersion	Film Thickness (k)	Dominant Wave-length (nm)	Purity (%)	Brightness (%)
LV-I-5	8.0	475.5	67.0	8.5
	5.8	475.7	65.2	10.9
	4.3	476.9	63.9	13.3
	2.7	478.5	59.2	18.4
LV-V-5	8.3	475.2	68.5	8.3
	6.0	475.6	67.5	10.1
	4.1	476.5	65.4	13.0
	3.0	477.8	64.0	15.3
LV-I-10	8.5	471.8	60.2	6.2
	5.1	472.5	62.2	8.3
	3.7	474.4	64.2	10.4
	2.8	475.7	65.0	12.1
LV-V-10	8.1	470.5	60.2	6.4
	5.4	472.0	63.0	8.4
	3.7	473.9	65.0	10.0
	2.9	474.7	65.3	11.1

Figure 28 - Influence of Ink Thickness on Purity for Data of Schaeffer (Ref. 99)

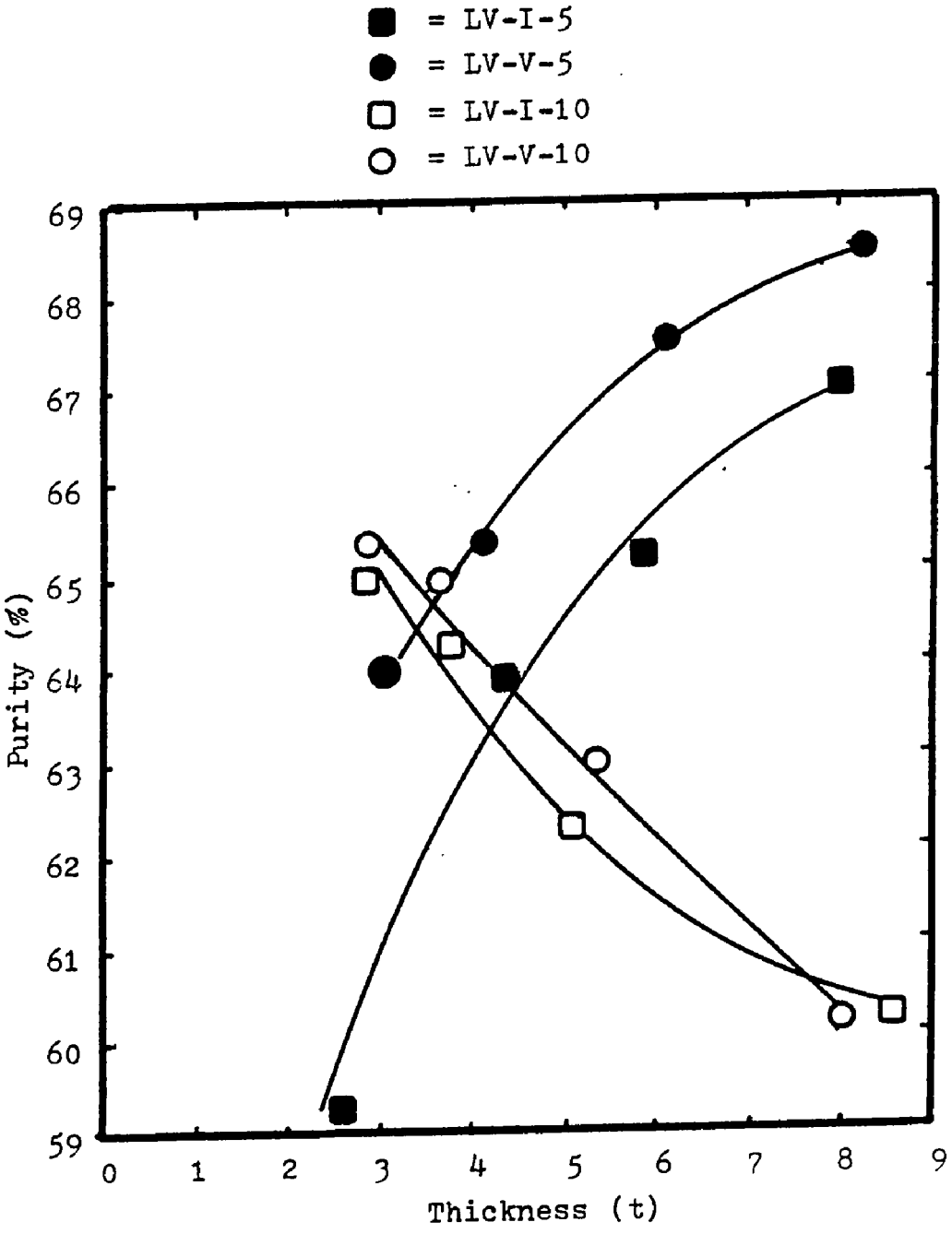

Part IV

CONCLUSIONS

The research described in Parts I, II and III has yielded several conclusions.

1. It has been demonstrated that existing bleach tests inadequately measure the color strength of inks and that an alternative method which uses the color of prints is advantageous, useful and feasible. Differences between bleach tests and actual printing conditions have been demonstrated to cause some pigment dispersions to appear stronger in bleach tests than they appear when printed. By using the simplified printing strength test presented here, the ink maker can avoid such pigments and produce his products more efficiently and cheaply.
2. In addition, it can be concluded that the primary mechanism of dispersion in

process equipment is collisions between aggregates caused by high shear. Proceeding from this assumption, it is possible to derive a system of ordinary differential equations which describe the change in the particular size distribution with time and which correctly predict the qualitative relationship between grindometer scratch count readings and dispersion time. This system of equations also predicts a quantitative relationship between pigment loading, dispersion time, and the particle size distribution observed by other workers. More detailed experimental research in this area is required before this system of equations can predict ink properties quantitatively. Controlled measurements of scratch count at various dispersion times and pigment loadings are needed to confirm the theoretical treatment (the effect of changes in

viscosity at various loading levels could also be included in such studies).

3. Modifying the Walker-Fetsko equation by replacing the first exponential term with a hyperbolic tangent gives a better fit of experimental data, especially for thin ink films. This is because the hyperbolic tangent is a better approximation of the distribution of the size of surface irregularities.

4. Wet gloss on a grindometer drawdown can be used as a measure of the quality of an ink. It has been proposed here that this measurement is related to the presence of aggregates smaller than those which cause scratches. The results may be influenced by extremely weak inks that do not hide the grindometer. For all other inks, this measurement may be a more reproducible alternative to measuring the mottle point.

relationship holds for the inks labeled "LV-I-5" and "LV-V-5" but not for "LV-I-10". For these last two inks, Schaeffer reported that surface bronzing occurred. Surface bronzing is a surface phenomena sometimes occurring when an ink does not penetrate the stock.

REFERENCES

1. "Printing Ink Handbook", Third Ed., 1976, National Association of Printing Ink Manufactureres, Inc.

2. Doubleday, D. and Barkman, A., Official Digest, 22 (307) 598-608, (Aug. 1950).

3. Walker, W. C. and Zettlemoyer, A. C., Am. Ink Maker, 27 (9) 67-69 (Sept. 1949).

4. Medalia, A. I. and Richards, L. W., J. Col. Int. Sci. 40 (2), 233-252 (Aug. 1972).

5. Mitton, P. B., "Opacity, Hiding Power and Tinting Strength", Pigment Handbook, Vol. III, Characterization and Physical Relationships, Temple C. Patton, ed., Wiley, New York, pp. 289-339, 1973.

6. Herbst, W., Farbe Lack, 76 (12), 1190-1208 (1970).

7. Herbst, W., J. Paint Tech., 45 (579), 39-50 (April 1970).

8. Gardner, H. A. and Sward, G. G., "Physical and Chemical Examination of Paint, Varnishes, Lacquers and Colors" 11th ed., Jan., 1950, Gardner Laboratory, Bethesda, Md.

9. Vanderhoff, J. W., Am. Ink Maker, 51 (7), 33, 45, 46 (Jan. 1973).

10. Austin, L. G., Powder Tech., 5 (1), 1-17 (Nov. 1971).

11. Taylor, J. H., Ph.D. Thesis, Lehigh University, 1959.

12. Sedlatschuk, K., Bass, L., Powder Met. Bull., 6 (5) 148 (May 1953).

13. Schmitz, O. J., Kroker, R., Pluhar, P., Farbe Lack, 79, 733-739 (Aug. 1973).

14. Zorll, U., Farbe Lack, 80 (1), 17-23 (Jan. 1974).

15. Patton, T. C., Off. Digest, 35 (467), 1328-1346 (Dec. 1963).

16. Weisberg, H. E., Off. Digest, 36 (478), 1261-1287 (Nov. 1964).

17. Crowl, V. T., J.O.C.C.A., 55, 388-420 (1972).

18. Von Smoluchowski, M., Physik, Z., 17, 557-585 (1916).

19. Wiegner, G. and Tourila, J., Kolloid Z., 38, 3 (1928).

20. Muller, H., Kolloidchem. Beihefte, 27, 223 (1928).

21. Overbeek, J. Th. G., "Colloid Science", Vol. 1, H. R. Kruyt, ed., Elsevier, New York, 1952.

22. Nippert, C. R., M.S. Research Report, Lehigh, (1972). "Analysis of Flow Behavior in a Two-Roll Mill: Navtoniandend Power Law Fluids.

23. Hellinchx, L. and Mewis, J., Rheologic Acta, 8 (4), 519-525 (1969).

24. Walker, W. C. and Zettlemoyer, A. C., Am. Ink Maker, 28 (7), 31-35, 55-57 (July, 1950).

25. DIN 53203.

26. NPIRI Test Method D-1.

27. ASTM D-1316-68.

28. ASTM D-1210-64.

29. Doubleday, D. and Parkman, A., Official Digest, 22 (307), 598-608 (Aug., 1950).

30. NPIRI Project Report No. 12, "The NPIRI Production Grindometer" (March, 1949).

31. NPIRI Project Report No. 24, "The NPIRI Production Grindometer II. Errors Affecting Measurement" (Feb. 1953).

32. Walker, W. C. and Zettlemoyer, A. C. Am. Ink Maker, 27 (7), 31-34, 55, 57 (July 1950).

33. Dixon, W. J. and Massey, F. J. "Introduction to Statistical Analysis", McGraw Hill, New York, 1951, pp. 102-103.

34. Walker, W. C. and Fetsko, J. M., Am. Ink Maker, 33 (12), 38 (Feb. 1955).

35. Schaeffer, W. D., Hammel, J. J., Fetsko, J. M. and Zettlemoyer, A. C., "Printing Inks and Color", Pergamon Press, New York, pp. 33-47 (1961).

36. Fetsko, J. M. and Zettlemoyer, A. C., Tappi, 45 (8), 667-681 (Aug. 1962).

37. Hungerm, G. K., Tappi, 54 (11), 1847-1852) (Nov. 1971).

38. Gate, L., Windle, W. and Hine, M., Tappi, 56 (3), 61-65 (March, 1973).

39. Ichiakawa, I., Sato, K., and Ito, Y., Res. Inst. Gov. Print. B. Japan, 1962, No. 1.

40. Cropper, M., J. Oil Color Chem. Assoc., 55 (2), 128-148 (1972).

41. Greene, R. K., Manual for the Lehigh Optimum Parameter Routine (LOPER), (Lehigh University Computing Center Program No. H20001) 1970.

42. Wyszecki, G. and Stiles, W., "Color Science, Concept and Methods, Quantitative Data and Formulas", Wiley, New York, 1967.

43. Judd, D. B. and Wyszecki, G., "Color in Business, Science and Industry", Wiley, New York, 1963.

44. Judd, D. B., "Color In Business, Science and Industry", Wiley, New York, 1952.

45. Born, M. and Wolf, E., "Principles of Optics, 2nd ed., Pergamon Press, New York, 1964.

46. Van de Hulst, H. C., "Light Scattering by Small Particles", Wiley, New York, 1957.

47. Allen, E., J. Paint Tech., 45 (584), 65-72 (Sept. 1973).

48. Saunderson, J. L., J. Opt. Soc. Am., 32 (12), 727-736 (Dec. 1942).

49. Dunstall, D. F., J. Oil Color Chem. Assoc., 55, 695-707 (1972).

50. Gate, L., Windle, W. and Hine, M., TAPPI, 56 (3), 61-65. (March 1973).

51. TAPPI Standard T 480, TAPPI, Atlanta, Ga., "Specular Gloss or Paper and Paperboard at 75 Degrees".

52. Witherell, F. E., "The Relationship Between Reflectance and Surface Roughness of Printed Ink Films", Lehigh University, M.S., Research Report, 1970.

53. Mie, G., Ann. Physik, 25 (4), 37, (1908).

54. Lowan, A. N., NBS Appl. Math. Series 4 (Jan. 25, 1945).

55. Dermedham, D., Clasen, R. and Viezce, W., J. Opt. Soc. Am., 51 (6), 620-30 (June 1961).

56. Chromey, F. C., J. Opt. Soc. Am., 50 (7), 730-737 (July, 1960).

57. Kubelka, P., J. Opt. Soc. Am., 38 (5), 448-457 (May 1948).

58. Kubelka, P., J. Opt. Soc. Am., 44 (4), 330-335 (April 1954).

59. Kubelka, P. and Munk, F., Zeit. Tech. Physik. 12, 593 (1931).

60. Duntley, S. Q., J. Opt. Soc. Am., 33 (5), 252-257 (May 1943).

61. Ross, W. D., J. Paint Tech., 39 (511), 515-521 (Aug. 1967).

62. Allen, E., "An Approach to the Computer Color Matching of Printed Ink Films", Tagungsberiet Internationale Farbtagung, COLOR 69.

63. Allen, E., J. Opt. Soc. Am., 64 (7), 991-993 (July, 1974).

64. El-Aasser, M.S., Iqbal, S., and Vanderhoff, J. W., "Model Microvoid Films, "Colloid Interface Sci. Kerker, M. ed. Academic Press, New York, 1976, 381-403, Vol. 4.

65. Kerker, M., Cooke, D. D. and Ross, W. D., J. Paint Tech., 47 (603) 33-42 (April 1975)

66. Billmeyer, F. W. and Abrams, R. L., J. Paint Tech., 45 (579), 23-40 (April 1973).

67. Billmeyer, F. W. and Abrams, R. L., J. Paint Tech. 45 (579), 31-38 (April 1973).

68. Billmeyer, F. W. and Phillips, D., J. Paint Tech., 46 (592), 36-39 (May 1974).

69. Mudgett, P. S. and Richards, L. W., Apl. Opt., 10 (7), 1485-1502 (July 1971).

70. Mudgett, P. S. and Richards, L. W., J. Col. and Int. Sci., 49 (2), 551-567 (June 1972).

71. Richards, L. W., J. Paint Tech., 42 (544), 276-286 (May 1970).

72. Brown, W. R. J., J. Opt. Soc. Am., 47 (2), 137-143 (Feb. 1967).

73. Brown, W. R. J., J. Opt. Soc. Am., 39 (10), 808-834 (Oct. 1949).

74. MacAdam, D. L., J. Opt. Soc. Am., 54 (2), 249-256 (Feb. 1964).

75. Mac Adam, D. L., J. Opt. Soc. Am., 54 (9), 1161-1165 (Sept. 1964).

76. MacAdam, D. L., J. Opt. Soc. Am., 55 (1), 91-92 (Jan. 1965).

77. MacAdam, D. L., J. Opt. Soc. Am., 56 (12), 1784-1785 (Dec. 1966).

78. Friele, L. F. C., J. Opt. Soc. Am, 55 (20), 1314-1315 (Oct. 1966).

79. Friele, L. F. C., J. Opt. Soc. Am., 56 (2), 259 (Feb. 1966).

80. Chickering, K. D., J. Opt. Soc. Am., 57 (4), 537 541 (April 1967).

81. Billmeyer, F. W., Color Engineering, pp. 28-29 (Nov. - Dec. 1967).

82. Stanley, H. D., Jr., "The Effect of Particle Size on the Color of Quinacridone Red: An Organic Pigment", Lehigh University, Master's Thesis, 1966.

83. New York Soc. for Paint Tech., Tech. Sub-Committee 83, J. Paint Tech., 45 (577), 55-59 (Feb. 1973).

84. Zettlemoyer, A. C., "Penrose Annual", 56, 116-119 (1962).

85. Hammel, J., Fetsko, J. M., Schaeffer, W. D., and Zettlemoyer, A. C., TAGA, Twelfth Meeting, June 20-22, 1960, pp. 63-79.

86. Hammel, J. J. & Fetsko, J. M. "Color Properties of PCN Blue Prints", Schaeffer, W. D., NPIRI Project Report No. 48 (Feb. 1962).

87. Garret, M. D., Am. Ink Maker, 52 (11), 20, 22, 24 (Nov. 1974).

88. Schmitz, O. J., Kroker, R. and Pluhar, P., Farbe Lack, 79 (8), 733-739 (Aug. 1973).

89. Garret, M. D., J. Paint Tech., 45 (582), 50-54 (July 1973).

90. Huelck, V., "Degree of Dispersion of Carbon Black Premixes", Lehigh University, Master's Thesis in Chem. Engr., 1969.

91. Cozzens, S. L., Schaeffer, W. D., and Zettlemoyer, A. C., J. Paint Tech., 40 (518, 99-104 (March 1968).

92. Pahlke, H., Farbe Lack, 72, 623-630; 747-758 (July, Aug. 1966).

93. Herbst, W., Am. Ink Maker, 51 (4), 60-62, 64, 66, 68, 108-111 (April 1973).

94. Schaeffer, W. D., Schiesser, R. H., Navidad, P. B. and Zettlemoyer, A. C., Official Digest, 37 (480), 78-87 (Jan. 1965).

95. NPIRI TM E2.

96. DIN 53 234.

97. Murray, A., J. Franklin Institute, (221), 721-744 (June 1936).

98. Yule, J. A. C. and Neilson, W. J., PAGA Proceedings, 3, 65-76 (1951).

99. Schaeffer, W. D., Hammel, J. J., Fetsko, J. M., Zettlemoyer, A. C., "Transfer and Color Studies With PCN Blue Dispersions, Printing Inks and Color", Pergamon Press, New York, 1961.

APPENDIX A
Grindometer Measurements

Ink	Number of Passes	Scratch Count (10^{-6}m) Two Scratch	Four Scratch	70° Gloss On Grindometer (Path Depth) 0.762×10^{-5}m (0.3 mil)	1.27×10^{-5}m (0.5 mil)	1.78×10^{-5}m (0.7 mil)	Average	Mottle
	1	9.0	8.0	91.8	90.6	92.2	91.5	
Cyanamid	3	7.9	5.6	94.2	93.8	94.0	94.0	
3456	10	3.5	2.2	94.3	94.3	94.5	94.4	
	25	2.6	1.7	95.1	94.4	94.4	94.6	
	50	3.9	2.8	94.7	94.4	95.1	94.7	
	1	4.7	3.0	99.2	99.3	99.5	99.2	
	3	3.2	2.8	98.7	98.7	98.7	98.7	
Crude	5	3.3	2.4	98.6	98.5	98.6	98.6	
	10	2.5	1.6	99.1	98.8	98.8	98.9	
	25	2.7	1.4	98.4	98.3	98.5	98.4	
	50	1.5	0.9	97.4	96.8	96.8	97.0	
	1	4.2	2.9	92.3	91.9	90.6	91.3	10
Ciba-	3	3.4	3.0	92.6	91.5	91.9	92.0	8
Giegy	5	4.4	3.0	93.4	91.7	91.5	92.2	0
PD-988	10	4.5	2.7	92.9	92.1	91.7	92.2	0
	25	2.5	1.0	92.9	91.9	91.5	92.1	0
	50	1.5	0.8	93.7	92.4	92.0	93.7	0
	1	5.1	4.6	93.2	92.8	93.8	93.3	10
DuPont	3	4.5	3.4	94.2	93.4	93.2	93.6	7.1
Bt-4490	5	4.9	2.8	94.5	93.4	92.8	93.6	5.5
Ps-92778	10	3.0	1.8	93.7	93.2	92.7	93.5	0
	25	2.3	1.0	94.8	93.2	92.8	93.6	0
	50	1.8	1.4	95.1	93.7	93.3	94.0	0

APPENDIX B

Calculated Values for the Original Walker-Fetsko and Modified Walker-Fetsko Equations Based on Transfer Measurements

Prints on Uncoated Stock

(NOTE: All prints prepared at 20kg/cm^2 unless otherwise moted)

Pigment	No. of Mill Passes	No. of Prints	Modified Walker-Fetsko Equation K'x10^{-5} (m^2/kg)	bx10^5 (kg/m^2)	f	S_e^2
American Cyanamid 3456 (no premix)	1	9	0.1626	4.917	0.2570	0.1348
	5	7	0.1231	10.95	0.0500	0.2470
	50	6	0.1930	7.219	0.5249	0.1381
(Printed @ 40)	50	20	0.1618	5.299	0.4150	0.0908
(Printed @ 60)	50	25	0.1703	5.862	0.4529	0.0384
American Cyanamid 3456 (5 Min. Premix)	3	15	0.1843	0.9331	0.5263	0.5409
	10	15	0.1900	0.4727	0.5588	0.0968
	50	13	0.1247	4.870	0.5588	0.0872
Crude	1	13	0.1461	0	0.5653	0.3098
	3	11	0.1732	0	0.6054	0.2871
	5	12	0.1472	0	0.6550	0.1817
	10	12	0.1440	0	0.6581	0.3319
	25	12	0.1821	0	0.5993	0.1614
	50	14	0.2036	0	0.5568	0.1058

Pigment	No. of Mill Passes	No. of Prints	Modified Walker-Fetsko Equation $K' \times 10^{-5}$ (m^2/kg)	$b \times 10^{5}$ (kg/m^2)	f	S_e^2
Ciba-Geigy PD-989	1	15	0.1535	8.261	0.1311	0.7108
	3	17	0.1509	8.583	0.0951	0.3314
	5	16	0.1252	7.924	0.1845	0.0810
	10	16	0.1353	9.184	0.0443	0.1117
	25	13	0.1306	8.127	0.1090	0.1181
	50	16	0.1365	8.397	0.1096	0.1096
DuPont BT-4490 PS-92778	1	13	0.1338	8,854	0.0528	0.0802
	5	15	0.1085	1.847	0.6985	0.0741
	10	15	0.1555	6.031	0.2696	0.0653
	25	18	0.1476	9.147	0.0799	0.2382
	50	17	0.1549	7.001	0.1738	0.2179

Pigment	No. of Mill Passes	No. of Prints	Original Walker-Fetsko Equation $Kx10^{-5}$ (m^2/kg)	$bx10^{5}$ (kg/m^2)	f	S_e^2	ΔS_e^2
American Cyanamid 3456 (no premix)	1	9	0.1960	9.545	0	0.1565	-0.0217
	5	7	0.1541	13.56	0.2112	0.3336	-0.0866
	50	6	0.2956	0.0065	0.5621	0.1786	-0.0866
(printed @ 40)	50	20	0.1923	15.47	0.1204	0.1055	-0.0405
(printed @ 60)	50	25	0.2095	17.65	0	0.056	-0.0172
American Cyanamid 3456 (5 Min. Premix)	3	15	0.1916	2.322	0.5247	0.5060	0.0203
	10	15	0.1541	9.057	0.2553	0.0929	0.0039
	50	13	0.1388	14.67	0.0039	0.0896	-0.0024
Crude	1	13	0.1257	2.490	0.2838	0.4741	-0.1673
	3	11	0.1347	17.87	0.0083	0.3432	-0.0561
	5	12	0.1169	31.82	0	0.2311	-0.494
	10	12	0.1175	29.61	0	0.4311	-0.0992
	25	12	0.1358	18.16	0	0.1772	-0.0158
	50	14	0.1456	13.32	0.0132	0.0543	0.1037
Ciba-Geigy PD-989	1	15	0.2045	10.57	0	0.6085	0.1023
	3	17	0.2002	10.74	0	0.4373	-0.1059
	5	16	0.1023	12.34	0	0.0964	-0.0154
	10	16	0.1807	10.49	0	0.2288	-0.1171
	25	13	0.1735	10.37	0	0.3491	-0.2310
	50	16	0.1769	11.02	0.0001	0.3561	-0.2465

Pigment	No. of Mill Passes	No. of Prints	Original Walker-Fetsko Equation $Kx10^{-5}$ (m^2/kg)	$bx10^{5}$ (kg/m^2)	f	S_e^2	ΔS_e^2
DuPont	1	13	0.1956	13.26	0	0.1204	-0.0402
BT-4490	5	15	0.1399	2.333	0.7127	0.0716	0.0025
PS-92778	10	15	0.1900	11.68	0	0.1028	-0.0375
	25	18	0.1984	11.05	0	0.3165	-0.0783
	50	17	0.2028	9.126	0.0812	0.3108	-0.0929

Prints on Coated Stock

Pigment	No. of Mill Passes	No. of Prints	Modified Walker-Fetsko Equation $K' \times 10^{-5}$ (m^2/kg)	$b \times 10^{5}$ (kg/m^2)	f	S_e^2
Ciba-Geigy PD-989	1	17	0.2724	1.570	0.2557	0.3167
	10	16	0.3480	1.207	0.2829	0.0639
	50	17	0.1578	2.100	0.2430	0.2168
DuPont	1	17	0.3631	1.225	0.3045	0.0526
	10	18	0.4017	1.237	0.2925	0.1186
	50	17	0.2831	1.617	0.2699	0.0347

Pigment	No. of Mill Passes	No. of Prints	Original Walker-Fetsko Equation $Kx10^{-5}$ (m^2/kg)	$bx10^5$ (kg/m^2)	f	S_e^2	ΔS_e^2
Ciba-Geigy PD-989	1	17	0.3881	1.690	0.2511	0.2950	0.2950
	10	16	-	-	-	-	-
	50	17	0.1762	2.959	0.2168	0.3345	-0.0753
DuPont	1	17	0.5053	13.46	0.2989	0.0476	0.0051
	10	18	0.6010	1.280	0.2907	0.1222	-0.0036
	50	17	0.3983	1.752	0.2644	0.0349	-0.0017

APPENDIX C

Printability Data On Uncoated Stocks

Dispersion	Number Of Roll Mill Passes	Ink On Cylinder ($kg/m^2 \times 10^5$)	Ink On Print ($kg/m^2 \times 10^5$)	Reflectance At Selected Wavelengths 460	500	540	620
Am.	1	12.34	6.146	.4443	.3339	.1200	.0495
Cyanamid		9.650	5.320	.4842	.3733	.1338	.0517
3456		8.117	4.482	.4923	.3791	.1330	.0504
No Premix		6.601	3.602	.5162	.4043	.1502	.0567
		5.864	2.887	.5272	.4165	.1580	.0604
		5.019	2.309	.5560	.4497	.1801	.0720
		3.766	1.657	.6122	.5243	.2497	.1059
		3.068	1.002	.6565	.5828	.3151	.1468
		2.681	.908	.6670	.5972	.3342	.1623
Am.	3	12.33	5.749	.4356	.3189	.1066	.0436
Cyanamid		9.637	4.867	.4198	.3019	.0932	.0422
3456		7.901	4.087	.4445	.3262	.1027	.0458
No Premix		6.104	2.702	.5164	.4073	.1544	.0646
		3.009	.654	.6998	.6419	.4048	.2326
Am.	5	14.86	8.09	.3569	.2467	.0835	.0394
Cyanamid		11.36	6.273	.3806	.2645	.0821	.0394
3456		7.345	4.174	.4528	.3349	.1121	.0462
No Premix		5.159	2.49	.5375	.4268	.1623	.0872
		3.991	1.274	.6375	.5572	.2934	.1406
		3.122	.783	.6869	.6238	.3722	.1944
		2.578	.63	.7047	.6503	.4142	.2302
Am.	25	9.285	5.107	.2890	.2658	.0801	.0411
Cyanamid		6.760	3.508	.4528	.3337	.1100	.0529
3456		5.747	2.786	.5008	.3852	.1338	.0590
No Premix		10.002	6.049	.3583	.2415	.0730	.0375

Dispersion	Number Of Roll Mill Passes	Ink On Cylinder ($kg/m^2 \times 10^5$)	Ink On Print ($kg/m^2 \times 10^5$)	Reflectance At Selected Wavelengths 460	500	540	620
Am. Cyanamid 3456 No Premix (cont'd)	25	5.793	2.251	.5157	.4404	.1856	.0818
		5.056	2.104	.5535	.4460	.1826	.0778
			.892	.6671	.5960	.3386	.1714
Am. Cyanamid 3456 No premix	50	11.99	6.381	.3459	.2296	.0673	.0368
		8.565	4.80	.4002	.2789	.0876	.0408
		6.518	3.18	.4860	.3681	.1309	.0548
		5.715	2.51	.5232	.4090	.1557	.0656
		4.542	1.89	.4705	.4663	.1998	.0833
		3.400	1.23	.6163	.5254	.2495	.1100
Am. Cyanamid 3456 5 Min. Premis	1	10.02	5.290	.4080	.2878	.0946	.0422
		8.800	4.629	.4279	.3057	.1305	.0430
		9.216	4.480	.4315	.3101	.1012	.0439
		8.041	4.160	.4365	.3141	.0970	.0413
		7.993	3.946	.4456	.3247	.1077	.0451
		6.912	3.475	.4767	.3592	.1282	.0516
		6.194	3.006	.5108	.3955	.1471	.0518
		5.377	2.177	.5575	.4509	.1916	.0813
		4.851	2.040	.5633	.4565	.1907	.0784
		4.292	1.655	.5999	.5032	.2339	.0987
		3.785	1.385	.6268	.5415	.2741	.1155
		3.404	1.088	.6508	.5735	.3085	.1443
		2.997	.736	.7007	.6434	.4089	.2266
		2.659	.682	.7012	.6449	.4094	.2226
Am. Cyanamid 3456 5 Min. Premix	3	12.03	6.898	.3308	.2243	.0747	.0369
		10.94	6.051	.3558	.2444	.0759	.0399
		9.659	4.591	.3704	.2559	.0826	.0397
		7.627	4.118	.4231	.3055	.1004	.0433
		6.616	3.398	.4595	.3108	.1195	.0509

Dispersion	Number Of Roll Mill Passes	Ink On Cylinder ($kg/m^2 \times 10^5$)	Ink On Print ($kg/m^2 \times 10^5$)	Reflectance At Selected Wavelengths 460	500	540	620
Am. Cyanamid 3456 5 Min. Premix (cont'd)	3	6.077	2.936	.4845	.3718	.1367	.0577
		5.426	2.429	.5249	.4177	.1653	.0703
		4.713	2.059	.5468	.4417	.1789	.0768
		4.045	1.637	.5924	.4998	.1983	.1022
		3.675	1.494	.6065	.5193	.2531	.1188
		3.291	1.175	.6354	.5563	.2896	.1355
		2.904	.928	.6690	.6037	.3499	.1786
		2.542	.816	.6777	.6164	.3678	.1911
		2.270	.604	.7048	.6559	.4244	.2378
		2.008	.540	.7195	.6760	.4547	.2639
Am. Cyanamid 3456 5 Min. Premix	10	11.68	6.409	.3419	.2316	.0760	.0400
		10.43	5.978	.3565	.2419	.0779	.0396
		8.851	4.859	.3953	.2761	.0879	.0431
		7.730	4.079	.4259	.3073	.1017	.0470
		7.008	3.582	.4496	.3322	.1137	.0504
		6.295	3.179	.4749	.3589	.1229	.0563
		5.225	2.347	.5080	.3948	.1462	.0622
		4.919	2.025	.5524	.4488	.1890	.0837
		4.297	1.737	.5840	.4866	.2164	.0949
		3.783	1.430	.6143	.5280	.2595	.1205
		3.345	1.173	.6255	.5437	.2746	.1271
		2.813	.901	.6623	.5937	.3336	.1663
		2.512	.800	.6736	.6086	.3492	.1768
		2.297	.578	.7043	.6550	.4191	.2304
		2.015	.445	.7231	.6839	.4754	.2851
Am. Cyanamid 3456 5 Min. Premix	50	10.66	5.850	.3674	.2458	.0804	.0377
		9.263	4.910	.4012	.2772	.0907	.0401
		8.345	4.430	.4164	.2907	.0937	.0412
		7.977	4.160	.4310	.3047	.099	.0432
		6.871	3.460	.4635	.3382	.112	.0496
		6.092	2.940	.5023	.3802	.135	.0576

Dispersion	Number Of Roll Mill Passes	Ink On Cylinder ($kg/m^2 \times 10^5$)	Ink On Print ($kg/m^2 \times 10^5$)	Reflectance At Selected Wavelengths 460	500	540	620
Am. Cyanamid	50	5.321	2.160	.5534	.441	.187	.0819
3456 5 Min.		4.594	1.800	.6016	.5013	.2397	.1104
Premix		4.109	1.580		.5009	.2327	.1021
(cont'd)		3.575	1.350	.6285	.5402	.270	.1230
		3.137	.857	.6906	.6252	.3769	.2016
		2.799	.861	.6967	.6326	.379	.1967
		2.355	.613	.712	.6592	.4231	.2291
Crude PCN	1	10.61	5.300	.3659	.3067	.1528	.0918
5 Min.		8.908	4.615	.4039	.3454	.1819	.1061
Premix		7.284	3.046	.4235	.3658	.1976	.1168
		7.037	3.170	.4762	.4217	.2413	.1451
		6.601	2.986	.4919	.4386	.2541	.1532
		5.837	2.270	.5456	.4963	.3107	.1951
		4.782	1.740	.5887	.5464	.3592	.2270
		5.318	2.310	.5574	.5101	.3202	.1987
		4.275	1.136	.6693	.6742	.4805	.3454
		3.888	1.077	.6577	.6268	.4599	.3220
		3.621	.816	.6878	.6628	.5107	.3740
		3.313	.894	.6822	.6582	.5060	.3653
		3.215	.368	.7450	.6654	.5157	.3758
		2.561	.368	.7450	.7344	.6282	.5068
Crude PCN	3	11.71	6.820	.3061	.24793	.1132	.0706
5 Min.		11.00	6.150	.3270	.26927	.1296	.7680
Premix		8.484	4.980	.3649	.30877	.1512	.0865
		7.791	4.320	.3939	.33400	.1679	.0955
		6.996	3.490	.4323	.37457	.1970	.1112
		5.353	2.330	.5347	.48483	.2894	.1687
		5.056	2.040	.5509	.50210	.3060	.1818
		4.043	1.590	.5926	.55023	.3577	.2193
		4.101	1.330	.6153	.57833	.3944	.2542

Dispersion	Number Of Roll Mill Passes	Ink On Cylinder ($kg/m^2 \times 10^5$)	Ink On Print ($kg/m^2 \times 10^5$)	Reflectance At Selected Wavelengths 460	500	540	620
Crude PCN	3	3.293	1.030	.6519	.62090	.4422	.2916
5 Min.		2.879	.674	.6986	.67857	.5276	.3780
Premix		2.600	.664	.6977	.67937	.5353	.3909
(cont'd)							
Crude PCN	5	9.966	5.777	.3384	.2773	.1286	.0756
5 Min.		9.730	5.674	.3411	.2786	.1366	.0795
Premix		8.058	4.351	.3908	.3299	.1624	.0901
		7.204	3.977	.4068	.3449	.1696	.0940
		6.023	2.922	.4778	.4210	.2298	.1259
		5.328	2.160	.5339	.4822	.2840	.1623
		4.772	1.933	.5451	.4937	.2898	.1652
		4.392	1.513	.5882	.5449	.3486	.2103
		3.827	1.291	.6093	.5703	.3752	.2290
		3.396	1.022	.6490	.6104	.4352	.2846
		3.359	.780	.6917	.6695	.5077	.3512
		2.529	.566	.7188	.7042	.5713	.4163
Crude PCN	10	11.38	6.745	.2993	.2399	.1044	.0612
5 Min.		9.434	5.631	.3309	.2692	.1166	.0690
Premix		8.051	4.386	.3789	.3155	.1455	.0782
		6.834	3.564	.4267	.3655	.1781	.0934
		6.276	3.167	.4760	.3819	.1883	.1008
		5.448	2.436	.4895	.4324	.2270	.1218
		5.078	1.990	.5318	.4786	.2715	.1498
		4.630	1.436	.5859	.5407	.3376	.1987
		3.893	1.181	.6167	.5747	.4725	.2216
		3.448	.982	.6516	.6167	.4214	.2604
		2.941	.596	.6879	.6622	.4910	.3303
		2.476	.505	.7150	.6952	.5375	.3726
Crude PCN	25	10.02	5.647	.3142	.2499	.0994	.0574
5 Min. Premix		8.531	4.777	.3425	.2753	.1127	.0617

Dispersion	Number Of Roll Mill Passes	Ink On Cylinder ($kg/m^2 \times 10^5$)	Ink On Print ($kg/m^2 \times 10^5$)	Reflectance At Selected Wavelengths 460	500	540	620
Crude PCN	25	7.688	3.956	.3828	.3140	.1337	.0693
5 Min.		6.969	3.734	.3950	.3264	.1417	.0765
Premix		5.771	3.711	.4689	.4041	.1926	.0963
(cont'd)		5.482	2.307	.4901	.4277	.2161	.1111
		4.327	1.943	.5439	.4856	.2589	.1347
		3.903	1.380	.6002	.5522	.3304	.1774
		3.499	1.137	.6228	.5788	.3633	.2077
		3.026	.885	.6519	.6249	.4193	.2523
		2.747	.735	.6800	.6483	.4488	.2708
		2.463	.553	.7036	.6788	.5019	.3249
Crude PCN	50	13.60	7.070	.2717	.206	.072	.0450
5 Min.		12.04	6.440	.289	.2221	.0811	.0462
Premix		10.10	5.970	.3102	.2396	.0	.0496
		8.893	5.160	.3373	.2643	.100	.0599
		7.598	3.915	.3948	.3214	.132	.0735
		6.716	3.416	.4129	.3390	.1003	.0784
		5.659	2.623	.4806	.4103	.1919	.0947
		5.201	1.977	.5315	.4678	.2456	.1290
		4.400	1.500	.5918	.5347	.308	.1726
		3.815	1.463	.5844	.5257	.2885	.1520
		3.614	1.187	.6080	.5555	.3264	.1819
		2.936	.875	.6540	.6105	.3916	.2265
		2.255	.161	.6790	.6448	.4486	.2826
		2.473	.528	.6953	.6646	.4777	.3092
Ciba-Geigy	1	29.14	9.402	.226	.1336	.033	.0315
PD-989		24.19	9.474	.2293	.1354	.0338	.0387
		21.80	9.564	.2289	.1350	.0332	.0363
		18.95	8.964	.2435	.1462	.0352	.0370
		17.35	8.173	.2534	.1542	.0370	.0370
		15.09	7.488	.2611	.1594	.0361	.0401

Dispersion	Number Of Roll Mill Passes	Ink On Cylinder ($kg/m^2 \times 10^5$)	Ink On Print ($kg/m^2 \times 10^5$)	Reflectance At Selected Wavelengths 460	500	540	620
Ciba-Geigy PD-989 (cont'd)	1	14.05	8.156	.2764	.1727	.0401	.0371
		8.492	4.864	.3623	.2503	.0705	.0574
		7.414	4.200	.3923	.2790	.0859	.0597
		6.494	3.519	.4073	.2915	.0892	.0592
		5.708	2.994	.4507	.3368	.1143	.0716
		4.973	2.582	.4770	.3633	.1249	.0787
		4.248	2.036	.5215	.4133	.1622	.0934
		3.832	1.630	.5648	.467	.2099	.1221
		3.315	1.337	.5893	.493	.2294	.1292
		2.904	1.158	.6097	.5214	.2580	.1535
		2.610	.928	.6395	.5606	.3013	.1737
Ciba-Geigy PD-989	3	21.49	9.087	.2371	.1414	.0357	.0306
		18.60	8.768	.2459	.1471	.0353	.0500
		16.77	8.171	.2541	.1529	.035	.0431
		14.70	7.437	.2768	.1718	.0408	.0417
		12.99	6.763	.2759	.1705	.0394	.0404
		11.19	6.329	.3002	.1914	.045	.0437
		9.850	6.003	.3304	.2170	.0522	.0522
		8.695	4.882	.3533	.2382	.0626	.0492
		7.566	4.273	.3807	.2652	.0758	.0546
		6.369	3.484	.4216	.3041	.0945	.0624
		5.744	3.173	.4440	.3261	.1044	.0713
		5.020	2.335	.4946	.3820	.1436	.0865
		4.358	2.010	.5217	.4138	.1660	.0965
		3.795	1.558	.5629	.4611	.2020	.1163
		3.271	1.320	.5860	.5890	.227	.1374
		2.936	1.001	.6265	.5421	.28	.1691
		2.534	.778	.6590	.5870	.3417	.2118
Ciba-Geigy PD-989	5	20.76	9.420	.2280	.133	.033	.0388
		18.19	8.926	.2386	.1406	.0337	.0445

Dispersion	Number Of Roll Mill Passes	Ink On Cylinder ($kg/m^2 \times 10^5$)	Ink On Print ($kg/m^2 \times 10^5$)	Reflectance At Selected Wavelengths 460	500	540	620
Ciba-Geigy PD-989 (cont'd)	5	15.81	8.440	.2497	.1500	.0369	.0407
		13.74	7.697	.2629	.1611	.0	.0418
		12.10	6.575	.287	.1812	.0444	.0427
		10.67	6.078	.3035	.1937	.045	.0476
		9.876	5.253	.3310	.2187	.0572	.0454
		8.190	4.483	.3672	.2511	.0701	.0499
		7.066	4.043	.3865	.2680	.073	.0540
		5.992	2.892	.450	.3342	.1140	.0684
		5.130	2.443	.4894	.3762	.14	.0820
		4.515	1.716	.5575	.4560	.2081	.1196
		3.822	1.156	.6259	.5395	.2868	.1703
		3.526	1.075	.6296	.5421	.2771	.1525
		2.926	.568	.6977	.6379	.408	.2617
		1.974	.213	.7547	.7256	.5585	.4072
Ciba-Geigy PD-989	10	20.09	8.664	.2348	.1401	.041	.0133
		17.05	7.845	.2538	.152	.0350	.0298
		15.13	7.568	.2563	.1558	.0388	.0249
		13.58	7.077	.2779	.1721	.0407	.0282
		11.90	6.380	.2938	.1848	.0408	.0399
		10.37	5.565	.3218	.2110	.0538	.0324
		9.187	5.080	.3434	.2311	.0622	.0349
		8.039	4.306	.3794	.2635	.0753	.0447
		7.020	3.865	.3992	.2818	.0811	.0494
		6.107	3.133	.4519	.3370	.1178	.0650
		5.360	2.495	.4865	.3758	.1424	.0759
		4.635	1.986	.5475	.4458	.1993	.1134
		4.106	1.719	.5618	.4594	.2031	.1181
		3.465	1.147	.6228	.5395	.2958	.1827
		3.144	1.028	.6384	.5564	.3051	.1848
		2.742	.903	.6595	.5832	.3314	.2022

Dispersion	Number of Roll Mill Passes	Ink On Cylinder ($kg/m^2 \times 10^5$)	Ink On Print ($kg/m^2 \times 10^5$)	Reflectance At Selected Wavelengths 460	500	540	620
Ciba-Geigy PD-989	25	18.35	7.945	.2424	.1448	.0377	.0175
		16.41	7.907	.2595	.1576	.0387	.0186
		12.33	6.520	.2809	.1760	.0439	.0193
		11.07	5.798	.3095	.1990	.0494	.0239
		9.787	5.309	.3304	.2189	.0583	.0268
		8.423	4.662	.3528	.2372	.0612	.0392
		7.346	3.777	.4107	.2976	.0998	.0494
		6.420	3.324	.4322	.3158	.1030	.0510
		5.531	2.491	.4982	.3878	.1530	.0786
		4.704	1.980	.5432	.4379	.1867	.0878
		4.214	1.713	.6139	.5252	.2756	.0966
		3.712	1.220	.6407	.5594	.3111	.1552
Ciba-Geigy PD-989	50	20.57	9.137	.2267	.1347	.0319	.0343
		17.52	8.196	.2389	.1447	.0344	.0311
		15.82	7.788	.2562	.1581	.0384	.0326
		13.11	6.871	.2714	.1683	.0352	.0399
		11.32	6.227	.2743	.1708	.0372	.0399
		9.775	5.465	.3174	.2103	.0515	.0417
		8.707	5.081	.3343	.2245	.0545	.0512
		7.502	4.060	.3671	.2545	.0699	.0510
		6.540	3.300	.4283	.3208	.1133	.0710
		5.526	2.665	.4739	.3683	.1423	.0901
		5.007	2.199	.4853	.3794	.1421	.0918
		4.339	1.968	.5390	.4416	.1975	.1195
		3.896	1.395	.5638	.4735	.2245	.1374
		3.421	1.188	.5862	.5020	.2522	.1502
		2.928	.970	.6393	.5719	.3377	.2229
		2.605	.702	.6618	.6047	.3789	.2438
DuPont BT-4490 PS-92778	1	18.22	8.072	.2706	.155	.0409	.0385
		15.00	7.483	.293	.1691	.0452	.0401
		13.00	6.693	.3126	.1839	.0495	.0524

Dispersion	Number of Roll Mill Passes	Ink On Cylinder ($kg/m^2 \times 10^5$)	Ink On Print ($kg/m^2 \times 10^5$)	Reflectance At Selected Wavelengths 460	500	540	620
DuPont	1	11.41	6.167	.3287	.1967	.0505	.0423
BT-4490		9.990	5.371	.3604	.2235	.0621	.0456
PS-92778		8.834	4.715	.3777	.2367	.0657	.0465
(cont'd)		7.564	4.064	.4209	.2785	.0860	.0673
		6.839	3.481	.4445	.3025	.0986	.0620
		6.795	3.355	.4493	.3090	.1039	.0667
		4.784	2.119	.5438	.4114	.1667	.1096
		4.358	1.875	.5667	.4409	.1916	.1208
		3.602	1.389	.6130	.4961	.2358	.1529
		2.950	0.758	.6597	.5625	.3136	.2148
		2.957	1.028	.6615	.5630	.3034	.2009
DuPont	3	18.40	8.267	.26	.147	.038	.0401
BT-4490		15.97	8.024	.2746	.1514	.0361	.0465
PS-92778		13.97	7.558	.2896	.1634	.0411	.0453
		12.17	6.589	.3090	.1792	.0447	.0469
		10.70	6.083	.326	.191	.0470	.0495
		92.33	5.518	.3490	.2102	.0529	.0550
		8.225	4.730	.379	.2364	.0623	.0527
		7.341	3.738	.4310	.288	.0893	.0666
		6.332	3.368	.4464	.3019	.0932	.0695
		5.852	2.876	.489	.3505	.1248	.0867
		4.919	2.315	.5322	.3979	.1537	.1067
		3.869	1.530	.6042	.4905	.2372	.1617
		3.462	1.175	.648	.5486	.2975	.2097
		2.990	.990	.648	.545	.2842	.1928
		2.649	.72	.687	.5046	.3625	.2683
DuPont	5	25.09	19.040	.258	.1398	.0371	.0484
BT-4490		15.76	8.619	.2710	.148	.0392	.0461
PS-92778		13.54	8.061	.2835	.1582	.0415	.0471
		11.74	7.069	.3046	.1738	.0455	.0486

Dispersion	Number of Roll Mill Passes	Ink On Cylinder ($kg/m^2 \times 10^5$)	Ink On Print ($kg/m^2 \times 10^5$)	Reflectance At Selected Wavelengths 460	500	540	620
DuPont BT-4490 PS-92778 (cont'd)	5	10.10	6.101	.3308	.194	.048	.0515
		8.847	5.367	.3620	.220	.057	.0593
		8.205	4.778	.384	.240	.064	.0584
		6.998	4.076	.425	.2803	.084	.0670
		6.055	3.373	.455	.2752	.096	.0719
		5.296	2.817	.4940	.3499	.1166	.0867
		4.023	1.771	.5777	.4510	.191	.1282
		3.553	1.495	.6001	.4792	.2146	.1435
		3.044	1.292	.621	.5058	.2335	.1534
		2.588	1.014	.6592	.5589	.2895	.1976
		2.027	.53	.7176	.8545	.4278	.3153
DuPont BT-4490 PS-92778	10	17.04	8.704	.2660	.1448	.0383	.0383
		15.35	7.992	.2674	.1452	.0369	.0445
		13.38	7.328	.286	.1589	.0400	.0423
		11.74	6.521	.3076	.1756	.0450	.0439
		10.29	5.867	.3348	.1993	.0527	.0487
		7.830	4.424	.4033	.2614	.0782	.0625
		8.288	4.930	.3654	.2228	.0565	.0543
		7.262	4.075	.4161	.2721	.0806	.0628
		6.388	3.426	.4447	.3002	.0924	.0678
		4.887	2.483	.5106	.3742	.1386	.0954
		4.234	1.892	.5765	.4514	.1913	.1259
		3.861	1.673	.6217	.5128	.2522	.1696
		3.308	1.257	.6500	.5502	.2877	.1945
		2.554	.790	.6741	.5840	.3263	.2245
		2.189	.665	.6987	.6193	.3664	.2593
DuPont BT-4490 PS-92778	25	22.85	9.611	.2132	.1267	.0328	.0394
		19.83	8.833	.2342	.1673	.0509	.0446
		18.23	8.622	.2431	.1513	.0402	.0450
		16.11	8.241	.2396	.1467	.0353	.0491

Dispersion	Number of Roll Mill Passes	Ink On Cylinder ($kg/m^2 \times 10^5$)	Ink On Print ($kg/m^2 \times 10^5$)	Reflectance At Selected Wavelengths 460	500	540	620
DuPont	25	13.72	7.259	.2652	.1683	.0413	.0460
BT-4490		12.25	6.801	.2806	.18	.0490	.0483
PS-92778		10.98	6.407	.2908	.192	.0503	.0489
(cont'd)		9.549	5.619	.3101	.2083	.0548	.0513
		8.171	4.590	.3536	.2478	.0686	.0629
		7.194	4.092	.3710	.2635	.0760	.0579
		6.374	3.340	.4176	.3115	.1054	.0732
		5.397	2.548	.4759	.3750	.1473	.0947
		4.780	2.428	.4804	.3768	.1392	.0926
		4.689	2.439	.5302	.4328	.1835	.1105
		3.700	1.561	.5576	.4652	.2135	.1271
		2.760	1.009	.6099	.5279	.2663	.1578
		2.427	.734	.6618	.5961	.3544	.2229
DuPont	50	22.68	9.640	.2429	.125	.0352	.0393
BT-4490		19.27	8.638	.2613	.1387	.0372	.0400
PS-92778		18.69	8.130	.2730	.1449	.0358	.0430
		15.23	7.748	.2850	.1555	.0400	.0428
		13.89	7.250	.2990	.1673	.0439	.0454
		12.66	6.802	.3176	.1828	.0490	.0476
		11.25	6.329	.3290	.1904	.0485	.0463
		10.01	5.492	.3564	.2145		.0535
		8.812	5.075	.3737	.2289	.0614	.0518
		7.777	4.419	.3915	.2433	.0653	.0525
		6.719	3.566	.4485	.3008	.0962	.0715
		6.009	3.249	.4584	.3100	.0940	.0700
		4.425	2.099	.5397	.4014	.1537	.1021
		4.664	2.129	.5458	.4104	.1640	.1121
		4.116	1.826	.5653	.4318	.1749	.1137
		3.146	1.164	.6329	.5201	.2522	.1653
		2.483	.850	.6726	.5752	.3051	.2028

APPENDIX D

Printability Data On Coated Stocks

Dispersion	Number of Roll Mill Passes	Ink On Cylinder ($kg/m^2 \times 10^5$)	Ink On Print ($kg/m^2 \times 10^5$)	Reflectance At Selected Wavelengths 460	500	540	620
Ciba-Geigy PD-988	1	24.85	7.342	.2718	.1709	.0415	.0353
		21.94	6.654	.2878	.1824	.0387	.0399
		18.92	6.442	.3031	.1941	.0388	.1417
		17.09	5.567	.3193	.2084	.0425	.0498
		15.05	4.948	.3473	.2338	.0513	.0601
		11.64	4.261	.3695	.2502	.0445	.0579
		10.54	3.748	.3966	.2791	.0620	.0740
		9.050	3.478	.4036	.2820	.0521	.0674
		7.911	2.947	.4334	.3133	.0684	.0807
		6.890	2.713	.4433	.3219	.0660	.0775
		5.935	2.405	.4777	.3592	.0856	.0882
		5.193	2.158	.4926	.3765	.0964	.0924
		4.721	1.980	.5033	.3878	.0998	.0952
		4.030	1.738	.5333	.4236	.1325	.1098
		3.531	1.559	.5513	.4447	.1482	.1161
Ciba-Geigy	10	23.47	7.404	.2741	.1675	.0361	.0393
		20.68	6.835	.2846	.1755	.0352	.0419
		18.28	6.048	.3057	.1928	.0382	.0461
		15.61	5.379	.3248	.2103	.0413	.0543
		14.34	4.799	.3701	.2498	.0495	.0680
		12.08	4.248	.3534	.2367	.0522	.0667
		11.42	4.135	.3720	.2496	.0430	.0515
		8.139	3.138	.4319	.3121	.0739	.0904
		8.438	3.232	.4191	.2974	.0594	.0783
		7.583	2.985	.4370	.3163	.0700	.0881
		6.584	2.714	.4487	.3253	.0638	.0805

Dispersion	Number of Roll Mill Passes	Ink On Cylinder ($kg/m^2 \times 10^5$)	Ink On Print ($kg/m^2 \times 10^5$)	Reflectance At Selected Wavelengths 460	500	540	620
Ciba-Geigy (cont'd)	10	5.798	2.345	.4797	.3608	.0875	.0946
		5.113	2.182	.4880	.3707	.0908	.0942
		4.378	1.895	.5098	.3939	.1025	.0942
		3.827	1.638	.5353	.4252	.1348	.1165
		3.288	1.480	.5617	.4563	.1563	.1224
		3.002	1.253	.5988	.5054	.2143	.1618
Ciba-Geigy PD-988	50	26.47	8.083	.2603	.1554	.0369	.0438
		22.90	7.118	.2782	.1700	.0528	.0469
		20.43	6.672	.2939	.1824	.0369	.0505
		15.78	5.290	.3303	.2130	.0376	.0545
		16.22	5.329	.3314	.2138	.0369	.0522
		14.34	4.802	.3546	.2351	.0437	.0601
		12.53	4.358	.3674	.2474	.0465	.0621
		10.80	3.935	.3884	.2668	.0505	.0654
		9.500	3.501	.4071	.3212	.0553	.0785
		8.325	3.308	.4232	.3003	.0554	.0735
		7.363	2.961	.4490	.2834	.0683	.0763
		6.329	2.424	.4793	.3639	.0959	.1011
		5.517	2.029	.5099	.3985	.1208	.1051
		4.593	1.506	.5790	.4742	.1895	.1342
		3.504	.999	.6431	.5665	.2974	.2116
		3.367	.801	.6685	.5993	.3353	.2323
		2.808	.472	.7106	.6606	.4230	.2956
DuPont BT-4490 PS-92778		21.49	5.317	.2988	.1691	.038	.0376
		19.26	6.743	.3035	.1746	.0379	.0384
		16.92	5.947	.3240	.1915	.0385	.0396
		14.79	5.302	.3469	.2094	.0395	.0415
		13.00	4.825	.3612	.2215	.0760	.0432
		11.57	4.492	.3814	.2395	.0418	.0440
		10.35	3.988	.4039	.2599	.0460	.0492

Dispersion	Number of Roll Mill Passes	Ink On Cylinder ($kg/m^2 \times 10^5$)	Ink On Print ($kg/m^2 \times 10^5$)	Reflectance At Selected Wavelengths 460	500	540	620
DuPont	1	8.854	3.554	.4255	.2811	.0498	.0528
BT-4490		8.004	3.314	.4466	.2988	.0536	.0551
PS-92778		6.513	2.779	.4859	.3368	.0661	.0648
(cont'd)		6.410	2.764	.4905	.2417	.0676	.0674
		6.090	2.484	.5104	.3695	.1032	.0968
		5.223	2.330	.5250	.3741	.0829	.0796
		4.432	2.033	.5475	.4025	.0952	.0827
		3.555	1.607	.5922	.4603	.1482	.1169
		3.394	1.565	.5956	.4619	.1434	.1077
		3.002	1.315	.6347	.5153	.2038	.1559
		2.627	1.205	.6476	.5295	.2100	.1534
DuPont	10	22.30	7.411	.2829	.1510	.0352	.0379
BT-4490		19.06	6.518	.3141	.1760	.0347	.0430
PS-92778		17.00	5.839	.3266	.1867	.0358	.0438
		15.16	5.254	.3533	.2416	.0373	.0485
		13.20	4.859	.3660	.2194	.0381	.0498
		12.40	4.233	.3766	.2286	.0375	.0479
		10.51	3.997	.4018	.2520	.0408	.0528
		9.655	3.671	.4183	.2685	.0471	.0572
		8.298	3.389	.4346	.2848	.0520	.0606
		7.333	3.034	.4501	.2994	.0502	.0642
		6.256	2.697	.4779	.3307	.0698	.0761
		5.656	2.454	.4964	.3527	.0814	.0816
		5.223	2.296	.5078	.3652	.0882	.0892
		4.481	2.061	.5257	.3835	.0923	.0879
		3.954	1.814	.5526	.4169	.1194	.1038
		3.377	1.581	.5714	.4392	.1338	.1090
		2.995	1.375	.6011	.4788	.1737	.1294
		2.617	1.226	.6287	.5151	.2104	.1535

Dispersion	Number of Roll Mill Passes	Ink On Cylinder ($kg/m^2 \times 10^5$)	Ink On Print ($kg/m^2 \times 10^5$)	Reflectance At Selected Wavelengths 460	500	540	620
DuPont	50	23.53	7.500	.2925	.1568	.0341	.0415
BT-4490		19.90	6.639	.3100	.1715	.0346	.0425
PS-92778		17.55	5.890	.3335	.1905	.0354	.0435
		15.97	5.398	.3444	.1994	.0358	.0444
		14.04	4.994	.3589	.2110	.0362	.0458
		12.47	4.563	.3801	.2307	.0378	.0476
		10.92	4.145	.3931	.2425	.0399	.0485
		9.951	3.842	.4067	.2560	.0431	.0513
		7.833	3.190	.4469	.297	.0586	.0625
		6.244	2.675	.4809	.335	.0779	.0748
		7.125	3.013	.4587	.3097	.0619	.0742
		6.315	2.643	.4823	.337	.0805	.0704
		5.144	2.217	.5176	.377	.1013	.0888
		4.780	2.166	.518	.3748	.0886	.0752
		4.241	1.834	.6002	.477	.1823	.0930
Am. Cyanamid	1	12.34	6.146	.4443	.3339	.1200	.0495
3456		9.650	5.320	.4842	.3733	.1338	.0517
No Premix		8.117	4.482	.4923	.3791	.1330	.0504
		6.601	3.602	.5162	.4043	.1502	.0567
		5.864	2.887	.5272	.4165	.1580	.0604
		5.019	2.309	.5560	.4497	.1801	.0720
		3.766	1.657	.6122	.5234	.2497	.1059
		3.068	1.002	.6565	.5828	.3151	.1468
		2.681	.908	.6670	.5972	.3342	.1623
Am. Cyanamid	3	12.33	5.749	.4356	.3189	.1066	.0436
3456		9.637	4.867	.4198	.3019	.0932	.0422
No Premix		7.901	4.087	.4445	.3262	.1027	.0458
		6.104	2.703	.5164	.4073	.1544	.0646
		3.009	.654	.6998	.6419	.4048	.2326

Dispersion	Number of Roll Mill Passes	Ink On Cylinder ($kg/m^2 \times 10^5$)	Ink On Print ($kg/m^2 \times 10^5$)	Reflectance at Selected Wavelengths 460	500	540	620
Am. Cyanamid	5	14.86	8.09	.3569	.2467	.0835	.0394
3456		11.36	6.273	.3806	.2645	.0821	.0394
No Premix		7.346	4.174	.4528	.3349	.1121	.0462
		5.159	2.49	.5375	.4268	.1623	.0875
		3.991	1.274	.6375	.5572	.2934	.1406
		3.122	.783	.6869	.6238	.3722	.1944
		2.578	.635	.7047	.6503	.4142	.2302
Am. Cyanamid	25	9.285	5.107	.2890	.2658	.0801	.0411
3456		6.760	3.508	.4528	.3337	.1100	.0529
No Premix		5.747	2.786	.5008	.3852	.1338	.0590
		10.002	6.049	.3583	.2415	.0730	.0375
		5.793	2.251	.5157	.4404	.1856	.0818
		5.056	2.104	.5535	.4460	.1826	.0778
			.892	.6671	.5960	.3386	.1714
Am. Cyanamid	50	11.99	6.381	.3459	.2296	.0673	.0368
3456		8.565	4.805	.4002	.2789	.0876	.0408
No Premix		6.518	3.182	.4860	.3681	.1309	.0548
		5.715	2.517	.5232	.4090	.1557	.0656
		4.542	1.899	.5704	.4663	.1998	.0833
		3.408	1.237	.6163	.5254	.2495	.1100
Am. Cyanamid	1	10.02	5.290	.4080	.2878	.0946	.0422
3456		8.800	4.629	.4279	.3057	.1305	.0430
5 Min. Premix		9.216	4.480	.4315	.3101	.1012	.0439
		8.041	4.160	.4365	.3141	.0970	.0413
		7.992	3.946	.4456	.3247	.1077	.0451
		6.912	3.475	.4767	.3592	.1282	.0516
		6.194	3.006	.5108	.3955	.1471	.0518
		5.377	2.177	.5575	.4509	.1916	.0813
		4.851	2.040	.5633	.4565	.1907	.0784

Dispersion	Number of Roll Mill Passes	Ink On Cylinder ($kg/m^2 \times 10^5$)	Ink On Print ($kg/m^2 \times 10^5$)	Reflectance At Selected Wavelengths 460	500	540	620
Am. Cyanamid 3456 5 Min. Premix (cont'd)	1	4.292	1.655	.5999	.5032	.2339	.0987
		3.785	1.385	.6268	.5415	.2741	.1155
		3.404	1.088	.6508	.5735	.3085	.1443
		2.997	.736	.7007	.6434	.4089	.2266
		2.659	.682	.7012	.6449	.4094	.2226
Am. Cyanamid 3456 5 Min. Premix	3	12.03	6.898	.3308	.2243	.0747	.0369
		10.94	6.051	.3558	.2444	.0759	.0399
		9.659	4.591	.3704	.2559	.0826	.3097
		7.627	4.118	.4231	.3031	.1004	.0433
		6.616	3.398	.4595	.3108	.1195	.0509
		6.077	2.936	.4845	.3718	.1367	.0577
		5.426	2.429	.5249	.4177	.1663	.0703
		4.713	2.059	.5468	.4417	.1789	.0768
		4.045	1.637	.5924	.4998	.1983	.1022
		3.675	1.494	.6065	.5193	.2531	.1188
		3.291	1.175	.6354	.5563	.2896	.1355
		2.904	.928	.6690	.6037	.3499	.1786
		2.542	.816	.6777	.6164	.3678	.1911
		2.270	.604	.7048	.6559	.4244	.2378
		2.008	.540	.7195	.6760	.4547	.2639
Am. Cyanamid 3456 5 Min. Premix	10	11.68	6.409	.3419	.2316	.0760	.0400
		10.43	5.978	.3565	.2419	.0779	.0396
		8.851	4.859	.3953	.2761	.0879	.0431
		7.730	4.079	.4259	.3073	.1017	.0470
		7.008	3.582	.4496	.3322	.1137	.0504
		6.295	3.179	.4749	.3589	.1229	.0563
		5.225	2.347	.5080	.3948	.1462	.0622
		4.919	1.025	.5524	.4488	.1890	.0837
		4.297	1.737	.5840	.4866	.2164	.0949
		3.783	1.430	.6143	.5280	.2595	.1205

Dispersion	Number of Roll Mill Passes	Ink On Cylinder ($kg/m^2 \times 10^5$)	Ink On Print ($kg/m^2 \times 10^5$)	Reflectance At Selected Wavelengths 460	500	540	620
Am. Cyanamid 3456 5 Min. Premix (cont'd)	10	3.345	1.173	.6255	.5437	.2746	.1271
		2.813	.901	.6623	.5937	.3336	.1663
		2.512	.578	.7043	.6086	.3492	.1768
		2.297	.578	.7043	.6550	.4191	.2304
		2.015	.445	.7231	.6839	.4754	.2851
Am. Cyanamid 3456 5 Min. Premix	50	10.66	5.850	.3674	.2458	.0804	.0337
		9.263	4.910	.4012	.2772	.0907	.0401
		8.345	4.430	.4164	.2907	.0997	.0432
		7.977	4.160	.4310	.3047	.1129	.0496
		6.871	3.460	.4635	.3382	.1354	.0576
		6.092	2.940	.5023	.3802	.1354	.0576
		5.321	2.160	.5534	.4410	.1870	.0819
		4.594	1.800	.6016	.5013	.2397	.1104
		4.104	1.580	.3999	.5009	.2327	.1021
		3.575	1.350	.6285	.5402	.2703	.1230
		3.137	.857	.6906	.6252	.3769	.2016
		2.799	.861	.6967	.6326	.3793	.1967
		2.355	.613	.7125	.6592	.4231	.2291
Crude PCN 5 Min. Premix	1	10.61	5.300	.3659	.3067	.1528	.0918
		8.908	4.615	.4039	.3454	.1819	.1061
		7.284	3.046	.4235	.3658	.1976	.1168
		7.037	3.170	.4762	.4217	.2413	.1451
		6.601	2.986	.4919	.4386	.2541	.1532
		5.837	2.270	.5456	.4963	.3107	.1951
		4.782	1.740	.5887	.5464	.3592	.2270
		5.318	2.310	.5574	.5101	.3203	.1987
		4.275	1.136	.6693	.6742	.4805	.3454
		3.888	1.077	.6577	.6268	.4599	.3220
		3.621	.816	.6878	.6628	.5107	.3740
		3.313	.894	.7822	.6582	.5060	.3653

Dispersion	Number of Roll Mill Passes	Ink On Cylinder ($kg/m^2 \times 10^5$)	Ink on Print ($kg/m^2 \times 10^5$)	460	500	540	620
Crude PCN 5 Min. Premix (cont'd)	1	3.215	.794	.6886	.6654	.5157	.3758
		2.561	.368	.7450	.7344	.6282	.5068
Crude PCN 5 Min. Premix	3	11.71	6.820	.3061	.2479	.1132	.0706
		11.00	6.150	.3270	.2692	.1296	.7680
		8.484	4.980	.3649	.3087	.1512	.0865
		7.791	4.320	.3939	.3340	.1679	.0955
		6.996	3.490	.4323	.3745	.1970	.1112
		5.333	2.330	.5347	.4848	.2894	.1687
		5.056	2.040	.5590	.5021	.3060	.1818
		4.043	1.590	.5926	.5502	.3577	.2193
		4.101	1.330	.6153	.5783	.3944	.2542
		3.293	1.030	.6519	.6209	.4422	.2916
		2.879	.674	.6986	.6785	.5276	.3780
		2.600	.664	.6977	.6793	.5353	.3909
Crude PCN 5 Min. Premix	5	9.966	5.777	.3384	.2773	.1286	.0756
		9.730	5.674	.3411	.2786	.1366	.0795
		8.058	4.351	.3908	.3299	.1624	.0901
		7.024	3.977	.4068	.3449	.1696	.0940
		6.023	2.922	.4778	.4210	.2298	.1259
		5.328	2.160	.5339	.4822	.2840	.1623
		4.772	1.933	.5451	.4937	.2898	.1652
		4.392	1.513	.5882	.5449	.3486	.2103
		3.827	1.291	.6093	.5703	.3752	.2290
		3.396	1.022	.6490	.6104	.4352	.2846
		3.359	.780	.6917	.6695	.5077	.3512
		2.529	.566	.7188	.7040	.5713	.4163

Dispersion	Number of Roll Mill Passes	Ink On Cylinder ($kg/m^2 \times 10^5$)	Ink on Print ($kg/m^2 \times 10^5$)	460	500	540	620
Crude PCN	10	11.38	6.745	.2993	.2399	.1044	.0612
5 Min.		9.434	5.637	.3309	.2692	.1166	.0690
Premix		8.051	4.386	.3789	.3155	.1455	.0782
		6.834	3.564	.4267	.3655	.1781	.0934
		6.276	3.167	.4760	.3819	.1883	.1008
		5.448	2.436	.4895	.4324	.2270	.1218
		5.078	1.990	.5318	.4786	.2715	.1498
		4.630	1.436	.5859	.5407	.3376	.1987
		3.893	1.181	.6167	.5747	.4725	.2216
		3.448	1.181	.6167	.5747	.4725	.2216
		2.941	.596	.6879	.6622	.4910	.3303
		2.476	.505	.7150	.6952	.5375	.3726
Crude PCN	25	10.02	5.647	.3142	.2499	.0994	.0574
5 Min.		8.531	4.777	.3425	.2753	.1127	.0617
Premix		7.688	3.956	.3828	.3140	.1337	.0693
		6.969	3.734	.3950	.3264	.1417	.0765
		5.771	2.711	.4689	.4041	.1926	.0963
		5.482	2.307	.4901	.4277	.2161	.1111
		4.327	1.943	.5439	.4856	.2589	.1347
		3.903	1.380	.6002	.5522	.3304	.1774
		3.499	1.137	.6228	.5788	.3633	.2077
		3.026	.885	.6519	.6249	.4193	.2523
		2.747	.735	.6800	.6483	.4488	.2708
		2.463	.553	.7036	.6788	.5019	.3249
Crude PCN	50	13.60	7.070	.2717	.2060	.0720	.0450
5 Min.		12.04	6.440	.2890	.2221	.0811	.0462
Premix		10.10	5.970	.3102	.2396	.0899	.0496
		8.893	5.160	.3373	.2643	.1002	.0599
		7.598	3.915	.3948	.3214	.1322	.0735
		6.716	3.416	.4129	.3390	.1003	.0784

Dispersion	Number of Roll Mill Passes	Ink On Cylinder ($kg/m^2 \times 10^5$)	Ink on Print ($kg/m^2 \times 10^5$)	Reflectance At Selected Wavelengths 460	500	540	620
Crude PCN	50	5.659	2.623	.4806	.4103	.1919	.0947
5 Min.		5.201	1.977	.5315	.4678	.2456	.1290
Premix		4.400	1.500	.5918	.5347	.3088	.1726
(cont'd)		3.815	1.463	.5844	.5257	.2885	.1520
		3.614	1.187	.6080	.5555	.3264	.1819
		2.936	.875	.6540	.6105	.3916	.2265
		2.255	.161	.6790	.6448	.4486	.2826
		2.473	.5280	.6953	.6646	.4777	.3092
Ciba-Geigy	1	29.14	9.402	.2260	.1336	.0338	.0315
PD-989		24.19	9.474	.2293	.1354	.0338	.0387
		21.80	9.564	.2289	.1350	.0332	.0363
		18.95	8.964	.2435	.1462	.0352	.0370
		17.35	8.173	.2534	.1542	.0370	.0370
		15.09	7.488	.2611	.1594	.0361	.0401
		14.05	8.156	.2764	.1727	.0401	.0371
		8.492	4.864	.3623	.2503	.0705	.0574
		7.414	4.200	.3923	.2790	.0859	.0597
		6.494	3.519	.4073	.2915	.0892	.0592
		5.708	2.994	.4507	.3368	.1143	.0716
		4.973	2.582	.4776	.3633	.1249	.0787
		4.248	2.036	.5215	.4133	.1622	.0934
		3.832	1.630	.5648	.4674	.2099	.1221
		3.315	1.337	.5893	.4936	.2294	.1292
		1.904	1.158	.6097	.5214	.2580	.1535
		2.610	.928	.6395	.5606	.3013	.1737
Ciba-Geigy	3	21.49	9.087	.2374	.1413	.0357	.0306
PD-989		18.60	8.768	.2459	.1471	.0353	.0500
		16.77	8.171	.2541	.1529	.0350	.0431
		14.70	7.437	.2768	.1718	.0408	.0417
		12.99	6.763	.2759	.1705	.0394	.0404

Dispersion	Number of Roll Mill Passes	Ink On Cylinder ($kg/m^2 \times 10^5$)	Ink on Print ($kg/m^2 \times 10^5$)	Reflectance At Selected Wavelengths 460	500	540	620
Ciba-Geigy PD-989 (cont'd)	3	11.19	6.329	.3002	.1914	.0450	.0437
		9.850	6.003	.3304	.2170	.0522	.0522
		8.695	4.882	.3533	.2382	.0626	.0492
		7.566	4.273	.3807	.2652	.0758	.0546
		6.369	3.484	.4216	.3041	.0945	.0642
		5.744	3.173	.4440	.3261	.1044	.0713
		5.020	2.335	.4946	.3830	.1436	.0865
		4.350	2.010	.5217	.4138	.1660	.0965
		3.795	1.558	.5629	.4611	.2020	.1163
		3.271	1.320	.5860	.4890	.2270	.1374
		2.936	1.001	.6265	.5421	.2829	.1691
		2.534	.778	.6590	.5870	.3417	.2118
Ciba-Geigy PD-989	1	20.76	9.420	.2280	.0330	.0330	.0388
		18.19	8.926	.2386	.1406	.0337	.0445
		15.81	8.440	.2497	.1550	.0369	.0407
		13.74	7.697	.2629	.1611	.0399	.0418
		12.02	6.575	.2870	.1812	.0444	.0427
		10.67	6.078	.3035	.1939	.0455	.0476
		9.876	5.253	.3310	.2186	.0572	.0454
		8.190	4.483	.3672	.2511	.0701	.0499
		7.066	4.043	.3865	.2680	.0733	.0540
		5.992	2.892	.4504	.3342	.1140	.0684
		5.130	2.443	.4894	.3762	.1429	.0820
		4.515	1.716	.5575	.4560	.2081	.1196
		3.822	1.156	.6259	.5395	.2868	.1703
		3.526	1.075	.6296	.5421	.2771	.1525
		3.926	.568	.6977	.6379	.4080	.2617
		7.974	.213	.7547	.7256	.5585	.4072
Ciba-Geigy PD-989	10	20.09	8.664	.2348	.1401	.0410	.0133
		17.05	7.845	.2538	.1520	.3050	.0298

Dispersion	Number of Roll Mill Passes	Ink On Cylinder ($kg/m^2 \times 10^5$)	Ink on Print ($kg/m^2 \times 10^5$)	Reflectance At Selected Wavelengths 460	500	540	620
Ciba-Geigy PD-989 (cont'd)	10	15.13	7.568	.2563	.1558	.0388	.0249
		13.58	7.077	.2779	.1721	.0407	.0282
		11.90	6.380	.2938	.1848	.0409	.0399
		10.37	5.565	.3218	.2110	.0538	.0324
		9.187	5.080	.3434	.2311	.0622	.0349
		8.039	4.306	.3794	.2635	.0753	.0447
		7.020	3.865	.3992	.2818	.0811	.0494
		6.107	3.133	.4519	.3370	.1178	.0650
		5.360	2.495	.4865	.3758	.1414	.0759
		4.635	1.986	.5475	.4458	.1993	.1134
		4.106	1.719	.5618	.4594	.2031	.1181
		3.465	1.147	.6228	.5395	.2958	.1827
		3.144	1.128	.6384	.5564	.3051	.1848
		2.742	.903	.6595	.5832	.3314	.2022
Ciba-Geigy PD-989	25	18.35	7.945	.2424	.1448	.0377	.0175
		16.41	7.907	.2595	.1576	.0387	.0186
		12.73	6.520	.2809	.1760	.0439	.0193
		11.07	5.798	.3098	.1990	.0494	.0239
		9.787	5.309	.3304	.2189	.0583	.0268
		8.423	4.662	.3528	.2372	.0612	.0392
		7.346	3.777	.4107	.2976	.0998	.0494
		6.420	3.324	.4322	.3158	.1030	.0510
		5.531	2.491	.4982	.3878	.1530	.0786
		4.704	1.980	.5432	.4379	.1867	.0878
		4.214	1.713	.6139	.5252	.2756	.0966
		3.712	1.220	.6407	.5594	.3111	.1552
DuPont BT-4490 PS-92778	1	18.22	8.072	.2766	.1550	.0409	.0385
		15.00	7.483	.2938	.1691	.0452	.0401
		13.00	6.693	.3126	.1839	.0495	.0524
		11.41	6.167	.3287	.1967	.0505	.0423

Dispersion	Number of Roll Mill Passes	Ink On Cylinder ($kg/m^2 \times 10^5$)	Ink on Print ($kg/m^2 \times 10^5$)	Reflectance At Selected Wavelengths 460	500	540	620
DuPont BT-4490 PS-92778 (cont'd)	1	9.99	5.371	.3604	.2235	.0621	.0456
		8.834	4.715	.3777	.2367	.0657	.0465
		7.564	4.064	.4209	.2785	.0860	.0573
		6.839	3.481	.4445	.3025	.0986	.0620
		6.795	3.355	.4493	.3090	.1039	.0667
		4.784	2.119	.5438	.4114	.1667	.1096
		4.358	1.875	.5667	.4409	.1916	.1208
		3.602	1.389	.6130	.4961	.2358	.1529
		2.950	0.758	.6592	.5625	.3136	.2148
		2.857	1.028	.6615	.5630	.3034	.2009
DuPont BT-4490 PS-92778	3	18.40	8.267	.2600	.1470	.0380	.0401
		15.97	8.024	.2746	.1514	.0361	.0465
		13.97	7.558	.2896	.1634	.0411	.0453
		12.17	6.589	.3090	.1792	.0444	.0469
		10.70	6.083	.3260	.1910	.0470	.0495
		9.233	5.518	.3490	.2102	.0529	.0550
		8.225	4.730	.3790	.2364	.0623	.0527
		7.341	3.738	.4310	.2880	.0893	.0666
		6.332	3.368	.4464	.3019	.0932	.0695
		5.852	2.876	.4895	.3505	.1248	.0867
		4.919	2.315	.5322	.3979	.1532	.1067
		3.869	1.530	.6042	.4905	.2372	.1617
		3.462	1.175	.6488	.5486	.2975	.2097
		2.990	.990	.6480	.5459	.2842	.1928
		2.649	.727	.6874	.5046	.3625	.2683
DuPont BT-4490 PS-92778	5	25.09	19.040	.2580	.1398	.0371	.0484
		15.76	8.619	.2710	.1481	.0392	.0461
		13.54	8.061	.2835	.1582	.0415	.0471
		11.74	7.069	.3046	.1738	.0455	.0486
		10.10	6.101	.3308	.1940	.0480	.0515

Dispersion	Number of Roll Mill Passes	Ink On Cylinder ($kg/m^2 \times 10^5$)	Ink on Print ($kg/m^2 \times 10^5$)	Reflectance At Selected Wavelengths 460	500	540	620
DuPont BT-4490 PS-92778 (cont'd)	5	8.847	5.367	.3620	.2200	.0574	.0593
		8.205	4.778	.3841	.2400	.0646	.0584
		6.998	4.076	.4250	.2803	.0847	.0670
		6.055	3.737	.4550	.2752	.0960	.0719
		5.296	2.817	.4940	.3499	.1166	.0867
		4.023	.1771	.5777	.4510	.1910	.1282
		3.553	1.495	.6001	.4792	.2146	.1435
		3.044	1.292	.6214	.5058	.2335	.1534
		2.588	1.104	.6592	.5589	.2895	.1976
		2.027	.535	.7176	.6545	.4278	.3153
DuPont BT-4490 PS-92778	10	17.04	.704	.2660	.1448	.0383	.0383
		15.35	7.992	.2674	.1452	.0369	.0445
		13.38	7.328	.2868	.1589	.0400	.0423
		11.74	6.521	.3076	.1758	.0450	.0439
		10.29	5.867	.3348	.1993	.0527	.0487
		7.830	4.424	.4033	.2618	.0782	.0625
		8.288	4.930	.3654	.2283	.0565	.0543
		7.262	4.075	.4161	.2721	.0806	.0628
		6.388	3.426	.4447	.3002	.0924	.0678
		4.887	2.483	.5106	.3742	.1386	.0954
		4.234	1.892	.5765	.4514	.1913	.1259
		3.861	1.673	.6217	.5128	.2522	.1696
		3.308	1.257	.6500	.5502	.2877	.1943
		2.544	.790	.6741	.5840	.3263	.2245
		2.189	.665	.6987	.6193	.3664	.2593
DuPont BT-4490 PS-92778	25	22.85	9.611	.2132	.1267	.0328	.0394
		19.83	8.833	.2342	.1673	.0509	.0446
		18.23	8.622	.2431	.1513	.0402	.0450
		16.11	8.241	.2396	.1467	.0353	.0491
		13.72	7.259	.2652	.1683	.0403	.0460

Dispersion	Number of Roll Mill Passes	Ink On Cylinder ($kg/m^2 \times 10^5$)	Ink on Print ($kg/m^2 \times 10^5$)	Reflectance At Selected Wavelengths 460	500	540	620
DuPont	25	12.25	6.801	.2806	.1800	.0490	.0483
BT-4490		10.98	6.407	.2908	.1920	.0503	.0489
PS-92778		9.549	5.619	.3101	.2083	.0548	.0513
(cont'd)		8.171	4.590	.3536	.2478	.0686	.0629
		7.194	4.092	.3710	.2635	.0760	.0579
		6.374	3.340	.4176	.3115	.1054	.0732
		5.397	2.548	.4759	.3750	.1473	.0947
		4.780	2.428	.4804	.3768	.1392	.0926
		4.689	2.439	.5302	.4328	.1835	.1105
		3.700	1.561	.5576	.4652	.2135	.1271
		3.200	1.132	.5988	.5144	.2588	.1558
		2.760	1.009	.6099	.5279	.2663	.1578
		2.427	.734	.6618	.5961	.3544	.2229
DuPont	50	22.68	9.640	.2429	.1250	.0352	.0393
BT-4490		19.27	8.638	.2613	.1387	.0372	.0400
PS-92778		18.69	8.130	.2730	.1449	.0358	.0430
		15.23	7.748	.2850	.1555	.0400	.0428
		13.89	7.250	.3990	.1673	.0439	.0454
		12.66	6.802	.3176	.1828	.0490	.0476
		11.25	6.329	.3290	.1904	.0485	.0463
		10.01	5.492	.3564	.2145		.0535
		8.812	5.075	.3737	.2289	.0614	.0518
		7.777	4.419	.3915	.2433	.0653	.0525
		6.719	3.566	.4485	.3008	.0962	.0715
		6.009	3.249	.4854	.3100	.0940	.0700
		4.425	2.099	.5397	.4014	.1537	.1021
		4.664	2.129	.5458	.4104	.1646	.1121
		4.116	1.826	.5653	.4318	.1749	.1137
		3.146	1.164	.6329	.5201	.2523	.1653
		2.483	.850	.6726	.5752	.3051	.2028

APPENDIX D

Printability and Data on Reflectance-Coated Stock

Dispersion	Number of Roll Mill Passes	Ink On Cylinder ($kg/m^2 \times 10^5$)	Ink On Print ($kg/m^2 \times 10^5$)	Reflectance At Selected Wavelengths 460	500	540	620
Ciba-Geigy PD-988	1	24.85	7.342	.2718	.1709	.0415	.0353
		21.94	6.654	.2878	.1824	.0387	.0399
		18.92	6.442	.3031	.1941	.0388	.0417
		17.09	5.567	.3193	.2084	.0425	.0498
		15.05	4.948	.3478	.2338	.0513	.0601
		11.64	4.261	.3695	.2502	.0445	.0579
		10.54	3.748	.3966	.2791	.0620	.0740
		9.050	3.478	.4035	.2820	.0521	.0674
		7.911	2.947	.4334	.3133	.0684	.0807
		6.890	2.713	.4433	.3219	.0669	.0775
		5.935	2.405	.4777	.3592	.0856	.0882
		5.193	2.158	.4926	.3765	.964	.0923
		4.721	1.980	.5033	.3878	.0998	.0952
		4.030	1.738	.5333	.4236	.1326	.1098
		3.531	1.559	.5513	.4447	.1482	.1161
Ciba-Geigy PD-988	10	23.47	7.404	.2741	.1675	.0361	.0393
		20.68	6.835	.2846	.1755	.0352	.0419
		18.28	6.048	.3058	.1928	.0382	.0461
		15.61	5.379	.3248	.2103	.0413	.0543
		14.34	4.799	.3701	.2498	.0495	.0680
		12.08	4.248	.3534	.2367	.0522	.0667
		11.42	4.135	.3720	.2496	.0430	.0615
		8.139	3.138	.4319	.3121	.0739	.0904
		8.438	3.232	.4191	.2974	.0594	.9783
		7.583	2.985	.4370	.3163	.0700	.0881
		6.584	2.714	.4487	.3253	.0638	.0805

Dispersion	Number of Roll Mill Passes	Ink On Cylinder ($kg/m^2 \times 10^5$)	Ink On Print ($kg/m^2 \times 10^5$)	Reflectance At Selected Wavelengths 460	500	540	620
Ciba-Geigy PD-988 (cont'd)	10	5.798	2.345	.4797	.3608	.0876	.0946
		5.113	2.182	.4880	.3707	.0908	.0942
		4.378	1.895	.5098	.3939	.1025	.0942
		3.288	1.480	.5617	.4563	.1563	.1224
		3.002	1.253	.5988	.5054	.2143	.1618
Ciba-Geigy PD-988	50	26.47	8.083	.2603	.1554	.0369	.0438
		22.90	7.118	.2782	.1700	.0528	.0469
		20.43	6.672	.2939	.1824	.0367	.0505
		15.78	5.290	.3303	.2130	.0376	.0545
		16.22	5.329	.3314	.2139	.0369	.0522
		14.34	4.802	.3546	.2354	.0437	.0601
		12.53	4.358	.3674	.2474	.0465	.0621
		10.80	3.935	.3884	.2668	.0505	.0654
		9.500	3.501	.4076	.3212	.0553	.0785
		8.325	3.308	.4232	.3033	.0554	.0735
		7.363	2.961	.4490	.2834	.0683	.0763
		6.329	2.424	.4793	.3639	.0959	.1011
		5.517	2.029	.5099	.3985	.1208	.1051
		4.593	1.506	.5780	.4743	.1895	.1342
		3.504	.999	.6431	.5665	.2974	.2116
		3.367	.801	.6685	.5993	.3355	.2323
		2.808	.4726	.7106	.6606	.4230	.2956
DuPont BT-4490 PS-92778	1	21.49	5.317	.2988	.1691	.0380	.0376
		19.26	6.743	.3035	.1746	.0379	.0384
		16.92	5.947	.3240	.1915	.0385	.0396
		14.79	5.302	.3469	.2094	.0395	.0415
		13.00	4.825	.3612	.2215	.0760	.0432
		11.57	4.492	.3814	.2395	.0418	.0440
		10.35	.3988	.4039	.2599	.0460	.0492
		8.854	3.554	.4255	.2811	.0498	.0528

Dispersion	Number of Roll Mill Passes	Ink On Cylinder ($kg/m^2 \times 10^5$)	Ink On Print ($kg/m^2 \times 10^5$)	Reflectance at Selected Wavelengths 460	500	540	620
DuPont	1	8.004	3.314	.4466	.2988	.0536	.0551
BT-4490		6.513	2.779	.4859	.3368	.0661	.0648
PS-92778		6.410	2.765	.4905	.3417	.0665	.0674
(cont'd)		6.090	2.484	.5104	.3695	.1032	.0968
		5.223	2.330	.5250	.3741	.0829	.0796
		4.432	2.033	.5475	.4025	.0952	.0827
		3.555	1.607	.5922	.4603	.1482	.1169
		3.394	1.566	.5956	.4619	.1434	.1077
		3.002	1.315	.6347	.5153	.2038	.1559
		2.627	1.206	.6476	.5295	.2100	.1534
DuPont	10	22.30	7.411	.2829	.1510	.0352	.0379
BT-4490		19.06	6.518	.3141	.1760	.0347	.0430
PS-92778		17.00	5.839	.3266	.1867	.0356	.0438
		15.16	5.254	.3533	.2416	.0373	.0485
		13.20	4.859	.3660	.2194	.0381	.0498
		12.40	4.233	.3766	.2286	.0375	.0479
		10.51	3.997	.4018	.2286	.0375	.0479
		10.51	3.997	.4018	.2520	.0408	.0528
		9.655	3.671	.4183	.2685	.0471	.0572
		8.298	3.389	.4346	.2848	.0520	.0606
		7.333	3.034	.4501	.2994	.0502	.0642
		6.256	2.697	.4779	.3307	.0698	.0761
		5.656	2.454	.4964	.3527	.0814	.0816
		5.223	2.296	.5078	.3652	.0882	.0892
		4.481	2.061	.5257	.3835	.0923	.0879
		3.954	1.814	.5526	.4169	.1194	.1038
		2.995	1.375	.6011	.4785	.1737	.1294
		2.617	1.226	.6287	.5150	.2104	.1535

Dispersion	Number of Roll Mill Passes	Ink On Cylinder ($kg/m^2 \times 10^5$)	Ink On Print ($kg/m^2 \times 10^5$)	Reflectance At Selected Wavelengths 460	500	540	620
DuPont	50	23.53	7.500	.2925	.1568	.0341	.0415
BT-4490		19.90	6.639	.3100	.1715	.0346	.0425
PS-92778		17.55	5.890	.3335	.1905	.0354	.0435
		15.97	5.398	.3444	.1994	.0358	.0444
		14.04	4.994	.3589	.2110	.0362	.0458
		12.47	4.563	.3801	.2307	.0378	.0476
		10.92	4.145	.3931	.2425	.0399	.0485
		9.951	3.842	.4067	.2560	.0431	.0513
		7.833	3.190	.4469	.2970	.0586	.0625
		6.244	2.675	.4809	.3351	.0779	.0748
		7.125	3.013	.4587	.3097	.0619	.0742
		6.315	2.643	.4823	.3370	.0805	.0704
		5.144	2.217	.5176	.3770	.1013	.0888
		4.780	2.166	.5180	.3748	.0886	.0752
		4.241	1.834	.6002	.4770	.1823	.0930

APPENDIX E

Absorption Coefficients for Bleaches and Prints

(All Premixing for 5 Min. Unless Otherwise Noted)

Dispersion	Number of Mill Passes	K (Model 2)	K/S Bleach	K Model 2 (K/S)
Cyanamid	1	1.420	0.855	1.661
3456	3	1.461	0.842	1.735
(0 Premix)	5	1.330	--	--
	25	1.534	0.798	1.922
	50	1.729	--	--
Cyanamid	1	1.584	0.759	2.087
3456	3	1.542	--	--
	10	1.576	0.786	2.005
	50	1.501	0.875	1.715
Crude	1	0.5585	0.266	2.100
PCN	3	0.5136	--	--
	5	0.7403	0.289	2.562
	10	0.8466	--	--
	25	0.9878	--	--
	50	1.035	0.410	2.524
Ciba-Geigy	1	1.313	1.09	1.205
PD-988	3	1.277	1.11	1.150
	5	1.215	1.11	1.095
	10	1.240	1.11	1.117
	25	1.404	1.10	1.117
	50	--	1.12	1.276
DuPont	1	1.140	0.694	1.643
BT-4490	3	0.9963	0.722	1.380
PS-92778	5	1.110	0.613	1.811
	10	0.9860	0.689	1.431
	25	1.167	0.726	1.607
	50	1.156	0.732	1.579

VITA

Charles R. Nippert was born in Allentown on May 10, 1947. He received a BS in Chemical Engineer from Lehigh University in 1969. In 1972, he received a Master's Degree in Chemical Engineering from Lehigh University. He is married to the former Carolyn Cochrane and is currently employed at Kawecki Berylco Industries (a division of Cabot Industries).